ECONADAPT

The Economics of Adaptation

Funded by the European Union

Description of uncertainties associated with planned investments and incorporation in decision rules

Elisa Sainz de Murieta, Ibon Galarraga and Luis M. Abadie (BC3); Kateřina Kaprová and Jan Melichar (CUNI); Paolo Scussolini and Onno Kuik (VUA); Alistair Hunt (UBAH)

Deliverable number 6.3	
Work Package Number 6	
Submission date	
Type of Activity	RTD
Nature	R = Report
Dissemination level	Public

Document information

Title:	
Authors:	Elisa Sainz de Murieta, Ibon Galarraga and Luis M. Abadie (BC3); Kateřina Kaprová and Jan Melichar (CUNI); Paolo Scussolini and Onno Kuik (VUA); Alistair Hunt (UBAH)
Other Contributors	Manuel Lago, Josselin Rouillard and Jenny Troeltzsch (ECOLOGIC INSTITUTE)
Date:	Submission Date
Contact details	Corresponding author: Paolo Scussolini (paolo.scussolini@vu.nl)
Work Package Number	WP6
Deliverable number	D6.3
Filename:	Deliverable 6.3 Final.docx
Document history:	Draft/ Final and version number
Type of Activity	RTD
Nature	R = Report
Dissemination / distribution level	PU = Public: PP = Restricted to other programme participants (including the Commission Services); RE = Restricted to a group specified by the consortium (including the Commission Services); CO = Confidential, only for members of the consortium (including the Commission Services)
Citation:	
Copyright:	

The ECONADAPT project has received funding from the European Union's Seventh Framework Programme for research, technological development and demonstration under grant agreement no 603906.

To find out more about the ECONADAPT project, please visit the web-site: www.econadapt.eu

For further information on the ECONADAPT project contact Alistair Hunt at: ecsasph@bath.ac.uk

Executive Summary

What is the aim of this deliverable?

In this deliverable we present the results of the appraisals conducted in the two case studies of Work Package 6 of ECONADAPT. For the Vltava (Czech Republic) and the Bilbao (Spain) case studies, we assessed the benefits and costs of investment to adapt to climate-induced variations in flooding. In these appraisals, we emphasize the methodologies that allow addressing the multiple sources of uncertainty that typically characterize appraisals of climate change adaptation investments.

Why is the work of this deliverable important?

By carrying out these two case studies we intend to explore the methodological challenges connected with dealing with the large and diverse uncertainties that are typical of investments in adaptation to climate change. So far, adaptation to future climate change, and the relevant uncertainties have rarely been explicitly included in economic appraisal studies, even when the investments under study have multi-decadal life times that make them particularly vulnerable to long-term climatic and socio-economic change. Damages result from extreme events that may become more frequent over time. It is therefore important to quantify the risks posed by changing future conditions, without and with the investment in adaptation.

Thanks to the lesson learned through the two cases we will be able to draw recommendations for practitioners to be followed in similar project appraisals in the EU context and beyond.

Which method was used?

In this deliverable, two methods have been applied and tested in terms of their suitability for tackling the challenges typical of appraisals of long-term investments with high uncertainties, such as those into adaptation to long-term climate change. In the Vltava case, we explored the boundaries of the Cost Benefit Analysis, a well-established method that has become routine in many contexts in the EU. In the Bilbao case, we set out to investigate the advantages that Real Option Analysis offers, especially the possibility it offers of explicitly considering the option of shifting the adaptation investment in time.

Further, in the two cases we also explore two different approaches to the calculation of economic returns, and of the risk, of investments that depend on stochastic processes, such as the occurrence of natural disasters. The Bilbao case considers the frequency of the extreme events modelled with three Poisson processes, and the stochastic growth rate of the damage due to climate and socio-economic effects. The Vltava case integrates the damages of various return periods of known floods under the so-called risk curve that is often adopted in the field of flood risk assessment.

What are the key results?

We have carried out simulations in a cascade of models, spanning several disciplines, from climate, to hydrology, to flood risk, through to economic modeling, and produced economic appraisals mostly in terms of the Net Present Values of the adaptation investments planned. Further, for the Bilbao case, results are also expressed in terms of Value-at-Risk, and of Expected Shortfall of the investment, two risk measures that are often used in financial risk analysis.

A final table of this Deliverable 6.3 provides a qualitative account of the relative importance of each source of uncertainty on the results of the two case study appraisals.

What are the main strengths and limitations of the method used?

We have observed that Cost Benefit Analysis presents the main advantage of allowing for the incorporation of different input data, reflecting the various sources of uncertainty, and therefore yielding results regarding the economic efficiency of the investment under the contemplated range of conditions. On the other hand, this method does not allow to explore the decision-making dimension of when the investment becomes optimal. The latter is indeed the main advantage of Real Option Analysis here presented, which calculates an analytical solution for the Net Present Value of investment at any given time, and applies a binomial tree to study whether the best decision at present is to invest or to wait until (some) uncertainty about the future is resolved.

What future research is recommended?

Handling different sources of uncertainties in appraisals such as those considered, generates a large amount of results, with dependency upon the multiple factors that reflect the uncertainties. Further research could be dedicated to devising ways of visualizing this wealth of information in a more user-friendly manner, and to formalizing the decision-making process in the presence of such large uncertainty into a rational and rigorous workflow.

Table of Contents

1 Introduction

1.1 Aims and structure of the ECONADAPT project

The ECONADAPT FP7 project carries out research in the context of Europe's adaptation to man-made climate change. The economics to support decision-making about adaptation actions are examined, and particular attention is bestowed to the aspects of uncertainty and multiplicity of scales inherent to the climate change predicament.

The project's aims are to provide decision-makers and stakeholders with economic methodologies, evidence and appraisal criteria to guide and coordinate adaptation action, at the various scales applicable in the European context. The climate change areas on which the project focuses range from the short-term effects of extreme weather events, to the long-term costs of climate-related risk, and from the macroeconomic consequences of impacts, to the assistance to developing countries in their response to expected climate developments.

The facilitate the project's scopes, ECONADAPT is organized in three methodological Work Packages (WP) (WPs 2 to 4), that are meant to inform and provide operational input to five WPs (WPs 5 to 9) that are centred on policy-relevant case studies. Besides these, other work packages focus on the project-supporting aspects of the framing of the policy-focussed economic analysis (WP1), stakeholder engagement (WP11), the final set-up of a toolbox for economic assessment of adaptation (WP10), dissemination (WP11) and project management and integration (WP12).

1.2 Work package 6

Among the policy-relevant case studies WPs, WP6 is dedicated to the economic appraisal of projects of adaptation to climate change. The aim here is "to provide illustrative examples of prototype appraisals in real-world contexts"[1]. To represent a variety of contexts, two case studies are selected:

- the fluvial flood protection in the Vltava river basin in the Czech Republic (Vltava case study);
- altering the topography of a district, Zorrotzaurre, by the Nervión river in city of Bilbao, Spain (Bilbao case study).

The Vltava case study is led and conducted by Charles University of Prague (CUNI partner), and the Bilbao case study by the Basque Centre for Climate Change (BC3 partner).

The two case studies explicitly address the two main threats that climate change poses to Europe, namely increased hazard from river floods, originating from modifications in the precipitation patters in continental regions (Vltava case study), and increased pressure on coastal zones from rising sea levels and intensifying storm surges (Bilbao case study).

The two case studies will present the evaluation of costs, benefits and related uncertainties of the two concrete projects of adaptation in the Czech and Spain contexts. Projections of the effects of climate change, in the form of altered rainfall, of and socioeconomic developments

[1] From the ECONADAPT project Description of Work.

will be explicitly taken into account. The methodologies applied will at least partially be derived from work in the methodological WPs of the project.

1.3 The challenges of uncertainty – This report

Deliverable 6.3 presents the final results of the appraisal exercises carried out in the two case studies of WP6, and emphasizes on the description, quantification, and techniques to address the uncertainties that are associated with appraisals of adaptation investments. Uncertainty is a defining aspect of climate-change adaptation action (Heal and Millner, 2014), and it has been suggested that decision-making and businesses alike need to enhance their capacity to rationally operate under uncertain future conditions (World Economic Forum, 2016).

With Deliverable 6.3 the appraisal exercises are complete, and the set of Deliverables 6.1, 6.2 and 6.3 will form the basis on which we compose the policy recommendations, lessons learned and guidance included in the final Deliverable 6.4.

Methodologically, the Vltava case study aims to examine whether cost-benefit analysis may contribute to the decision-making on climate change adaptation investments, to show which uncertainties affect the results, assess how uncertainties may be treated in cost-benefit analysis so that the results are more robust, and to discuss also the limitations of the method in relation to assessment of climate change adaptation investments.

The Bilbao case study the opportunity of investing in an adaptation measure is considered from an economic point of view, and the decision is taken on the basis of real option analysis, in turn informed by the complete assessment of the benefits (in terms of avoided damages) and costs of the measure.

1.3.1 Climate uncertainty

The uncertainties in the phase of climate modelling represent a key problem in evaluating climate-sensitive investments. Uncertainties have different sources, such as the natural climate variability that causes changes in short term climate, incomplete knowledge about the climate system and representation of its processes in climate models, measurement errors, and also uncertainty in future emissions of greenhouse gases (Figure 1). Another source of uncertainty stems from downscaling, when local impacts of global climate change is estimated (Heal and Millner, 2014). For a more extensive discussion on the uncertainties related to climate change, see Deliverable 4.1.

No single climate model is able to produce a reliable prediction of the climate and the uncertainty increases for the far future. To address the climate change-related uncertainties, in the case studies of WP6 we adopted datasets from a set of climate models. This enables assessing the potential variability of the climate until year 2100.

Uncertainties in future emissions of greenhouse gases have been addressed by employing a range of scenarios from a set of the Representative Concentration Pathways (RCPs; IPCC, 2014), the most recent in the research community. In the case studies, we focus on two of them, RCP4.5 and RCP8.5. In this manner, two realistic emission paths are investigated, one that entails 21st century stabilization of emissions at a moderate rate, and one that represents emissions in the absence of serious global mitigation policies. We explicitly disregard, in WP6, the potential impacts of scenarios of drastic and immediate reduction in emissions, such as represented in RCP2.6 (although in the Vltava case study one model run is employed with RCP2.6 forcings, to get an impression of the variability with respect to the other scenarios).

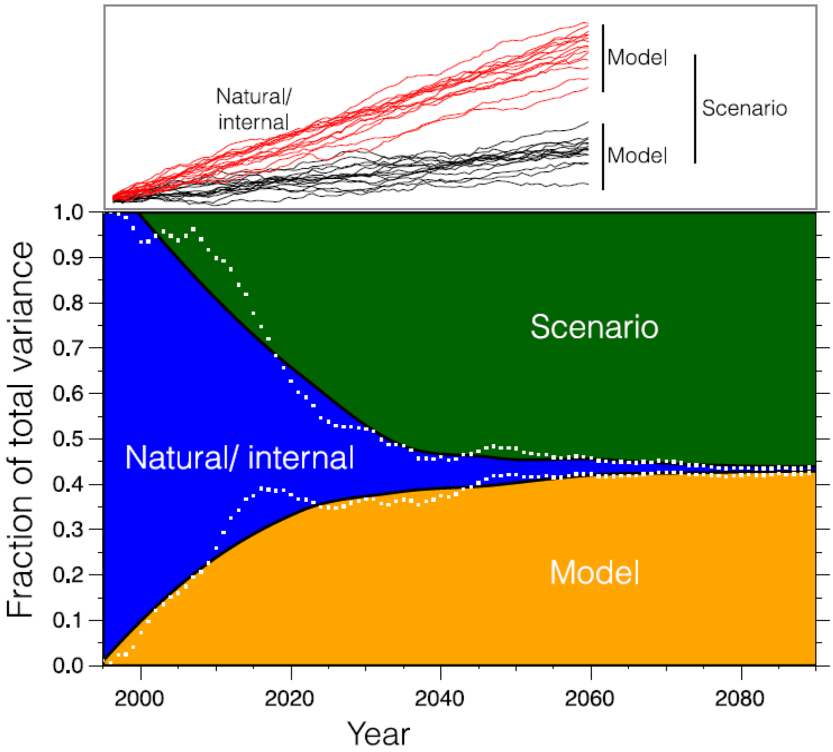

Fig.1. Representation of the different sources of uncertainty in climate change projections. In the bottom panel the relative contribution to the total variance is quantified for the example of regional North Sea sea level rise in the 21st century. Adapted from de Vries et al. (2014).

1.3.2 Hydraulic/hydrologic model uncertainty

There are two main sources of **uncertainty** in the phase of hydrological modelling: from the datasets, which comprise the uncertainties associated with the modeling of future climate variability (see 1.3.1), and from the modeling itself, i.e., model parameters, and model structure.

The uncertainties in the hydrological modeling are summarized in Arcadis (2004). The uncertainty is related to the following factors (Ibid.):

- Hydraulic/hydrological models
- Flood protection systems
- Flood factors

Hydraulic models describe complex hydraulic processes necessarily via simplifications, which accounts for the first contribution to uncertainty in this type of modeling. Other uncertainties regard geographic/spatial datasets, the simulation of constructed structures in and close to the water body (e.g., flood protection structures) into the model, and errors in estimating slope and surface unevenness. The most frequently used model is the water depth-inflow model, in which the relationship between water depth and inflow from the watercourse depends on parameters of high uncertainty that change over time, such as the profile and shape of the riverbed, temperature of water, the extent of sedimentation in the riverbed, instable impact of flowing, changes in the profile of the riverbed during the flood etc. The amount of uncertainty is usually reported using the deviation of the measured values with respect to the fitted curve.

The flood protection systems are composed of a series of elements with different construction characteristics (height, materials etc.). The behaviour and response of flood protection systems during flooding is often simplified in simulations, and is associated with large uncertainty due to limited experience and knowledge. Models that account for this type of uncertainty may stem from generic data or local measurements; but often are based on very limited experience and expert technical assessment (ibid.).

The area of flood is often simplified using models that are used for the definition of flood factors. The simplification does not take into account some specific features of the flooded area (forests or buildings) that may affect the water streaming, and also the behaviour of obstacles that are in the way of the flood (ibid.).

1.3.3 Other sources of uncertainty

Other sources of uncertainty that are relevant to the appraisals dealt with here include:

- Uncertainty about the exposed assets, people, infrastructure and buildings. This implies that impacts of flood may differ largely, based on the accuracy of the exposure datasets, or on the assumptions made when these datasets are missing or incomplete.
- Uncertainty about the vulnerability of the exposed assets and people. The vulnerability, or in other words, the susceptibility to be damaged is a very difficult to quantify parameter, which moreover has been shown to be markedly site-specific. In the ideal situation, results from specific survey performed in the site and at the time of the analysis should be used. Moreover, it should be kept in mind that it is not possible to know how the vulnerability of people and assets will change in the future.
- Uncertainty about the indirect and intangible damages. Adaptation measures typically aim to also reduce climate change impacts that are not directly translatable to direct economic losses. Also, side-effects (such as benefit, but also damages) can result from the adaptation investment, such as in the case of building a dam that also creates a lake with recreational function and that endangers the ecology of a river trait. Because of their non-trivial monetization, these type of damages and effects are difficult to incorporate into the appraisal, and the results of it are therefore more uncertain.
- Uncertainty about the costs of the adaptation measure(s). This source of uncertainty can be limited when the investment has been formally assessed, and its realization is near in the future, while it can be much larger in case realizations of larges-scale structures/investments are planned for the longer-term future, and/or there is no local experience with the realization.
- Uncertainty about the future economic developments. This type of uncertainty is encapsulated normally in the discussions about which is the best rate that should be used to discount future assets to present values. Large- and local-scale economic predictions are notoriously challenging and necessarily inaccurate, therefore it is good practice to explore the results of the appraisal under a range of discount rates.

1.3.4 Appraisal approaches to address uncertainty

In this section we provide an explanation of the two economic techniques we employed in the two case studies, with more detail than in the descriptions included in Deliverable 6.2.

Cost-Benefit Analysis

Cost-benefit analysis (CBA) is a classical economic method employed for decision-making on investments, and is at present the most sophisticated tool that is used for major budgetary decisions in the Czech Republic, as well as in other countries including USA (Chichilnisky, 2011). The application of this method requires to explicitly determine all costs and benefits, as well as to determine future scenarios that will be assessed. The analysis of adaptation investments associated with hazard events such as floods is characterized by imperfect knowledge on the distribution of future avoided damage (for further discussion, see Deliverable 4.2) and requires the researcher to make several assumptions that may dramatically affect the results, such as adoption of a specific discounting approach.

CBA can be used in the assessment of alternative options in decision and policy-making process. It is particularly important to private investment projects and public programmes that involve large expenditure with high environmental impacts. New investment projects and public spending in flood protection falls within this category.

CBA is one of many tools in economic analysis that can provide valuable information, and thus help in answering the following questions: i) what are the main outcomes of the intended project, ii) are there better ways to achieve these outcomes, and iii) are there better uses for the available resources. By expressing all costs and benefits in monetary terms, CBA is able to aggregate all social costs and benefits of the project over time, and to rank project alternatives in terms of Net Present Value (NPV); and therefore to compare the outcomes to the status quo (development without the project).

The general practice of CBA is characterized by several features. First, all consequences of a project to all individuals of society (i.e., stakeholders) at multiple scales are considered. Second, these costs and benefits are quantified in monetary terms. Third, the project is evaluated to determine if it provides net economic benefits to society. The net social benefits (NSB) are expressed as the social benefits (B) minus the social costs (C), and aggregated over the life span of the project and expressed as NPV:

$$NPV = PV(B) - PV(C)$$

The present value of the stream of benefits, denoted *PV(B)*, is:

$$PV(B) = \sum_{t=0}^{N} \frac{B_t}{(1+s)^t}$$

where Σ (*t*, *n*) is the sum of all the benefits, *B*, incurred at different time periods (from $t = 0$ to the end of the evaluation period *N*), with benefits at each time period (*t*) discounted to the present using the discount rate *s*.

Similarly, C_t denotes the incurred in period *t* for $t = 0, 1, \ldots, n$. Then, the present value of stream of costs, denoted *PV(C)*, is:

$$PV(C) = \sum_{t=0}^{N} \frac{C_t}{(1+s)^t}$$

The net social benefits can then be used to quantitatively rank alternative projects and to test the (economic) efficiency of an intended project. Comparison could be done:

- between a given project and the status quo (or development without the project), or
- between competing alternative projects.

In the first case, one single project is evaluated in order to determine whether it provides net social economic benefit to society. In this case, we should invest in the project if its NPV is positive:

$$NPV = PV(B) - PV(C) > 0$$

In the second case, several project alternatives are compared, and that with the highest NPV is considered the best and should be selected. If no NPV is positive, then the status quo is preferred.

Real Option Analysis

Real Option Analysis **(**ROA) is a decision support tool specifically suited for economic decision making under conditions of uncertainties. It works by assessing the risk associated with implementing investments to which considerable future uncertainties are associated, and was applied in the evaluation of financial options and the transfer of risk on financial markets. The technique was then transferred to the valuation of investments in physical assets, the "real options", that are characterized by future uncertainty of diverse nature. It takes into account the flexibility of the investment over time. It has gained attention in the literature in its application in the domain of investments in adaptation in climate change, as dealt with in WP6, where the flexibility of an adaptation measure refers to the possibility of bringing adjustments in different points in time, such as if new climatic developments/information emerge, and the adaptation can be improved, made more efficient. The technique enables evaluation about the optimal timing of realization, and the evaluation of alternative measures which might ensure more flexibility. The common implementation of the ROA: develops decision trees, defines possible outcomes and indicates probabilities.

In climate change adaptation investments, ROA features along with other approaches, such as adaptive management and iterative decision making. ROA shows advantages as the estimation of information takes place in quantitative and economic terms and first applications. Nevertheless, its usage is limited by its technical complexity and its resource/information requirements. Indeed, one of the main difficulties is the need of probabilistic (or probabilistic-like) information on outcomes. The approach is best used for investments which have large upfront costs and are irreversible, such as dikes, which are flexible in timing and for which relevant new information may emerge in the years after initial realization. The technique tends to support measures or investment options which have short-term benefits and the flexibility to be adjusted in the future.

In the Bilbao case study below, ROA has been used to determine the value of the option to postpone the investment or to "wait" with the investment. Postponing a climate adaptation investment, may have the benefit that (some) uncertainty about future climate change may be resolved over time and therefore maladaptation may be avoided. The cost of postponing is that early benefits of adaptation are foregone. If the benefits of reduced uncertainty exceed the cost of foregone short-term adaptation benefits, then ROA would advise to "wait" with the investment. If the benefits of waiting do not exceed the costs (the foregone benefits) and if the standard Net Present Value of the project is positive, then there is no reason to wait and from an economic point of view the project should be executed immediately. In the Bilbao case study below, we will see the standard NPV of the adaptation project is positive and that the benefits of waiting do not exceed the costs (the foregone benefits), so that the economic advise would be to execute the project immediately.

2 Costs and benefits of adaptation – The Vltava case study

In the following sections we outline the details of the final methodology adopted, and the results of the quantification of benefits and cost of the measures, with inclusion of uncertainties. In section 2.1 we recap on the adaptation investment that is analysed, and on its costs. Appraisal methods and results are reported in sections 2.2 and 2.3 for the several steps of the assessment in separate sections: the obtainment of climate data, the hydrological modeling, the modeling of avoided damage and risk. In turn, these results will constitute the input to the economic CBA.

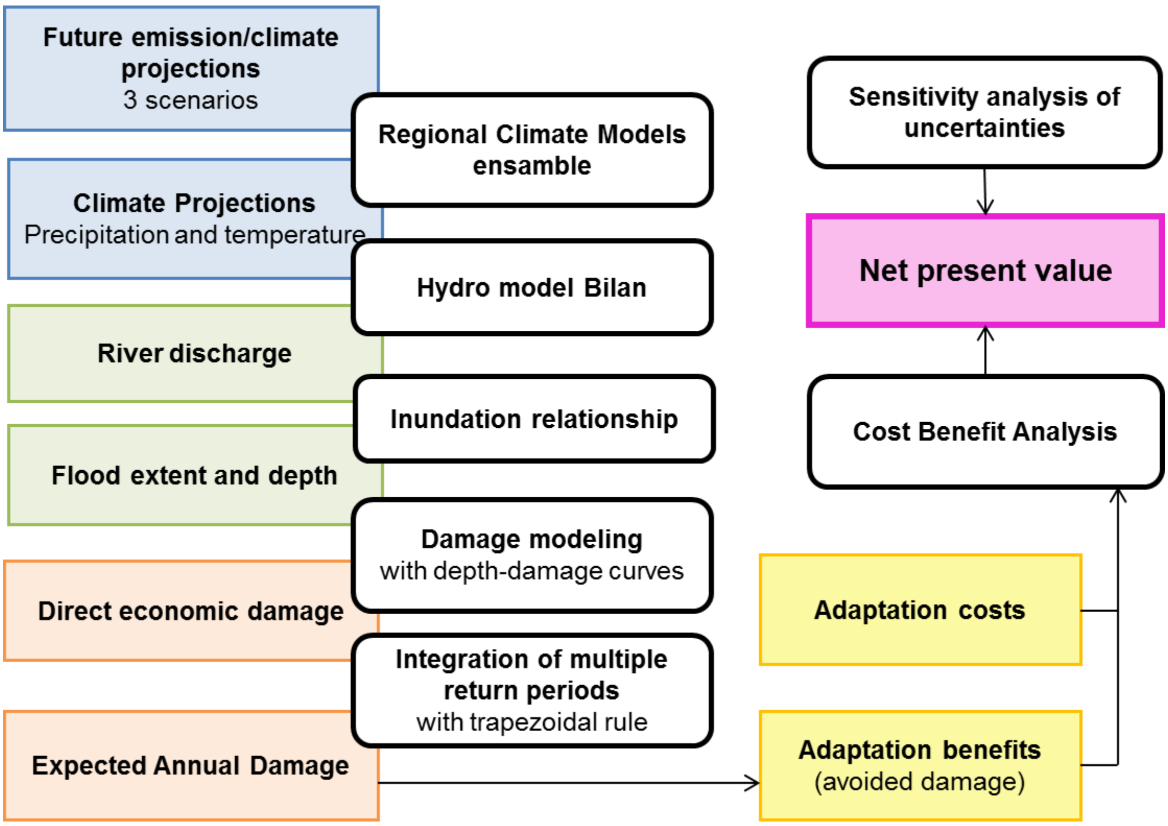

Fig. 2. Methodological framework of the appraisal of adaptation investments in the Vltava case study. Coloured square boxes indicate datasets, rounded empty boxes indicate models and methods.

2.1 Summary of the adaptation investment analyzed and of its costs

The scope of the study is to assess ex-post the implementation of the Prague flood protection measures that have been carried out in the period 1999 to 2014. The project represents one of the largest adaptation investments in the Vltava river basin, totalling ca. 256 M €, and unlike other investments into flood protection in the basin (see Deliverable 6.1), it has substantial effect on flood mitigation and will likely avoid flood damage into the far future.

The flood protection project consists of several types of measures: line measures (i.e., fixed anti-flood earth dikes, reinforced concrete walls, mobile barriers etc.) and barriers in the waste-water system (i.e., backflow preventors etc.).

The project was subdivided in several stages, reflecting the realization of flood protection measures in particular districts of Prague, as listed in the following Table 1.

Table 1. Overview on the stage of the flood protection project in Prague (data: City Hall of Prague, 2015).

Stage	District
1	Old Town and Josefov
2	Lesser Town and Kampa
3	Karlín and Libeň
4	Holešovice and Stromovka
5	Výtoň, Podolí and Smíchov
6a	Zbraslav and Radotín
6b	Chuchle
7	Troja
8	Modřany
10	Mobile measures
11	The other watercourses

Before the initialization of the flood protection project in Prague, the flood protection could cope with a 10-year flood only. That is due to the fact that during the 20th century flood events have been very scarce in Prague and in the whole country, in comparison with the high-flood risk that characterizes the history of the low Vltava basin (Elleder, 2015). The largest flood event during the whole century was a 50-year flood in year 1940 (TGM WRI, 2009). Due to the infrequency of extreme flood events for such a long period, the flood protection of the city of Prague has not been designed until year 1997, when a catastrophic flood event occurred in another part of the country. The urgency of proper flood protection raised interest in the flood protection in the whole country and also in Prague, the complex project of flood protection on Vltava and Berounka rivers has been prepared in 1997. The aim of the flood protection project in Prague was to resist a 100-year flood, defined using the runoff the of last catastrophic flood in Prague in year 1890, when the runoff amounted to 4030 m^3/s (City Hall of Prague, 1997). In 2002, Prague experienced a catastrophic flood of even larger scale (runoff of 5300 m^3/s) and subsequently, the flood protection project of Prague has been redesigned to manage the level of flood in year 2002, plus a freeboard of 30 cm (City Hall of Prague, 2002).

The project finished in year 2014 (PIPD, 2014). Even after the realization of the project, some areas in the north and south of Prague, for which the cost of reaching the protection against catastrophic flood of year 2002 would exceed severalfold the value of the exposed (private and public/municipal), remained unprotected. Also in the city centre, there are several objects that are located outside the line measures, because it was not technically feasible to cover them in the enhanced flood protection project of year 2002. As follows, while for most of Prague the flood protection is relatively high, in case of even relatively small floods some of the districts experience flood damages.

Costs

The investment costs are summarized in Table 2. The data are recalculated to € 2015 using EU HICP deflator and PPP exchange rate. The majority of the costs were paid by the City Authority of Prague, which has received a state subsidies covering 37.3 M €, about 15% of the 256 M € total cost.

Apart from the investment costs, the City Authority of Prague covers yearly also the operating costs, such as the storage of mobile barriers, the maintenance, testing, revisions and reparation of the mobile measures, installed immobile flood walls and terrain adjustments, adjustments of the sewerage system etc. The estimate of yearly operating costs is about 0.23-0.45 M €. However, the estimation is characterized by a large uncertainty, due to the fact that most of the flood protection measures has been until recently under the warranty provided by the constructors, and have not been budgeted yet by the City Authority of Prague.

Further, “one-off” costs are associated with the individual flood events. These are due to the launching the flood protection into operation, installation of the mobile barriers, allocation of the water pumps and all associated transport. The procedure is based on the schedule of flood protection construction by the City Authority of Prague, which has several stages that depend on the observed runoff. The estimate of the one-off costs by the City Authority of Prague is 0.34-0.7 M € for flood events of at least 50-year return period.

Table 2: Investment cost on the flood protection in Prague (in thousand €). Source: City Authority of Prague.

No. and stage / Year	**1997**	**1998**	**1999**	**2000**	**2001**	**2002**	**2003**	**2004**	**2005**	**2006**	**2007**	**2008**	**2009**	**2010**	**2011**	**2012**	**2013**	**2014**	**Total**
1 - Old Town and Josefov	.	.	1920	1593	28	2	4		4	4									**3,554**
2 - Lesser Town and Kampa	.	.	83	109	59	1366	3031	14348	2190	243	120	118	8					13	**21,688**
3 - Karlín and Libeň	.	.		48		1	391	11195	25989	7251	926	99		13	730	1258	2	14	**47,917**
4 - Holešovice and Stromovka	.	.		39	10	57	502	5754	17248	19884	42	86	3			10	0	4	**43,638**
5 - Výtoň, Podolí and Smíchov	.	.			39	5	234	2039	1616	30	2							0	**3,965**
6 – Zbraslav, Radotín, Chuchle	.	.			79	3	199	378	367	329	727	4705	36858	15801	965	8934	1992	1101	**72,437**
7 - Troja	.	.			63	39	125	788	1195	635	4435	494	19046	7665	5522	184	287	339	**40,819**
8 - Modřany	.	.					148	4437	12246	2646	106	129	24	5					**19,741**
10 – Mobile measures	.	.											7	2481	20				**2,509**
11 - The other watercourses	.	.														82	12	27	**121**
Total	**8**	**89**	**2003**	**1789**	**278**	**1473**	**4635**	**38939**	**60853**	**31022**	**6358**	**5631**	**55945**	**25966**	**7238**	**10468**	**2293**	**1497**	**256,485**

2.2 Benefits of adaptation and associated uncertainties

2.2.1 Climate data

As the occurrence of floods inherently depends on the climate of the catchment area, present and future climate data represent the first input into the analysis of investments on protection from flooding. Simulation of future climate at the regional and local scale is based on regional climate models (RCMs). For the simulation of future hydrological regime in the Vltava river basin, i.e., river runoff, datasets from climate models were selected and provided by the Danish Meteorological Institute, also partner in ECONADAPT. Namely, daily time series of precipitation and temperature, until year 2100, were acquired from 14 simulation sets from the WCRP CORDEX database[2] (see also Jacob *et al.*, 2014). These simulations were run with greenhouse forcing boundary conditions based on the Representative Concentration Pathway (RCP) scenarios RCP4.5 and RCP8.5 (see Table 3). As a test exercise, to test the sensitivity of the hydrological system to a wider range of climate scenarios, one RCM was also run for scenario RCP2.6. This set of models is considered by the Danish Meteorological Institute to approximate the variability in the potential evolution of climate. Since this model selection does not cover the entire possible range of emission scenarios, nor the range of global model results, we cannot expect the full variability to be represented; it is, however, considered to include a large part of this variability.

Table 3: Overview of employed regional climate models (simulation sets) and climate scenarios.

	Future climate scenarios		
Regional climate models and simulation sets	**RCP2.6**	**RCP4.5**	**RCP8.5**
CNRM-CERFACS-CNRM-CM5_r1i1p1_CLMcom-CCLM4-8-17		x	x
CNRM-CERFACS-CNRM-CM5_r1i1p1_CNRM-ALADIN53		x	x
CNRM-CERFACS-CNRM-CM5_r1i1p1_SMHI-RCA4		x	x
ICHEC-EC-EARTH_r1i1p1_KNMI-RACMO22E		x	x
ICHEC-EC-EARTH_r3i1p1_DMI-HIRHAM5		x	x
ICHEC-EC-EARTH_r12i1p1_CLMcom-CCLM4-8-17		x	x
ICHEC-EC-EARTH_r12i1p1_SMHI-RCA4	x	x	x
IPSL-IPSL-CM5A-MR_r1i1p1_IPSL-INERIS-WRF331F		x	x
IPSL-IPSL-CM5A-MR_r1i1p1_SMHI-RCA4		x	x
MOHC-HadGEM2-ES_r1i1p1_CLMcom-CCLM4-8-17		x	x
MOHC-HadGEM2-ES_r1i1p1_KNMI-RACMO22E		x	x
MOHC-HadGEM2-ES_r1i1p1_SMHI-RCA4		x	x
MPI-M-MPI-ESM-LR_r1i1p1_CLMcom-CCLM4-8-17		x	x
MPI-M-MPI-ESM-LR_r1i1p1_SMHI-RCA4		x	x

The climate datasets were obtained for the whole Vltava river basin, in the native model grid resolution of 12 km. All simulations have been run for years 1970-2010. The simulated data for period 1970-2000 has been used further by the T. G. Masaryk Water Management Institute (TGM WRI) as a baseline for bias-correction of the model climate dataset, prior to inclusion in the hydrological modeling.

The climate projections of two climate parameters, precipitation and temperature, considered further in the hydrological modeling are summarized in Table 4. Both mean annual values for

[2] http://www.cordex.org

the period representing current climate (historical projections of 1970-2005), and future climate (2006-2100) are presented here for each RCP and simulation set.

Table 4. Mean annual values of precipitation (pr; in mm/day) and temperature (temp; °C) in the Vltava river basin.

Regional climate models and simulation sets	Historical projections (1970-2005)		Future climate simulations (2006-2100) per scenario					
			RCP2.6		RCP4.5		RCP8.5	
	pr	temp	pr	temp	pr	temp	pr	temp
CNRM-CERFACS-CNRM-CM5_CLMcom-CCLM4-8-17	2.2	7.9			2.3	9.0	2.4	9.5
CNRM-CERFACS-CNRM-CM5_CNRM-ALADIN53	2.3	7.1			2.6	7.9	2.7	8.5
CNRM-CERFACS-CNRM-CM5_SMHI-RCA4	2.4	7.6			2.5	9.1	2.6	9.6
ICHEC-EC-EARTH_KNMI-RACMO22E	2.0	6.7			2.0	8.1	2.1	8.9
ICHEC-EC-EARTH_DMI-HIRHAM5	2.4	7.8			2.5	9.2	2.5	9.9
ICHEC-EC-EARTH_CLMcom-CCLM4-8-17	2.1	7.8			2.2	9.1	2.2	9.8
ICHEC-EC-EARTH_SMHI-RCA4	2.2	7.2	2.3	8.3	2.3	8.9	2.3	9.7
IPSL-IPSL-CM5A-MR_IPSL-INERIS-WRF331F	2.7	8.1			2.9	9.9	3.1	10.5
IPSL-IPSL-CM5A-MR_SMHI-RCA4	2.5	7.9			2.6	9.8	2.7	10.6
MOHC-HadGEM2-ES_CLMcom-CCLM4-8-17	1.9	8.9			2.0	11.2	2.0	12.1
MOHC-HadGEM2-ES_KNMI-RACMO22E	1.9	9.3			2.1	11.7	2.1	12.7
MOHC-HadGEM2-ES_SMHI-RCA4	2.2	8.6			2.4	10.8	2.4	11.7
MPI-M-MPI-ESM-LR_CLMcom-CCLM4-8-17	2.6	8.3			2.7	9.2	2.7	10.1
MPI-M-MPI-ESM-LR_SMHI-RCA4	2.5	8.7			2.6	10.0	2.7	10.8

Projected changes of mean annual values (2006-2100 minus 1970-2005) of simulated climate variables express the difference between future and current climate conditions, and are reported in Table 5.

Table 5. Mean percentage changes by year 2100 (with respect to historical baseline) in annual values of daily precipitation (pr; in mm/day) and temperature (temp; °C) in the Vltava river basin.

Regional climate models and simulation sets	RCP2.6		RCP4.5		RCP8.5	
	pr	temp	pr	temp	pr	temp
CNRM-CERFACS-CNRM-CM5_CLMcom-CCLM4-8-17			6.3	14.0	9.5	19.8
CNRM-CERFACS-CNRM-CM5_CNRM-ALADIN53			13.7	11.0	19.5	19.7
CNRM-CERFACS-CNRM-CM5_SMHI-RCA4			4.7	19.6	11.2	26.6
ICHEC-EC-EARTH_KNMI-RACMO22E			2.9	21.1	6.3	33.3
ICHEC-EC-EARTH_DMI-HIRHAM5			3.4	18.3	5.7	28.2
ICHEC-EC-EARTH_CLMcom-CCLM4-8-17			4.6	16.0	5.1	25.4
ICHEC-EC-EARTH_SMHI-RCA4	3.5	15.2	5.6	23.8	5.8	35.5
IPSL-IPSL-CM5A-MR_IPSL-INERIS-WRF331F			9.5	22.4	18.6	30.2
IPSL-IPSL-CM5A-MR_SMHI-RCA4			7.2	24.3	10.1	35.0
MOHC-HadGEM2-ES_CLMcom-CCLM4-8-17			4.9	26.7	6.2	36.4
MOHC-HadGEM2-ES_KNMI-RACMO22E			10.9	26.7	12.3	37.0
MOHC-HadGEM2-ES_SMHI-RCA4			9.1	25.3	9.7	35.4
MPI-M-MPI-ESM-LR_CLMcom-CCLM4-8-17			6.2	10.7	6.3	21.0
MPI-M-MPI-ESM-LR_SMHI-RCA4			5.8	14.8	7.7	24.4
Average annual change	**3.5**	**15.2**	**6.8**	**19.6**	**9.6**	**29.1**

2.2.2 Hydrological modeling

The runoff of the Vltava river in Prague until year 2100 was predicted by TGM WRI using the simulations of climate variables. As the first step, TGM WRI performed the bias correction of raw climate data provided by the Danish Meteorological Institute. In this step the climate input data provided by regional climate models are corrected for systematic deviations from observational data. The data used by TGM WRI to model the impact of climate change on the hydrological regime include the climatological simulations explained above and data on observed precipitation extremes for the baseline period, provided by the Czech Hydrometeorological Institute.

For the simulation of changes in maximum runoffs, the hydrological model Bilan, run by TGM WRI (TGM WRI, 2015), was used. The input to the model was the bias-corrected time series of precipitation and temperature for period 1970-2100 from the above-mentioned regional models. The changes in extreme runoffs were further assessed using a non-stationary model of extremes (Hanel et al., 2009). For the assessment of the reliability of the estimates of maxima of higher return periods, a stochastic generator of climatologic data, a precipitation generator, that is based on an vector autoregressive model was employed, RMAWGEN (Hanel and Vizina, 2015). For the period 1970-2000, the changes in the flood extent of 5, 20, 50, 100, 250 and 500-year return period were estimated. The analysis was done under the assumption that the derived relationship between (extreme) precipitation and (extreme) runoff holds also under changed climate conditions. The runoff has been calculated at the water gauging profile in Malá Chuchle, where the Vltava enters urban Prague.

For the flood simulations, hydraulic modelling was not employed, and most of the uncertainty associated with it (see chapter 1.3.2) could not be addressed. The study is rather based on a simplified approach that utilizes the observed relationship between runoff and flood extent, and the extrapolation of available data on flood extents of several return periods of flood. The simulation of changes in maximum runoff and flood extent in Prague was done by interpolating of available data on flood extents of return periods of 5-, 20- and 100-years and of the maximal historical flood of August 2002 (the return period of the last mentioned flood has been assessed as 500-year flood by TGM WRI and CHMI, 2003). The flood extent data come from the DIBAVOD database (www.dibavod.cz) and has been interpolated between 141 flood extents, ranging from 1.5-year to 500-year period.

The outputs of the hydrological modelling, the discharge and water level at the Malá Chuchle gauge, were converted by TGM WRI into flood extent and depth based on a digital terrain model. The total 141 floods from the database were modelled. Also, for climatological data produced by particular regional climatological models and for each RCP scenario, several time series on the occurrence of N-year period floods were predicted.

In the Vltava case study, uncertainties mostly refer to the climate datasets used. The output of the hydrological modelling, concerning the impact of climate change on the maximum runoffs in the Vltava river at Malá Chuchle water gauging profile for six return periods are summarized in Figure 3 and 4. Figure 3 illustrates how the uncertainties in climate conditions modelled by respective RCM are reflected in the hydrological modelling: large differences exist among the predicted maximum runoffs for each RCM simulation are apparent and (as may be expected) increase with the horizon of the prediction. The changes according to particular simulations are between -60% to +350%, the average values for the sets of models and the respective RCP scenarios are much less varying from the original values in the base year 1985.

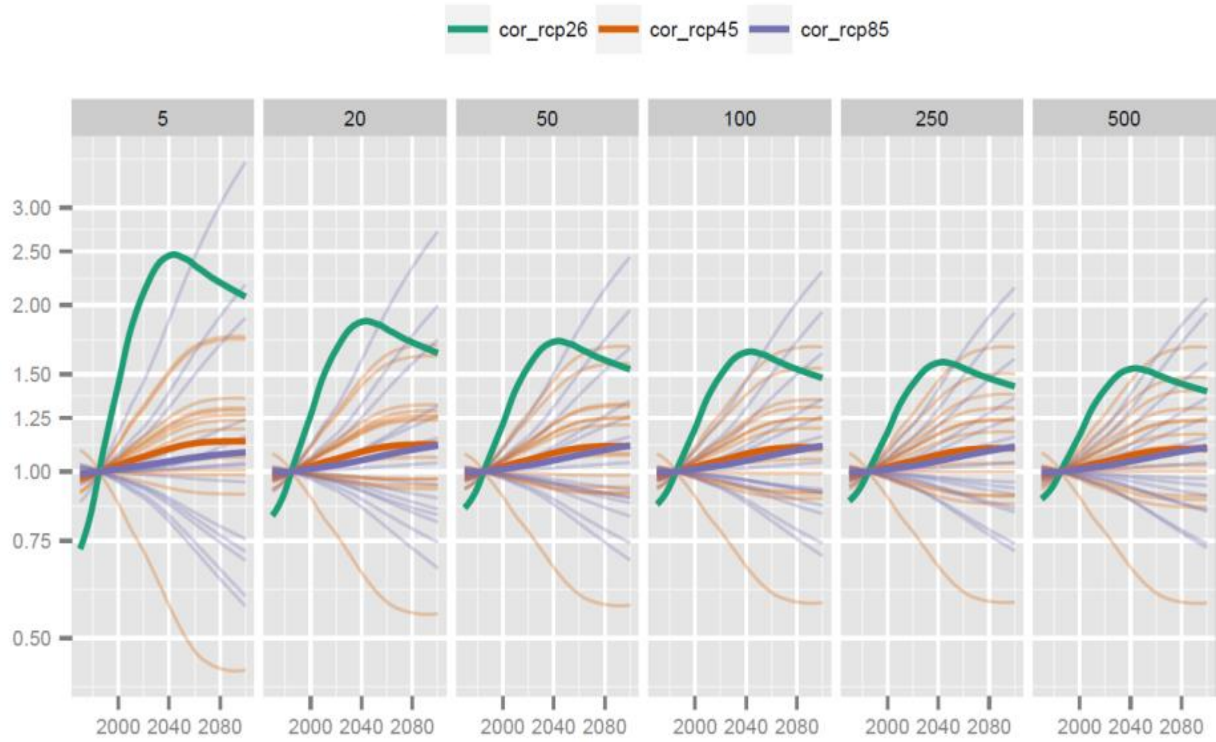

Figure 3: Relative changes (in factor units) of the maximum runoffs, simulated with data from the ensemble of RCMs, for the assessed period (thin lines represent individual RCMs, and bold lines the average for each RCP scenario) and for floods of six return periods (5- to 500-year), compared to base year 1985. Source: Hanel and Vizina (2015), produced for ECONADAPT.

As it can be seen from the comparison of Figures 3 and 4, while large relative variations in the maximum runoff for the short return period floods do not entail important changes in the absolute discharge values, even small relative changes imply massive absolute increases in the discharge of rarer events. The most serious scenario of climate change, RCP8.5, is related to larger increases in discharge than RCP4.5. For the mildest scenario of climate change, RCP2.6, the increases in discharge at the considered gauge station are unexpectedly even higher than for the other two. However, the RCP2.6 scenario is here represented by only one model simulation, which prevents drawing conclusions on its outcome.

In the modelled hydrologic data, extreme events such as 1000-year and even 5000-year floods are present. According to the climate data availability on baseline for a 30-year period (1970-2000), the estimation of runoffs for floods greater than the 100-year event are associated with excessive uncertainty and TGM WRI advises to exclude 500-year events and greater from the modelling of economic impacts.

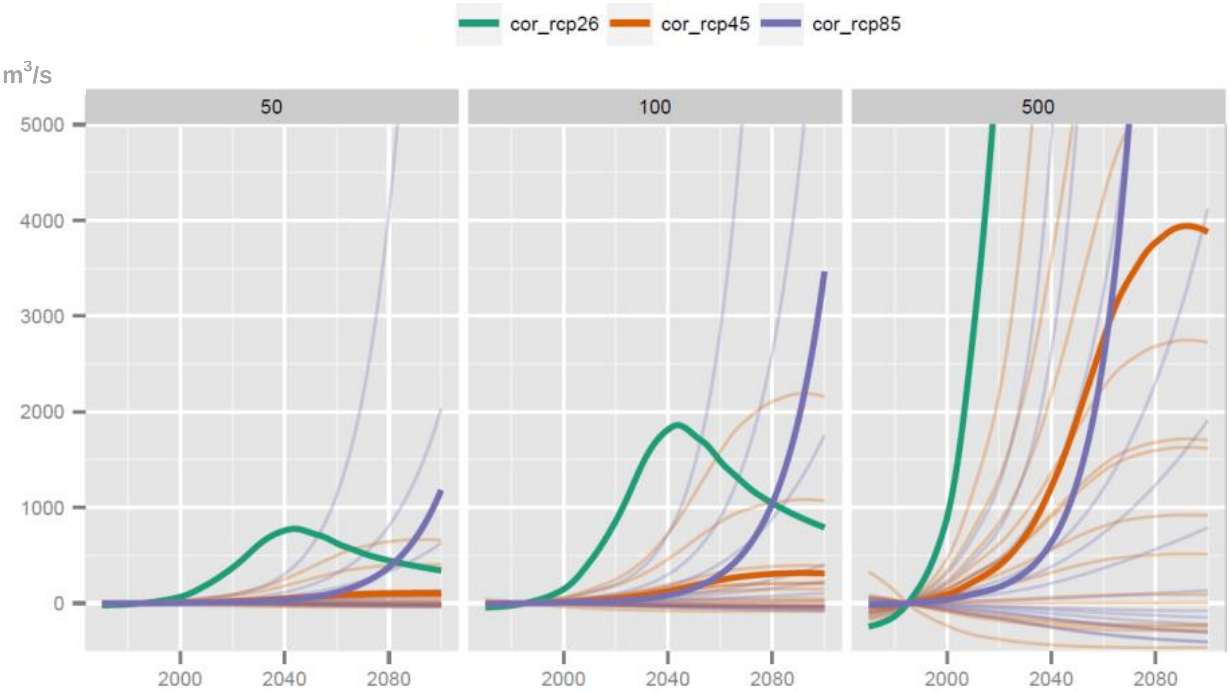

Figure 4: Changes in maximum runoffs for the assessed period (in m^3/s). Thin lines represent individual RCMs, and bold lines the average for each RCP scenario) and three selected return periods of floods. Data are normalized such that the present runoff of the N-year flood is 0. Source: Hanel and Vizina (2015), produced for ECONADAPT.

Uncertainty in the input data is reflected also in the water depth results, that have been estimated using a digital elevation model for interpolated flood extents. As the analysis is based on a statistical relationship and a more advanced hydrodynamic model has not been used, the uncertainties associated with the water depth data are large. The water depth data represent an input into modelling of economic damage on buildings. However, we cannot count on more reliable estimates from hydrodynamic modeling, and this source of uncertainty remains therefore unquantified.

Another category of uncertainty in the hydrological modelling is associated with the model fit used to obtain the extreme values. In the case study, the maximum runoffs and precipitation were obtained with the use of a generalized extreme value distribution (Hanel et al., 2009). Two models have been tested: a model with constant shape parameter, and a full nonstationary model with varying shape parameter. The fit between modeled and observed values is high, as figure 5 shows, and it is equivalent for the two models, therefore the simpler model with constant shape parameter was adopted. The figure shows that for large floods with large discharge heights, there are fewer observations and for this range the quality of the fit decreases, with the model systematically underestimating the observed discharge heights; while for floods with lower discharge heights, the model predicts with higher accuracy, which is in line with the recommendations of TGM WRI to use a cut-off for very large floods for which the fit is not satisfactory. The effect of the hydrological modelling uncertainty on the results may be estimated using the whole predicted scope of return periods and compare it to the results using a cut-off.

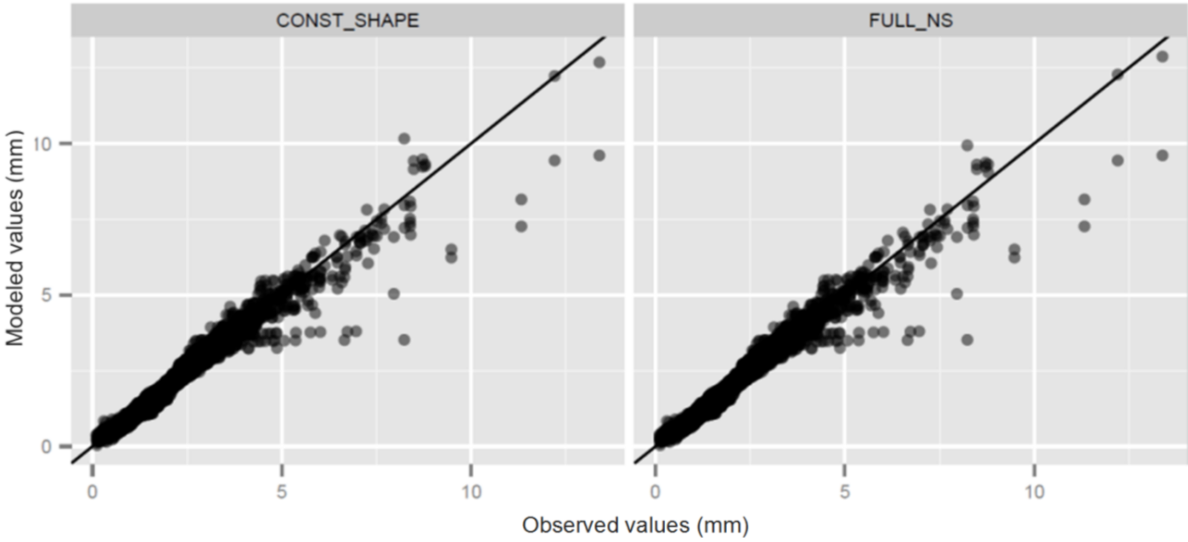

Figure 5: Comparison of observed vs. modeled values of maximum discharge heights (mm) for two considered models, with constant shape parameter (CONST_SHAPE) and with full nonstationary shape parameter (FULL_NS). Source: Hanel and Vizina (2015), produced for ECONADAPT.

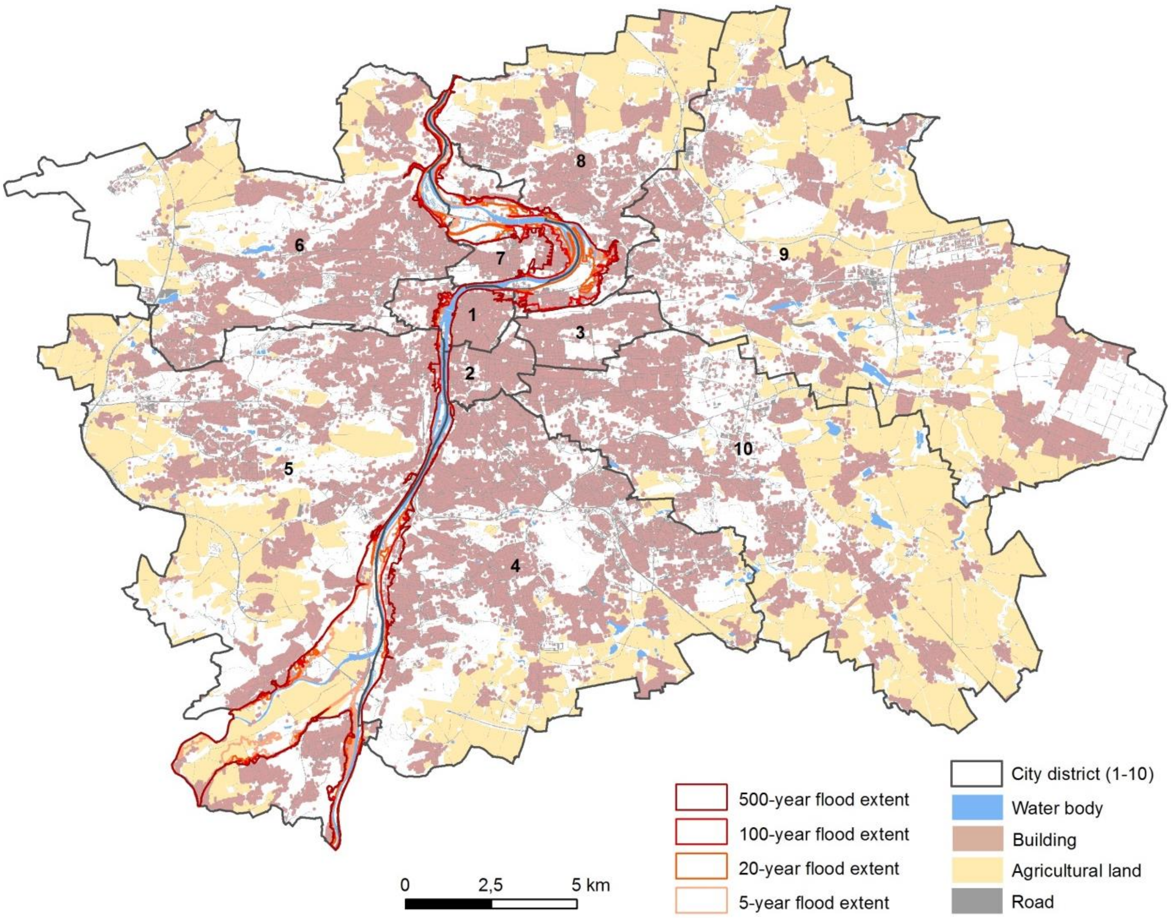

Figure 6: Floodplain areas in Prague for selected return periods and distribution of main assets under risk. Source: PIPD (2013), CZSO (2011), DIBAVOD database (2014; www.dibavod.cz).

2.2.3 Damage and risk modeling

In the phase of the damage modelling, it is first necessary to determine the boundaries of the system for the damage calculation and for the cost-benefit analysis. For the Vltava case study, the investment in flood protection in Prague affects not only the Prague region, but it is possible that the enhanced protection of Prague alters the behaviour of floods (velocity, extent etc.) also in the areas downstream of Prague. Also, the flood protection in Prague affects functioning of essential services such as transport during a major flood event, from which not only Prague itself, but surrounding region may benefit. However, the majority of the investment cost has been paid from the budget of the City Hall of Prague, and it is supposed that most of the effects of the flood protection are within the boundaries of Prague. For the sake of simplicity therefore, the geographic boundaries of the study correspond with the city of Prague proper.

Flood damage definition

The flood damage comprises several categories of damage and the results of the cost-benefit analysis may depend heavily on which categories of damage are or are not covered within the study. The flood damage may be split into the categories tangible and intangible, and direct and indirect (based on Foudi et al., 2015; Table 6):

Table 6: Categories of flood damage, based on the distinctions of Foudi et al. (2015).

Damage categories	Direct	Indirect
Tangible	• damage to property, to stocks, to capital for production • damage to buildings - housing and commerce (including equipment) • damage to infrastructure (roads, underground services, irrigation systems etc.) • damage on hydraulic structure and water management measures • damage to agricultural production and cattle • cleaning costs	• disruption of the consumption of flows of goods and services (transport, supply of intermediate goods for production, supply of public services and electricity, water etc.)
Intangible	• loss of life • injuries • health • damage to cultural heritage • damage to ecosystems • recreation loss	• post-traumatic stress • trust in public interventions • modification of preferences • risk perception and acquisition of experience in flood prevention

Direct and tangible flood damage is the only damage that is reported by public authorities after major floods in the Czech Republic (TGM WRI, 2002, 2009; CHMI, 2013) and that is taken into account in budgetary decisions on flood protection in the country. On the other hand, research on socio-economic impacts of floods usually considers also the other categories of damage listed above.

The uncertainties on the assessment of damage differ by category, and generally the direct tangible damage is most easily estimated; and it is also the only category where the assessment of damage by modelling may be compared to reported data (Merz et al., 2010). For the other categories of damage, the estimates are based on non-market valuation techniques and concepts of willingness to pay (for safety) and willingness to accept (damage), and on the value of statistical life. In the absence of local studies, the estimated value function may be transferred from the literature (e.g., Brouwer and van Ek, 2004). The uncertainty of the estimated measures of utility (willingness to pay, willingness to accept) or the value of statistical life may be measured using the distribution of the estimate from a primary study. Transfer of values from the literature adds to the uncertainty about the estimate itself also the uncertainty associated with value transfer in time and space, as the original estimates are dependent on the socio-economic context of the original study. Foudi et al. (2015) for example uses a value function transfer.

The following types of flood damages have been estimated for the Vltava case study:

- Damage to immovable:
    - buildings (housing, commerce and public sector)
    - infrastructure (roads)
- Loss of agricultural production

Method of damage assessment

The expected annual damage (EAD) that is avoided by the adaptation measures serves as welfare measure of socioeconomic benefits attributed to the investment. EAD is calculated from an exceedance probability loss curve which represents a relationship between different levels of flood damage of a particular return period and the corresponding probabilities of flood events.

As outlined in chapter 2.2, potential flood damage for each of the 141 return periods (from 1.5 to 500-year recurrence interval) was calculated for several asset categories – buildings, road infrastructure and crops – using GIS-interpolated inundation extents, inundation depths and depth-damage functions. For each of the 141 return periods *e* (1 to 141), the total damage to buildings, D_{build}, because of heterogeneity in property structure and usage, was calculated for different categories of buildings following Li et al. (2016):

$$D_{build(e)} = \sum_{i=1}^{m} \sum_{j=1}^{n} f_{DR}(w) \cdot A_{ij} \cdot F_{ij} \cdot P_i$$

where *m* represents the number of building categories, *n* is the total number of buildings in a given building category *m*, f_{DR} represents the depth-damage function linking the water depth *w* to the relative damage on flood-exposed buildings, A_{ij} is the floor area of building *j* and category *i*, F_{ij} is the number of floors of building *j* and category *i*, and P_i is the price of 1 m^2 of floor of building category *i*.

Total flood damage to road infrastructure, D_{road}, for return periods *e*, is not supposed to be dependent on water depth and was calculated for each return period as follows:

$$D_{road(e)} = \sum_{i=1}^{n} DR \cdot A_i \cdot P_{road}$$

where *n* is the number of road segments exposed to a given flood, *DR* represents the damage ratio for road infrastructure, A_i is the surface area of road segment *i* and P_{road} is the price of 1 m^2 of road infrastructure.

Flood damage to agricultural crops, D_{crop}, is also assumed independent from the inundation depth and is calculated as follows:

$$D_{crop(e)} = \sum_{i=1}^{n} P_{crop} \cdot A_i$$

where n is the number of agricultural land exposed to a given flood event e, A_i is their corresponding surface area, P_{crop} represents unit crop damage and is calculated as average costs of growing plants weighted by their sowing area in Prague:

$$P_{crop(e)} = \frac{\sum_{j=1}^{m} C_j \cdot SA_j \cdot DR_j}{\sum_{j=1}^{m} SA_j}$$

where m is the number of plants, C_j represents the costs of planting a given plant j, SA_j is a sowing area of plant j in Prague and DR_j is the damage ratio for plant j.

The total value of flood damage for a given return period e is calculated as the sum of damages of the analyzed categories:

$$D_{total(e)} = D_{build(e)} + D_{road(e)} + D_{crop(e)}$$

According to Saint-Geours et al. (2014), EAD [€/year] is an indicator that measures potential flood damage over a certain level of floodplain inundation. The EAD is defined as the expectation of flood damage *D(e)* over a vector of possible flood events (*e*) with respective return period. EAD is expressed as integral:

$$EAD = \int_0^1 D(f)df$$

where f is the annual exceedance frequency of flood event e_i.

Several different methods for numerical integration are available. A simple trapezoidal rule, which approximates this integral from the range of flood events with corresponding annual exceedance frequencies and flood damages, is often used. The trapezoidal rule, which we applied for EAD estimation, could be expressed using following equation (Olsen et al., 2015):

$$EAD = \frac{1}{2}\sum_{i=1}^{n}\left(\frac{1}{RP_i} - \frac{1}{RP_{i+1}}\right)(D_i + D_{i+1})$$

where RP_i is a given return period, n represents a number of return periods chosen, so that all relevant RPs are covered, from frequent floods with limited damage to exceptional floods with catastrophic consequences. We tested the EAD estimation on parameter n with $n = 6$ and $n = 141$, to potentially provide recommendations on the value added of considering a very large amount of flood damage observations.

The purpose of this study is to compare the economic efficiency of the adaptation measure to the *status quo* situation (without the adaptation measure). Therefore, our key result is the avoided EAD resulting from the investments with respect to the *status quo*, which can be defined as:

$$\Delta B = \Delta EAD = EAD_{adapt} - EAD_{sq}$$

where ΔB represents socioeconomic benefits of the adaptation, and EAD_{sq} and EAD_{adapt} indicate the EAD of the *status-quo* and with the adaptation, respectively. The distribution of assets under risk within four selected return periods of flood is depicted in Figure 6.

For the damage modelling of direct tangible damage, we adopt the approach of expected annual damage, which relates the flood damage to the probability of flood (Arnell, 1989). Two approaches are common: either data on reported damage on several historical floods is assessed and extrapolated, or (more frequently) an exposure assessment and vulnerability assessment of assets under risk is done for several return periods using geographic data.

None of the two approaches is ideal. The historic/actual flood damage data depend on the actual characteristics and flood factors of the respective flood (velocity, awareness of people, month of occurence etc.) and for two floods of the same return period in the same area, the damage may differ vastly. This is true especially for data on smaller floods (Downtown and Pielke, 2005).

The modelling of flood damage is done under simplifying assumptions and the models do not account for all specific damage-influencing factors, such as contamination, damage-reducing measures on particular buildings (enhanced materials etc.), temporal variability of the vulnerability of assets within a year, etc. The flood damage was estimated using spatial data on the location of assets exposed to flooding in Prague, based on the methodology of flood risk assessment by TGM WRI (2009).

The data on exposed assets was provided by the Prague Institute of Planning and Development (PIPD, 2013) in geographic layer on technical use of the area and include data on buildings, infrastructure and land use. The data on buildings was supplemented by detailed data by the Czech Statistical Office from the 2011 census of “Counting of people, houses and flats”, which occurs every 10 years. The data describe the use of the building (whether the main use is housing, commerce or public sector), the number of floors and other relevant characteristics. Further, the outputs from hydrological modelling: projected flood extents and water depths for N-year return period floods have been employed for the damage modelling.

Damage on buildings

The estimation of damage on buildings applies depth-damage function for buildings and introduces minimum and maximum percent damage for 0-10 m of water depth (see Figure 7). From 10 m of water depth on, the damage on buildings is assumed not to grow further.

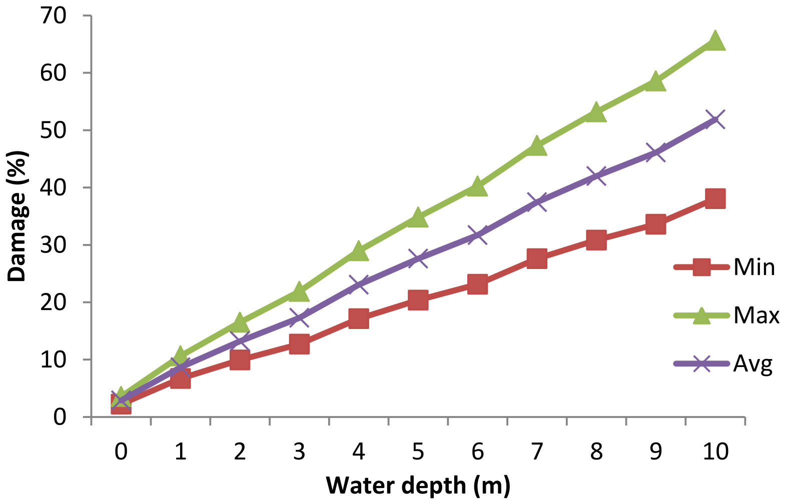

Figure 7: Depth-damage functions for buildings in the Czech Republic. Source: Data based on TGM WRI (2009).

There exist an uncertainty on the shape of the depth-damage function. The above estimate has been done using pooled detailed data on flood damage from several localities in the Czech Republic (not directly in Prague), including towns and municipalities (Horský, 2008). Another depth-damage function in the Czech Republic has been estimated by the Morava River Basin Management, s. e. for several categories of built-up areas (Arcadis, 2004). There exist also foreign estimates of depth-damage functions (e.g. Dutta et al., 2003; Penning-Rowsell et al., 2005; Thieken et al., 2008; Ward et al., 2011; Lasage et al., 2014; Koks et al., 2015) for different types of buildings - some estimates vary by building use or building material, other are general. de Moel et al. (2016) have set up a global database of damage functions, specific for regions and for land-use. Mostly, unlike the results suggested by TGM WRI (2009), the shape is concave. Also, the TGM WRI (2009) study brings relatively conservative (low) estimates of percentage damage on buildings compared to the other studies. Figure 7 and Figure 8 show for comparison the depth-damage functions from the Czech study by Arcadis (2004). A sensitivity analysis of the damage estimates to the depth-damage function employed would reveal the impact of the choice of depth-damage function on the CBA results; however, it is not inspected within this case study.

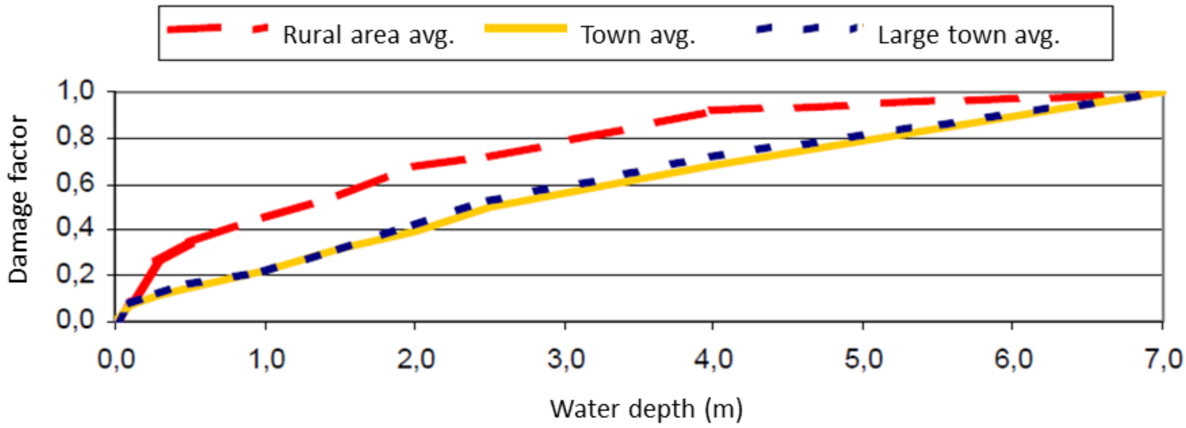

Figure 8: Depth-damage functions - built-up areas. Source: Arcadis (2004).

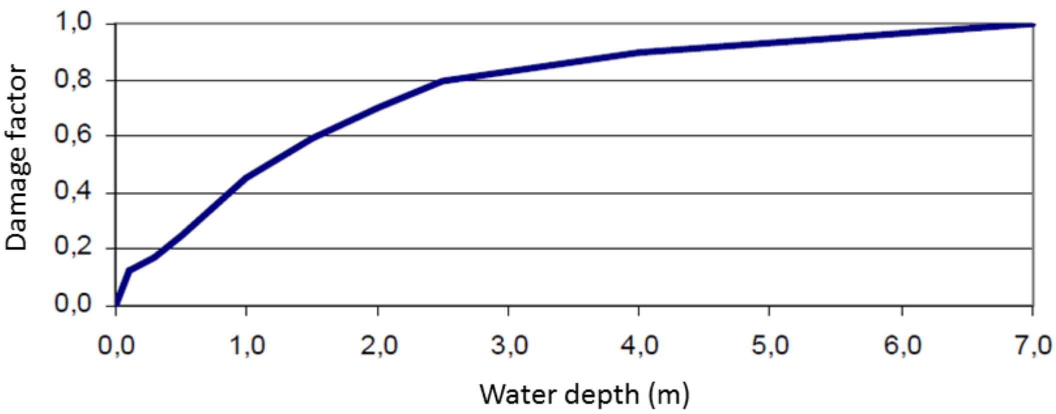

Figure 9: Depth-damage function - industrial areas. Source: Arcadis (2004).

The value of buildings has been estimated according to the TGM WRI (2009) methodology, using actualised prices per square meter of respective type of building published by the

Czech construction standards (2015) and recalculated to € using PPP exchange rate (Table 7).

Table 7: Prices per square meter by type of building (€ 2015). Source: Own calculations based on Czech construction standards (2015) and TGM WRI (2009).

Building type	**Price of 1 floor (€/m^2)**
Buidling for industrial production, energy production and storehouses	1 005
Building for animal farming, plant growing,adjustment and storage of crop farming and animal farming, greenhouse	750
Buildings for housing	831
Building for purposes of public administration and management, school and educational purposes, cultural and public enlightenment, sport, medical, social and commercial	1 141
Building for the purpose of automobile, railway, air transport and public transport	989
Building for family recreation	816
Building for vehicle parking	1 028
Building of other use than above stated	937
Multi-purpose buildings	992

As the Czech construction standards use a different classification of buildings than the Czech Statistical Office, similar categories have to been matched manually. The unit price for the category on “multi-purpose buildings” has been calculated as average of the other categories (no information is available about which of these buildings serve which purposes, whether e. g. the mix of housing and commercial purpose prevails etc., and no weights may be therefore employed).

We have assessed the uncertainty associated with the accuracy and completeness of the spatial asset data used against a study that monitored the assets under significant flood risk in part of the Vltava river basin (Sweco Hydroprojekt and DHI, 2014) and which uses data from ZABAGED (Fundamental Base of Geographic Data of the Czech Republic).Table 8 shows the results of the mapping by Sweco Hydroprojekt and DHI for Prague, and the results of our inventarization.

Table 8: Number of buildings exposed to flooding of different return periods - comparison of spatial datasets.

Spatial data source/ return period	**5-year**	**20-year**	**100-year**	**500-year**
ZABAGED database[a]	343	646	846	3 856
PIPD+CZSO layers[b]	416	813	1 365	2 479

[a]Sweco Hydroprojekt and DHI (2014); [b]Own calculation based on PIPD (2013) and CZSO (2014).

The results of inventarization based on data by the PIPD and CZSO that are more readily available yield a higher number of buildings exposed to floods of small return periods (5-year), but from 20-year to higher return periods the number of buildings exposed found is lower than for the ZABAGED database. The differences are explained by different actualisation of the data (PIPD data are for year 2013, CZSO for year 2011; ZABAGED is updated every three years); also, the CZSO layer lacks certain details on buildings that feature in the PIPD database; no information on the completeness and reliability of the ZABAGED database is available to the authors.

Damage on infrastructure

In the damage to infrastructure only the damages related to roads were included. The data on infrastructure come from the PIPD unit (Technical use of the area; PIPD, 2013). Unit price is based on TGM WRI (2009) and, as no actual unit prices are available in the Czech construction standards database, the unit prices by TGM WRI (2009) are adjusted for inflation of construction works (using producer index of construction works by CZSO) to the price level of year 2015. The price per m^2 is set at 194 € (recalculated using EU HICP deflator and PPP exchange rate). Table 9 lists the data included in the uncertainty analysis.

Table 9: Unit price and price range for damage to infrastructure (roads) for floods of any return period. Source: TGM WRI (2009), *TGM WRI (2009) and CZSO data (2015).

Infrastructure type	**Unit price per m^2 (€ 2015)**	**Damage (%)**		**Unit damage per m^2 (€ 2015)**	
		Min	Max	Min	Max
Roads	194.0*	2.06	4.12	4.0	8.0

Unlike damage on buildings, infrastructure damage is assumed not to be related to water depth.

Damage on agriculture

Damage on agriculture consists in direct damage to crops. The methodology is based on TGM WRI (2009). The unit price is based on the average cost of planting five categories of basic crops published by the Institute of Agricultural Economics and Information (IAEI). The unit price is the average of prices of five main basic crops, weighted for the area of the respective crop in Prague in May 2014 (as reported by the CZSO, 2014). The values of agricultural production are actualised using the latest published report by IAEI (2014).

The damage is assumed to occur at the maximum risk scenario, where all production is damaged by the flood, irrespective of the water depth. This approach is in line with e. g. study by Foudi et al. Arcadis (2004) reports on a depth-damage function estimated by the Morava River Basin Management, s. e., where the full damage is associated with water depth of 40 cm and more; from 0 to 40 cm, the damage factor increases linearly. Adoption of this approach leads only up to 5% decrease in the agricultural area in the floodplain for Q500 which, together with the low unit price (see later in the text) would have practically no effect on the results. There exist also some foreign studies that take the water depth into account when estimating the flood damage on agriculture, but they are focused on a single crop (e. g. Brémond, 2011) and the results may not be generalized over the whole range of crops.

The following Table10 shows the unit values and range of values associated with flooding 1 ha of agricultural land.

Table 10: Unit price and price range - damage on crops. Source: TGM WRI (2009), CZSO (2014), IAEI (2014).

Crop	Area in Prague (ha; CZSO 2014)	Cost of planting (€/ha; IAEI 2014)	Loss in % (TGM WRI 2009)		Unit damage (€/ha)	
			Min	**Max**	**Min**	**Max**
Cereal	6 564	1 412	15	80	212	1 129
Corn	217	1 885	15	80	283	1 508
Rape	2 119	1 886	10	90	189	1 697
Potato	6	1 583	20	80	317	1 266
Sugar beet	362	6 436	15	80	965	5 149
Weighted average - Prague					**221**	**1 338**

Other uncertainties in the analysis

Cost-benefit analysis requires to precisely define the costs and benefits occurring in different time periods and requires to make assumptions also on the dynamics of the socio-economic system. Within the time horizon until year 2100, there is large uncertainty on the demographic and socio-economic trends (population growth, migration, density, economic growth) which affect the amount, state and value of assets under risk – see Deliverable 4.1 for the discussion.

Also, the future urban development in Prague (increasing urbanisation, urban policy, changes in land use in general) is uncertain and has to be dealt with in the analysis. For the Vltava case study, the urban planning in Prague does not favour further development of the areas in the flood zones. We therefore assume that the real value of assets does not change among time, and that the present urban development is fixed in the long-term. A more precise approach has been used e. g. by Lasage et al. (2014) - they study employs for the definition of the future development existing planning documents and land-use maps; from the year where no further data are available, the urban development is assumed to be fixed at the latest available state.

A further uncertainty that affects the value of costs and benefits is related to technology. The costs of potential future investments into flood protection may be directly driven by technological uncertainty, and potentially, a different scheme of the flood protection investments made in the future when the technologies might be more efficient and/or less expensive than the scheme that has been already designed. However, CBA enables only a static evaluation of a particular investment project and does not allow for the assessment of the flexibility of future investment schemes under uncertain evolution of climate, hydrology and occurrence of flood events in the future. To achieve an assessment of a dynamic scheme of flood protection investments, other decision support tools than CBA may be more appropriate (see Deliverable 4.2 for a detailed review of decision support tools under uncertainty).

Technological uncertainty in a more general sense relates also to the scale and carbon intensity of the economic activities and affects the climate modelling, socio-economic trends and affect also the value of assets at risk in the long-term (Heal and Millner, 2014). Other climate-related and population-related effects may also in the long-term affect the agriculture (change of crops planted, changes in the area of planted crops) and associated flood damage on agricultural land. These general uncertainties are very complex and are not in most cases considered in the cost-benefit analyses of flood protection (Lasage et al., 2014; Foudi et al., 2015).

2.2.4 Avoided damages and risk

Figure 9 shows the average estimated damages for each return period of flood in Prague and damage category (four categories of buildings, agricultural loss and infrastructure - roads). Regardless of the return period, the damage on buildings account for the largest portion of the total damage. Within the category of damage on buildings, the most damage occurs to housing. Figure 10 disaggregates the total damage for Prague into the damage in respective Prague districts.

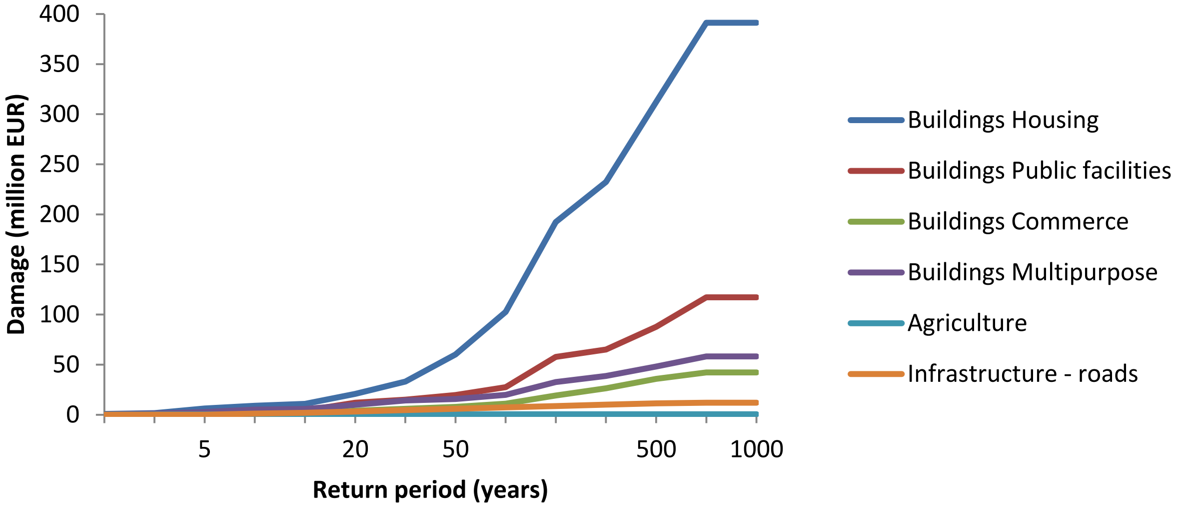

Figure 10: Damage by damage category for return periods 1– to 100-year.

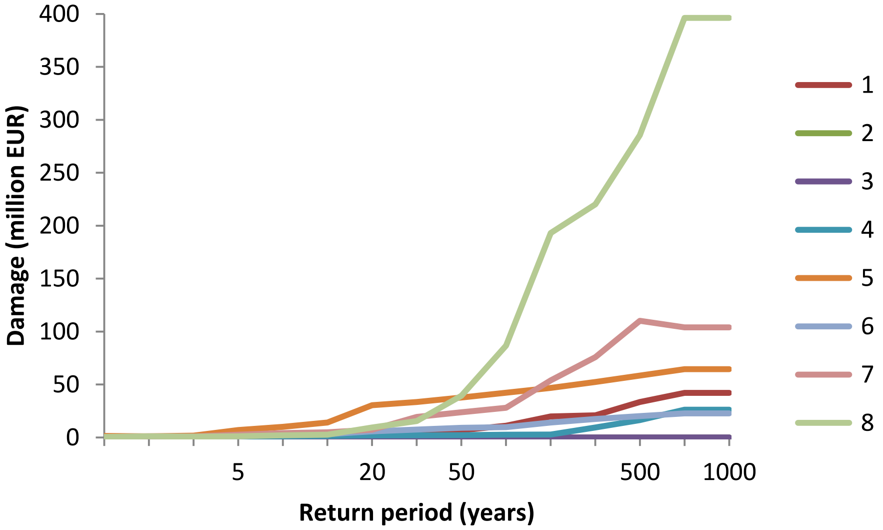

Figure 11: Damage by Prague districts (1-8) for return periods 1– to 100-year.

To assess how the estimates of flood damage on buildings fit the real damages, Table 11 reports the estimated damage for four selected return periods of floods and compares them with actual historic damage from recent floods of the respective return period. There was no flood of return period 100-year in the past 50 years, so we have chosen 5-, 20-, 50- and 500-year.

The detailed damage categories from the evaluations of actual historic flood damage are reported only for 500-year in year 2002, for the other return periods only total damage is reported. The data on damage on buildings were therefore estimated under the assumption that the share on total flood damage is equal to that in year 2002. Flood 2013 is categorised as between 20- and 50-year (CHMI, 2013). All the reported numbers are recalculated to € 2015 using EU HICP deflator and PPP exchange rate.

Table 11: Estimated vs. observed damages on buildings in Prague (M €). Source: Own calculations, TGM WRI (2002), TGM WRI and CHMI (2006), CHMI (2013).

Return period	5-year	20-year	50-year	500-year
Estimated average damage	2.8	46.6	85.2	596.6
Actual historic damage (Floods 2002-13)	0.8*	80.7*		570.3

* *The actual damages related to historic floods in 2006 (5-year) and 2013 (20-50-year) were estimated from the reported total damage under assumption that the share is similar to the share of damages on buildings on total damage in year 2002 (500-year)*

The results show that the estimated results are in a very similar range to the actual historic damage. Our model slightly overestimates the damage associated with floods of small return periods, but actually for the 500-year one, for which the actual historic damage data on buildings are available, the estimation is remarkably close to the actual damage. Although protection standard is formally 20-year, minor damage occurs also in the 5-year event as some buildings and agricultural areas are outside of the protections works.

The actual loss of agricultural output was estimated also only for the flood in year 2002(500-year); the reported loss is 3.5 M € (TGM WRI, 2002). The estimated average damage for a 500-year flood is of 0.4 M € and underestimates this number. The estimated damage covers only the direct loss of the agricultural output in the year of flood event and does not cover other damages, such as damage to the soil itself. Agricultural land is located in the south of Prague, in the natural floodplain of the Vltava river where there is only a few built-up areas and where the flood protection is therefore relatively weak. The loss is therefore not very much responsive to the change in the flood extent and the damage occurs even if the flood is of a relatively low return period.

Figure 12 shows that even for small scale floods such as 5-year flood event, the area of agricultural land under risk is very similar to floods of larger return period; the differences among the agricultural area flooded by a 20-year, 100-year or 500-year flood are negligible.

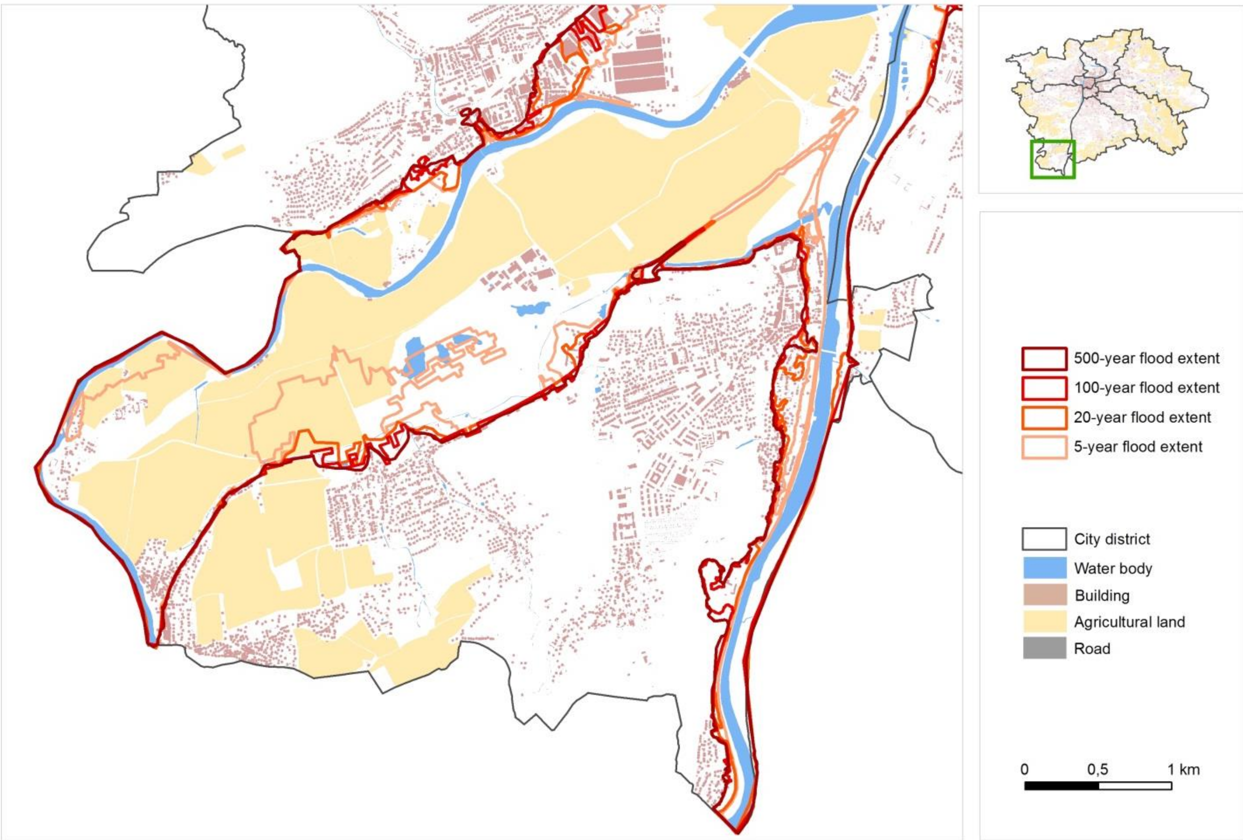

Figure 12: Location of agricultural land within flood extents of floods of selected return periods in the district of Prague 8. Own processing of datasets from TGM WRI (2015), Prague Institute of Planning and Development (2015).

For infrastructure, the reported flood damage in year 2002 for a 500-year flood event has been 65 M €. The estimated value is only 33.3 M €, so the estimates of damage for this category also may be underestimated.

2.3 Cost-benefit analysis of adaptation measures

The case of this study is to investigate economic efficiency of investments into flood protection measure built up in Prague at the beginning of 21st century. In this section we calculate the net present value of the flood protection investments recently built in Prague under future climate variability, and compare them to the status quo, represented by the current climate conditions (base year is 1985) without flood protection.

2.3.1 CBA methodology applied

Economic appraisal of adaptation to climate change variability and the investigation of associated uncertainties is made possible by means of a wide range of appraisal tools (see Deliverable 4.2). Cost-benefit analysis (CBA), which is used in the Vltava case study, belongs to a set of traditional economic decision supporting tools. Considering a set of possible alternatives, CBA involves the systematic identification of project consequences, followed by the assessment of all social benefits and costs and thereafter the application of appropriate decision criteria (Fuguitt and Wilcox, 1999).

Investing in flood prevention measures such as dike and mobile barriers is an important part of flood risk management, especially in the face of empirical evidence of increasing flood damages and the ongoing and future climate change (de Moel et al., 2014). An equally important question to flood risk management is whether flood damage-reducing measures promote economic efficiency. Economic evaluation of adaptation investment into flood prevention under different climate projections is of particular interest for an analysis in the Vltava case study, and it seems particularly interesting to investigate economic efficiency of investments using a traditional appraisal tool such as CBA.

The principle focus of our case study is to investigate the economic efficiency of the investments in measures recently built in Prague: line measures (fixed earth dikes, reinforced concrete walls, mobile barriers) and barriers in the waste-water system - and their operating consequences. We follow the steps of the procedure displayed in Figure 2 to estimate the EAD, under future climate variability (until year 2100), for:

(a) The situation without the new adaptation investment, the *status-quo* situation (with a 10-year protection), which we compare with
(b) The adaptation investment (with a 500-year protection), which was realized in the period of 1999-2014.

We regard the difference between these two EAD as the benefits of adaptation.

Net present value

The avoided EAD represents the socioeconomic benefit of the adaptation investment and is further used in the cost-benefit analysis. The economic efficiency is estimated by a widely used decision criterion, the net present value, which can be applied when evaluating a single investment. A NPV above zero suggests that the adaptation project promotes economic efficiency.

Some variables considered in the calculation of the NPV are deterministic, i.e., there is no uncertainty involved in the lifespan of the measure. The EAD, the lump-sum / one-off of costs associated with the occurrence of a flood event and the discount rate under intertemporal risk aversion are random variables contributing uncertainty (and risk, from a certain point of view) into the CBA. Thus, instead of the simple NPV, we are interested in the expected NPV, which could be formulated for the Vltava case study as follows:

$$E[NPV] = -\sum_{t=ts}^{t=-1} CI + \sum_{t0=0}^{T} (\Delta EAD_t - CV_t - CL_t) \cdot \tau_t \cdot \prod_{to=0}^{T} (1 + \eta \cdot g_t)$$

where τ_t is the discount factor in year *t* with the social discount rate r_s, assumed to by:

$$\tau_t = \frac{1}{(1 + r_s)^t}$$

The costs of the adaptation measures include the initial investment cost *CI*, the yearly maintenance and variable costs CV_t and lump-sum costs CL_t. Lump-sum costs are spent when 50-year flood and higher will occur. The investment costs were incurred during the period 1997-2014. The social benefits in year *t* are measured by the ΔEAD_t indicator and represent the avoided flood damage in year *t.* The indicator ΔEAD_t, for a given year represents the increased flood protection standard in Prague, from 1 in 10-year flood to 1 in 500-year. The product in the third term adjusts real values of social benefits and costs for possible changes in income over time. Parameter η is the elasticity of marginal utility and g_t is the growth rate of consumption in year *t*.

The values of benefits and costs over a time period are discounted to 2015, which is indexed as $t_0 = 0$. An investment horizon starts in year 1997 ($t_s = -18$) and ends in 2100 ($T = 85$) after 104 years. Thus the ENPV of the adaption investment is then calculated over a time period of t = 1, …, 104. All values are converted to € of 2015 using PPPs for GDP and the OECD HICP (http://stats.oecd.org).

A positive ENPV shows that the sum of the discounted social benefits exceeds the sum of the discounted costs over time, which implies that the adaptation investment strategy into flood protection is beneficial in economic terms. The larger the ENPV value is, the more efficiency the flood protection measure promotes.

Discount rate

Flood protection investments and other climate change adaptation measures are typically based on a series of costs in time and yield long-run benefits that accrue both to present and future generations. To aggregate costs and benefits across time using the concept of NPV, discounting of costs and benefits is essential. The social discount rate, δ_S, is an important but uncertain parameter, which is exogenously determined, and its choice may dramatically affect the results of the project appraisal. Ermoliev et al. (2008) show that for a relatively modest interest rate of 3.5%, the policy evaluation time horizon of a project does not exceed 30 years.

The calculation of discount rates involves uncertainties of two sources (Heal and Millner, 2014): empirical uncertainties that are associated with the lack of information on future economic growth rates; and normative disagreements about the values of welfare parameters. Deliverable 4.1 discusses several approaches to discounting, including using a constant discount rate (most frequently based on the Ramsey formula – Ramsey, 1928), certainty-equivalent discount rate / declining discount rate (Weitzman, 1998), and other schedules. Moreover, Deliverable 2.2 discusses discounting approaches under uncertain growth and accounting for intertemporal risk.

The most recent approaches to discounting favour more complex and flexible ways of determining the discount rate, and this can also be observed in the decision-making practice of European countries that shift to applying non-constant discount rates (HM Treasury, 2013) that do not lower the importance of the benefits occurring in the far future as much as the constant discount rate does. However, in the decision-making practice in the Czech Republic it is still most common to stick to a constant discount rate, even if it is (based on the results of the discussion in Deliverables 4.2. and 2.2) not considered as appropriate for evaluating projects with long-term benefits such as climate change adaptation. Recent studies also develop endogenously-determined discount rates, which is of high importance for the adaptation to catastrophic events, because the catastrophic events may affect discount rate (Ermoliev et al., 2008). It is necessary to state that CBA, unlike some recently developed discounting approaches (see Deliverable 4.2 or Ermoliev et al., 2010) does not allow for the endogeneity of this parameter, and thus the discount rate is always exogenously determined in the CBA.

To investigate the effect of the choice of the discount rate on the results, we have applied several discounting approaches, and tested the influence of this exogenously determined parameter on the ENPV in a sensitivity analysis. The approaches adopted are four:

(a) The constant discount rate, which is a typical approach applied in CBAs in the Czech decision-making context. We compare rates of 0 % and 4 %.

(b) The standard neoclassical Ramsey formula:

$$r_s = \delta + \eta \cdot g_t$$

where parameter δ characterizes the pure rate of time preference, η represents the consumption elasticity of marginal utility and g_t is the growth rate of consumption. In this classic Ramsey formula, we expressed the social discount rate r_s as scenario-dependent. The parameter g_t was approximated by GDP growth projections with respect to the Shared Socioeconomic Pathways (SSPs). The SSP Database (https://tntcat.iiasa.ac.at/SspDb) provided two series of the GDP growth simulations - modelled by IIASA and by OECD - for each of five SSP scenarios in the period 2005-2100 for the Czech Republic (Figure 13).

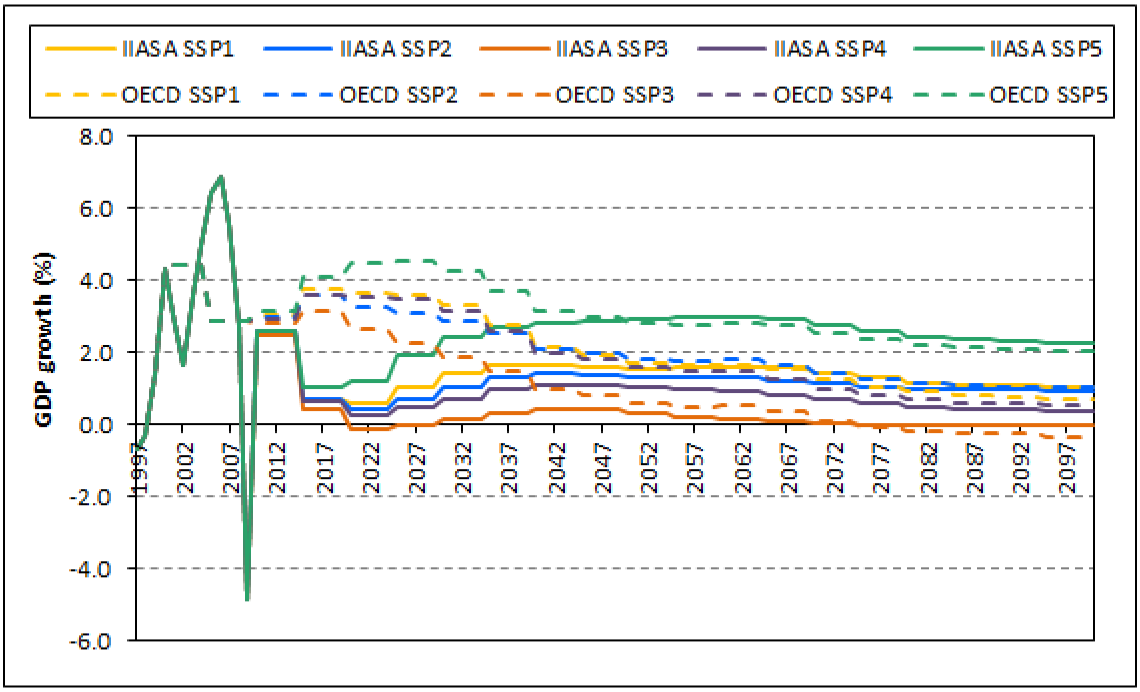

Figure 13. GDP growth projections for the 21st century, produced by OECD and by IIASA, with respect to specific Shared Socioeconomic Pathways for the Czech Republic.

Following the recommendations from the European project IMPRESSIONS (http://www.impressions-project.eu), we formulate one-to-one, plausible links between SSPs to the RCP scenarios we adopted: RCP2.5 with SSP1, RCP4.5 with SSP3 and RCP8.5 with SSP5.

(c) The extended Ramsey formula with stochastic growth (Traeger, 2014; Deliverable 2.2):

$$r_s = \delta + \eta \cdot \mu - \eta^2 \cdot \frac{\sigma^2}{2}$$

where parameter μ is the expected growth rate and σ represents the standard deviation of the expected growth rate. The term $\eta \cdot \mu$ characterizes the decrease in marginal utility in relation to consumption growth. According to Traeger (2014), the parameter η represents aversion to intertemporal consumption changes. The third term is referred to as the standard risk term that is interpreted as the costs of expected variability because of the aversion to non-smooth intertemporal consumption.

In order to estimate r_S, the expected growth rate μ and its variance σ^2 are needed. We adopted a Lebegue (2005) approach, assuming that the expected growth rate has *n* possible values μ_i with corresponding probabilities p_i, where *i = 1, .., n* (Groom, 2014). Then the expected growth rate is computed as:

$$\mu = \sum_{i=1}^{n} p_i \cdot \mu_i$$

For an empirical estimation of the parameter μ, we used the GDP growth projections from SSP Database for the Czech Republic (as described see above). We merged the SSPs' projections modelled by IIASA and OECD, and computed relative frequencies as probabilities p_i for each μ_i value in the dataset. Finally, we estimated the mean value and its standard deviation, μ = 0.015, and σ = 0.011.

(d) Discounting under intertemporal risk aversion (Traeger, 2014; Deliverable 2.2):

$$r_s = \delta + \eta \cdot \mu - \eta^2 \cdot \frac{\sigma^2}{2} - RIRA \cdot |1 - \eta^2| \cdot \frac{\sigma^2}{2}$$

where the parameter RIRA measures the relative intertemporal risk aversion. The fourth term represents the intertemporal risk aversion, and the magnitude of its contribution compared to the contribution of the standard risk term is computed as:

$$\frac{RIRA \cdot |1 - \eta^2| \cdot \frac{\sigma^2}{2}}{\eta^2 \cdot \frac{\sigma^2}{2}}$$

The RIRA parameter depends on RRA, which is the coefficient of Arrow-Pratt risk aversion:

$$RIRA = \begin{cases} 1 - \frac{1-RRA}{1-\eta} & if\ \eta < 1 \\ \frac{1-RRA}{1-\eta} & if\ \eta > 1 \end{cases}$$

In the sensitivity analysis, we decided to use the following set of values of the RRA parameter: RRA $\in$ [1, 2.5, 5, 10].

Uncertainty analysis

The CBA assessment realized for the Vltava case study encompasses a variety of models, which we used in the different steps of the analysis, and different types of input data. As a consequence, the ENPV is characterized by uncertainties, which should be treated appropriately when interpreting the results (de Moel et al., 2014). The expected NPV is an important measure when evaluating projects of which each possible outcome has a known probability. When the probabilities are unknown for each input parameter, one should compute NPVs using a sensitivity analysis performed under plausible ranges of the variables, and demonstrates how the NPV, our decision criterion, varies depending on the choice of values of the input variables. In other words, the sensitivity analysis measures the influence of changes in key input parameters independently, holding all other parameters constant, i.e., *ceteris paribus* (Fuguitt and Wilcox, 1999).

Performing a sensitivity analysis in the CBA of flood adaptation in Prague allows us to address the issue of uncertainty in the investment appraisal, and thus to explore and rank sources of uncertainty. We try to answer the question: Which are the key input parameters with significant influence on the ENPV?

We identified and listed several uncertainty sources in the CBA assessment, which we were able to describe and simulate in terms of the ENPV change (Saint-Geours et al., 2014). We considered eight categories of uncertain inputs, which are presented in Table 12: (X_1) projections of GHG emissions with respect to RCPs, (X_2) simulation of climate parameters by the regional climate models, (X_3) depth-damage functions, (X_4) method of approximation of EAD, (X_5) maintenance costs, (X_6) lump-sum costs, (X_7) assumptions about future socio-economic development, and (X_8) assumptions in discounting.

Table 12. Sources of uncertainty in the CBA assessment explored in the Vltava case study (adapted from Saint-Geours et al., 2014). n represents the number of realizations of the value of each input parameter.

	Input parameter	n	Source of uncertainty
X1	Representative Concentration Pathways	3	Difference in the GHG forcing boundary conditions
X2	Climate simulations from RCM	14	Assumptions behind the regional climate models
X3	Depth-damage function	3	Variability in the damage rates
X4	Approximation of EAD	2	Trapezoidal rule with different number of return periods
X5	Variable costs	3	Range of values
X6	Lump-sum costs	3	Range of values
X7	Economic growth	10	Variability in the GDP growth projections, different SSPs and models
X8	Discounting approach	4	Assumptions behind discounting

2.3.2 Results of the CBA assessment

Benefits – Expected annual damage avoided

This section presents the results in terms of the avoided EAD, and we explore how various climate change scenarios – RCP2.6, RCP4.5 and RCP8.5 – affect this metric.

The curves in Figure 14 show that the avoided EAD (not discounted) for the adaptation investment increases across time. The avoided EAD slightly increases under climate change scenarios without flood protection. The RCP2.6 scenario provides the largest benefits, but this result should be interpreted with caution, because only one simulation set is behind this RCP. The new flood protection system immediately after the realization of the investment generates several times higher benefits, and the flow of annual benefits is almost constant across time, from the time point when the flood protection measures are completed. This means that the adaptation is effective against floods both in the early and in the late 21st century.

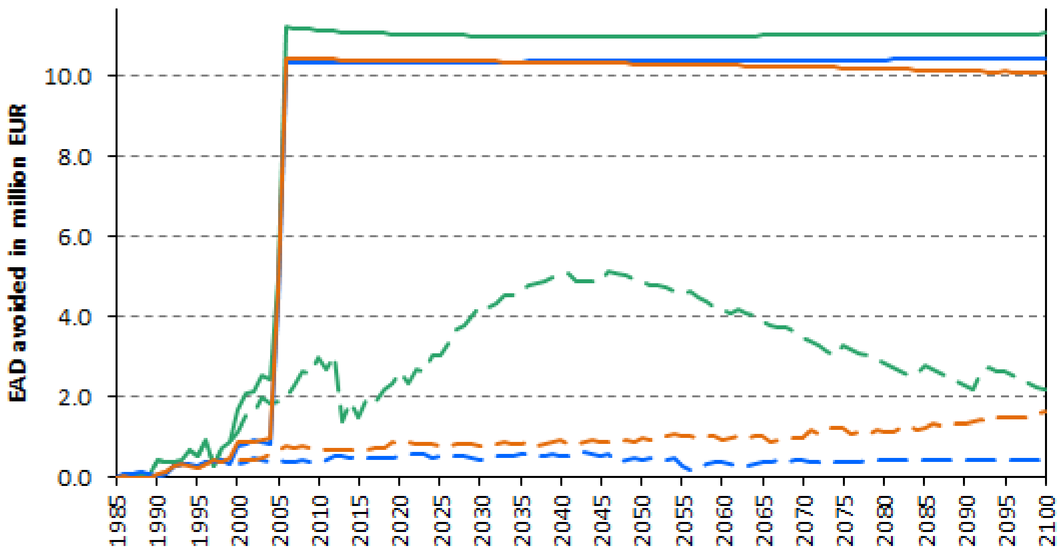

Figure 14. Avoided expected annual damage (not discounted) according to RCP scenarios, with the adaptation investment (protection up to 500-year floods) in solid lines, and in the status quo situation without the adaptation investment (protection up to 10-year floods), compared to the EAD of the base year 1985. Green lines refer to RCP2.6, blue lines to RCP4.5, and orange lines to RCP8.5.

Under future climate conditions without the realization of the new adaptation investment, the total avoided flood damage for the entire period 1997-2100 is estimated at more than € 341 million for RCP2.6, € 47 million for RCP4.5 and € 101 million for RCP8.5, compared to damages of the base year 1985, without even the status quo protection (of 10/year return period). With the adoption of the adaptation measure, the avoided damages increase up to € 1067 million (RCP2.6), 996 million (RCP4.5) and 988 million (RCP8.5). By taking the adaption measures, flood damages can be reduced substantially, 3 times in the case of RCP2.6, 21 times and 10 times for RCP4.5 and RCP8.5, respectively.

The results of the relative changes of the EAD avoided thanks to the adaptation, with respect to the no adaptation for each of the 14 simulations and RCPs are shown in Figure 15, depicting the relative increase in the avoided EAD. In mean the relative change is 71% (standard deviation = 13.61%), and if the single RCP2.6 simulation is excluded the mean relative change is 72% (s.d. = 13.56%). The relative changes per RCP are 54% for RCP2.6, 74% for RCP4.5 (with an inter-simulation range of 33 to 95%), and almost the same, 70%, for RCP8.5 (inter-simulation range 53 to 86%).

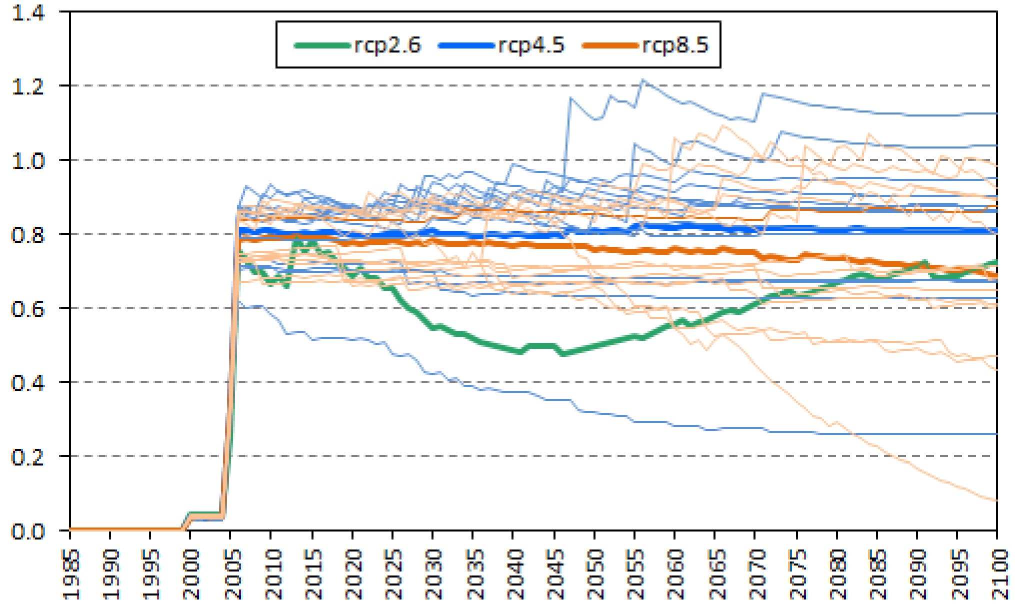

Figure 15. Relative changes (in factor units) of the expected annual damage avoided thanks to the adaptation investment, for the three RCP scenarios. Thin lines represent individual RCM simulations and bold lines the multi-simulation mean for each RCP scenario.

Costs – Investments into flood protection

The temporal distribution of the annual total costs of the flood protection measure in Prague has two peaks during the period of 1997-2100. Figure 16 shows that two main investments are realized around years 2005 and 2009. The annual total costs cumulated across the period amount to € 285 million. Variable and lump-sum costs amount to € 22.5 million for the entire period. Investment costs cover 92% of the total costs. This entails small differences in the temporal development of total costs across RCPs, because different occurrence of floods in different scenarios imply differences in the one-off costs of deployment of the measures.

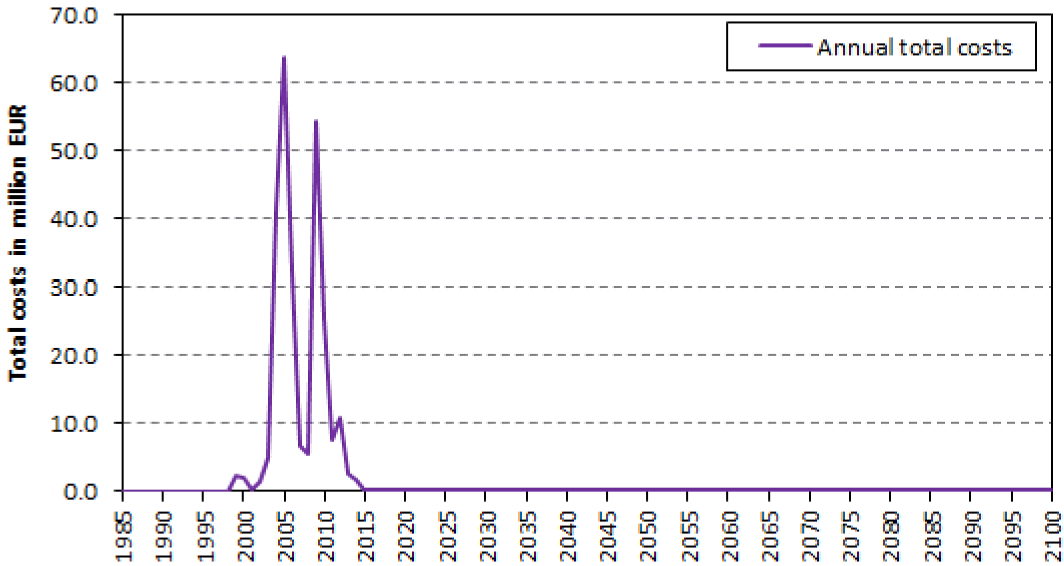

Figure 16. Total costs (not discounted) of flood protection measure invested in Prague.

Net present value of flood protection under climate change

Under future climate conditions, the ENPV of the adaptation investments (Table 13), averaged across all simulations and RCPs, is € 626 million (s.d. € 174 million), with 0% discount rate. The ENPV at 0% discount rate excluding RCP2.6 is € 633 million (s.d. 173 million). ENPV is the lowest for RCP2.6, € 440 million, and ENPVs for RCP4.5 and RCP8.5 are similar, € 664 million (range 138-931; s.d. 191) and 602 million (range 388-807; s.d. 147), respectively.

Table 13. Cumulative net present value (in million €) of adaptation in Prague compared to the baseline of year 1985 without flood protection, shown for the whole 1997-2100 assessment period, according to the three scenarios, for each Regional Climate Model, at 0 and 4 % discount rate.

Regional climate models and simulation sets	**RCP2.6**		**RCP4.5**		**RCP8.5**	
	0%	**4%**	**0%**	**4%**	**0%**	**4%**
CNRM-CERFACS-CNRM-CM5_r1i1p1_CLMcom-CCLM4-8-17	-	-	516	21	411	2
CNRM-CERFACS-CNRM-CM5_r1i1p1_CNRM-ALADIN53	-	-	683	76	535	30
CNRM-CERFACS-CNRM-CM5_r1i1p1_SMHI-RCA4	-	-	521	20	505	25
ICHEC-EC-EARTH_r12i1p1_CLMcom-CCLM4-8-17	-	-	741	89	548	32
ICHEC-EC-EARTH_r12i1p1_SMHI-RCA4	440	-4	931	123	757	91
ICHEC-EC-EARTH_r1i1p1_KNMI-RACMO22E	-	-	138	-78	558	33
ICHEC-EC-EARTH_r3i1p1_DMI-HIRHAM5	-	-	813	108	742	88
IPSL-IPSL-CM5A-MR_r1i1p1_IPSL-INERIS-WRF331F	-	-	827	102	388	47
IPSL-IPSL-CM5A-MR_r1i1p1_SMHI-RCA4	-	-	650	59	715	82
MOHC-HadGEM2-ES_r1i1p1_CLMcom-CCLM4-8-17	-	-	771	96	807	100
MOHC-HadGEM2-ES_r1i1p1_KNMI-RACMO22E	-	-	741	88	770	90
MOHC-HadGEM2-ES_r1i1p1_SMHI-RCA4	-	-	741	93	774	96
MPI-M-MPI-ESM-LR_r1i1p1_CLMcom-CCLM4-8-17	-	-	743	90	501	21
MPI-M-MPI-ESM-LR_r1i1p1_SMHI-RCA4	-	-	479	13	416	3
RCP Average	**440**	**-4**	**664**	**64**	**602**	**53**

ENPV are dramatically lower for a 4% discount rate, by as much as 91% less than with 0% discount rate: 101%, 90% and 91% for RCP2.6, RCP4.5 and RCP8.5, respectively. The ENPV under the climate conditions of RCP2.6 is even negative, amounting to € -4 million, indicating that the project doesn't promote efficiency in this case. RCP4.5 and RCP8.5 at 4% promote efficiency, ENPVs are positive and amount to € 64 and 53 million, respectively.

The temporal distribution of annual ENPV is displayed for 0% and 4% discount rate in Figure 17. The curves show that the annual ENPVs are distinctly negative in the first phase, until the investments are completed.

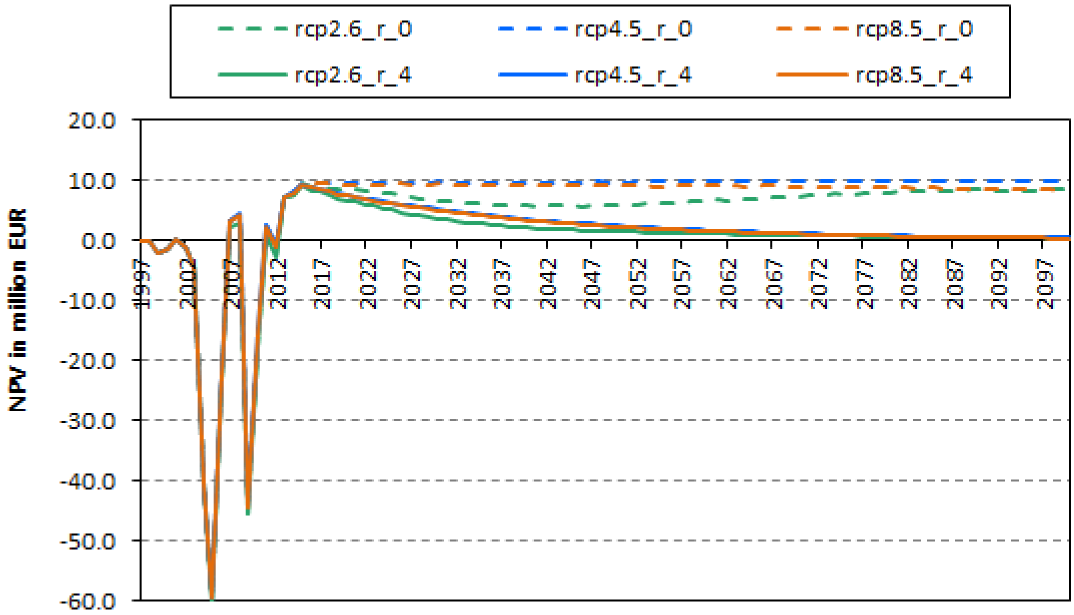

Figure 17. Annual net present value of flood protection measure in Prague according to RCP scenarios, compared to climate of the base year 1985 without flood protection (dashed and continue lines are 0% and 4% discount rates, respectively).

When considering the climate conditions of the RCP2.6 scenario, the annual ENPV at 0% discount rate is on average € 4.2 million (s.d. 10.3 million). At 4% discount rate the annual value is negative, € -0.04 million. The RCP4.5 and RCP8.5 scenarios raise the annual ENPV to € 6.4 and 5.8 million, respectively. The range of the annual ENPVs across the RCP4.5 and RCP8.5 simulation sets are € 1-9 million (s.d. 10.7 million) and € 4-8 million (s.d. 10.5 million), respectively.

The average value of ENPV for all RCP scenario is € 626 million, if we assume 0% discount rate. The differentiation between RCPs will have a moderate impact on ENPV, the RCP2.6 scenario will decrease the value by 30%, RCP4.5 will increase ENPV by 6% and RCP8.5 decreases by 4%. When considering 4% discount rate, then the effect of RCPs on ENPV is larger, the change is -107%, 14% and -7% for RCP2.6, RCP4.5 and RCP8.5, respectively.

The variability in the estimation of ENPV among RCPs and climate simulations is clearly evident in Figure 18. The ENPV value varies among the RCP4.5 simulations in the range from -79% to 40% compared to the RCP4.5 average (at 4% is the range larger, from -221% to 91%). The variability of ENPV for the climate simulations of RCP8.5 is in the range from -35% to 34 % (at 4% discount rate the range is from -238% to 91%).

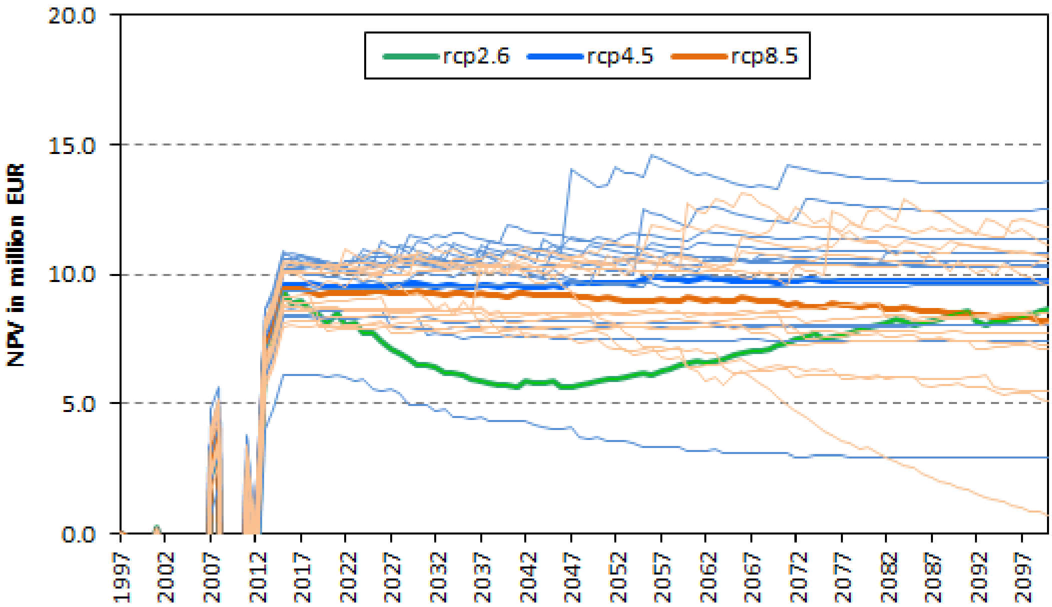

Figure 18. Annual net present value (not discounted values) of flood protection measure in Prague. The thin lines represent individual RCMs, and bold lines the average for each RCP scenario.

2.3.3 Uncertainty behind the results of CBA

Minimum and maximum values of input parameters

This section presents the results of sensitivity analysis which investigates the influence of different values of single input parameters – depth-damage function, variable costs and lump-sum costs - on the cumulative ENPV. For 0% and 4% discount rate, we estimate ENPV with minimum or maximum values of each input parameter.

The results in Table 14 show that both cost variables – variable (maintenance) and one-off (lump-sum) costs - have a negligible influence on estimated ENPV. The depth-damage function has a moderate effect on ENPV, changing the ENPV value by 37-158% according to RCP scenario. But the ENPV changes drastically when different discount rates are assumed.

Table 14. Sensitivity analysis of cumulative NPV (in million €) on minimum, average and maximum value of input parameters under investigation.

Parameters under investigation		**RCP2.6**		**RCP4.5**		**RCP8.5**	
		0%	**4%**	**0%**	**4%**	**0%**	**4%**
Damage function rate	average	440.4	-3.9	664.1	64.4	601.9	52.7
	minimum	253.6	-72.1	419.0	-21.7	373.1	-30.3
	maximum	627.2	64.3	909.1	150.6	830.7	135.7
Variable costs	average	440.4	-3.9	664.1	64.4	601.9	52.7
	minimum	442.0	-3.4	665.7	64.9	603.5	53.2
	maximum	438.8	-4.4	662.5	63.9	600.3	52.2
One-off-costs	average	440.4	-3.9	664.1	64.4	601.9	52.7
	minimum	440.7	-3.8	664.3	64.5	602.2	52.8
	maximum	440.1	-4.0	663.8	64.3	601.7	52.6
All parameters	average	440.4	-3.9	664.1	64.4	601.9	52.7
	minimum	255.5	-71.5	420.8	-21.1	375.0	-29.7
	maximum	625.3	63.7	907.3	150.0	828.9	135.1

Method of integration to obtain the EAD

Further, we performed a sensitivity test to explore the dependence of the ENPV results from the methodological choice of the number of return periods that are taken into account when approximating the EAD integral with a trapezoidal rule. We run the test with either 6 or 141 return periods, i.e., the full range of available damage results for the case study. For each of the two choices, a range of discounting rate are applied (Table 15).

Table 15. Sensitivity analysis of cumulative NPV (in million €) depending on the number of return periods (6 or 141) used in calculating EAD by the trapezoidal rule, for different discount rates.

	Discount rates	**EAD with 6 Return Periods**	**EAD with 141 Return Periods**
RCP2.6	0%	440.4	482.9
	1%	231.8	261.5
	2%	112.9	132.4
	3%	41.4	53.3
	4%	-3.9	2.2
RCP4.5	0%	664.1	462.3
	1%	387.5	248.7
	2%	226.5	124.0
	3%	127.9	47.4
	4%	64.4	-2.1
RCP8.5	0%	601.9	475.8
	1%	350.5	257.8
	2%	202.9	130.5
	3%	111.8	52.2
	4%	52.7	1.6

There are non-negligible differences between the two return period approximations when calculating EAD, especially for RCPs 4.5 and 8.5, giving absolute differences between 10 - 63% for the discount rate in the range of 0 - 3%. The higher discount rate at 4% leads to a larger difference, up to 158%. The implication is that the computation-expensive choice of running damage simulations for a very high number of return periods does entail significant differences in the result of the economic appraisals.

Discounting rate

We performed a number of sensitivity tests to understand the dependence of the results on the choice of the discount rate. We applied four different methodologies for discounting: (i) constant discount rate, (ii) Ramsey formula with scenario-dependent discount rate on GDP projection, (iii) extended Ramsey formula under uncertain growth, and (iv) discounting under intertemporal risk aversion.

(i) The constant discount rate at 0% and 4%.

> The results in the previous section 2.3.2 revealed that the choice of constant discount rate has a significant impact on the ENPV, in the range 90-101% depending on the RCP scenario.

(ii) The standard Ramsey formula with scenario-dependent discount rate.

> Table 16 provides the ENPV estimates according to different methodological assumptions about parameters δ (pure rate of time preference) and η (consumption

elasticity of marginal utility), type of GDP growth projections and the choice of SSP. We rely on the following combinations of SSP and RCP: RCP2.5 and SSP1; RCP4.5 and SSP3; RCP8.5 and SSP5, highlighted in bold in Table 16. We run the sensitivity test with the following values of parameters $\delta \in$ [0%, 1.5%] and $\eta \in$ [1, 2].

Table 16. Sensitivity analysis of cumulative NPV (in million €) on different parameters assumed in Ramsey discounting, with the IIASA and OECD SSP-dependent growth rates. Plausible selected combinations of SSP and RCP are in bold.

		Shared Socioeconomic Pathways				
		SSP1	**SSP2**	**SSP3**	**SSP4**	**SSP5**
	Parameter values:	δ = 0%	η = 1			
Average discount r.	IIASA	0.0128	0.0106	0.0012	0.0069	0.0243
	OECD	0.0193	0.0195	0.0081	0.0175	0.0302
RCP2.6	IIASA	**440**	501	934	663	200
	OECD	**440**	400	876	500	207
RCP4.5	IIASA	664	747	**1312**	953	344
	OECD	664	615	**1232**	742	356
RCP8.5	IIASA	602	678	1188	862	**311**
	OECD	602	560	1116	672	**323**
	Parameter values:	δ = 1.5%	η = 2			
Average discount r.	IIASA	0.0407	0.0361	0.0174	0.0288	0.0636
	OECD	0.0536	0.0540	0.0311	0.0499	0.0753
RCP2.6	IIASA	**169**	229	785	392	7
	OECD	**170**	150	687	221	15
RCP4.5	IIASA	303	386	**1125**	600	78
	OECD	304	280	**991**	373	91
RCP8.5	IIASA	273	350	1021	543	**66**
	OECD	274	254	899	337	**78**

The results show that there is a dramatically large difference in the value of discount rate, in the range 16-2802%, caused by different values of δ and η parameters. The discount rate for δ = 0.015 and η = 2 and SSP5 reaches ca. 7.5%. There is only a relatively small difference in the range 0-61% between the two types of GDP growth projection (modelled by IIASA and OECD), depending on RCP and SSP scenario. The choice of SSP scenario has a moderate effect on NPV, when we consider parameters δ = 0 and η = 1. The range of variability caused by SSP scenarios is 9-282%. When we assume δ = 0.015 and η = 2, the variability of NPV increases, with range 11-1141%.

(iii) The extended Ramsey formula under uncertain growth.

This sensitivity test investigates the dependence of the NPV estimates from the choice of parameters in the extended Ramsey formula under stochastic growth. We use these values of parameters $\delta \in$ [0, 1, 1.5] and $\eta \in$ [1, 1.5, 2].

Table 17. Sensitivity analysis of cumulative NPV (in million €) on different parameters assumed in Ramsey discounting with stochastic growth, for different RCPs and methods of EAD estimation.

Values of parameters				
discount rate	0.0150	0.0160	0.0234	0.0448
δ	0.0000	0.0010	0.0010	0.0150
η	1.0000	1.0000	1.5000	2.0000
μ	0.0150	0.0150	0.0150	0.0150
σ	0.0110	0.0110	0.0110	0.0110

	ημ	0.0150	0.0150	0.0225	0.0301
	standard risk term	0.0001	0.0001	0.0001	0.0002
RCP2.6	EAD with 6 Return Periods	442	416	418	172
	EAD with 141 Return Periods	485	457	459	197
RCP4.5	EAD with 6 Return Periods	666	631	634	308
	EAD with 141 Return Periods	464	437	439	187
RCP8.5	EAD with 6 Return Periods	604	572	575	277
	EAD with 141 Return Periods	478	450	452	195

Table 17 shows that there is a relatively moderate difference in the range 4.8-60.1% caused by the choice of δ and η parameters, depending on RCP scenario and on the number of return periods chosen when approximating EAD by trapezoidal rule.

(iv) Discounting under intertemporal risk aversion with RIRA coefficient.

As in the previous approach of discounting, we performed a sensitivity analysis to explore the dependence of the ENPV values on the methodological assumptions of parameters in the discounting approach under intertemporal risk aversion. We run the sensitivity test with different values of parameters $\delta \in$ [0, 1.5], $\eta \in$ [0.99, 2] and *RIRA* $\in$ [1, 2.5, 5, 10].

Table 18. Sensitivity analysis of cumulative NPV (in million €) on different parameters assumed in discounting under intertemporal risk aversion with RIRA coefficient.

Values of parameters								
discount rate	0.015	0.015	0.014	0.014	0.045	0.045	0.044	0.043
RRA	1	2.5	5	10	1	2.5	5	10
δ	0	0	0	0	0.015	0.015	0.015	0.015
η	0.99	0.99	0.99	0.99	2	2	2	2
μ	0.0150	0.0150	0.0150	0.0150	0.0150	0.0150	0.0150	0.0150
σ	0.0110	0.0110	0.0110	0.0110	0.0110	0.0110	0.0110	0.0110
ημ	0.0149	0.0149	0.0149	0.0149	0.0301	0.0301	0.0301	0.0301
standard risk term (SR)	0.0001	0.0001	0.0001	0.0001	0.0002	0.0002	0.0002	0.0002
RIRA	1	151	401	901	-1	0.5	3	8
intertemporal risk aversion (IRA)	1.2E-06	1.8E-04	4.9E-04	1.1E-03	-1.8E-04	9.1E-05	5.5E-04	1.5E-03
magnitude of IRA/SR contribution	0.020	3.066	8.142	18.294	-0.750	0.375	2.250	6.000
RCP2.6	439	447	456	473	170	174	179	190
RCP4.5	662	673	684	707	305	309	317	332
RCP8.5	600	610	620	641	275	279	286	300

Table 18 shows that there is a negligible difference in the range from 3.2-10.5% caused by the choice of RIRA coefficient, depending on the value of δ and η parameter and on the RCP scenario.

2.3.4 Economic decision

The aim of the Vltava case study is to determine if the adaptation investments into flood protection system in Prague promote economic efficiency.

We calculate the EAD for the status quo and for the adaptation investment:

(a) The situation without the new adaptation investment, the *status-quo* situation (with a 10-year protection), which we compare with
(b) The adaptation investment (with a 500-year protection), which was realized in the period of 1999-2014.

We regard the difference between these two EAD as the benefits of adaptation.
In our case, the status quo option serves as the benchmark against which the adaptation is compared. The value of our interest is the incremental impact of the adaptation investment, which we estimate by analyzing the project option's deviations from the status quo. This means describing the differences in the project option impacts in comparison to status quo (in terms of marginal costs and benefits). Therefore, our interest is the reduction of potential food damage due to new flood protection system, which represents marginal social benefits *(ΔB)*, and incurred investments and corresponding maintenance and lump-sum costs, which represent marginal social costs *(ΔC)*.

The decision criterion appropriate for an evaluation and to test the economic efficiency of one single project against the status quo alternative is the NPV. In our case, we support the adaptation project into flood protection because its NPV is generally positive:

$$\Delta NPV = PV(\Delta B) - PV(\Delta C) > 0$$

Our results show that the adaptation project into the new flood protection system in Prague promotes efficiency in the scenarios of changing future climate. The flood protection measure provides positive value of the net present value in the order of millions of €, depending on the characters of input data and methodological assumptions.

We revealed that, as expected, the selection of a discount rate becomes a critical decision in our CBA assessment, as the NPV values shows sensitivity to the choice of discount rate. Discount rates in the range up to 3% still enable that the adaptation option generates positive ENPV. However, if discount rate is set at 4% and above, we conclude that the project is no longer efficient.

It must be noted anyway, that the benefits, which we quantified as the avoided flood damage, are in all likelihood underestimated, because they cover only direct tangible damages on buildings, road infrastructure and agricultural crops, and the other damage categories are not included in the CBA.

3 Costs and benefits of adaptation – The Bilbao case study

In section 3.1 we recap on the adaptation investment analysed and on its costs, and then in sections 3.2 and 3.3 describe the methodology (fig. 18) and the results relative to the appraisal of the benefits of the adaptation investment, in terms of avoided damages.

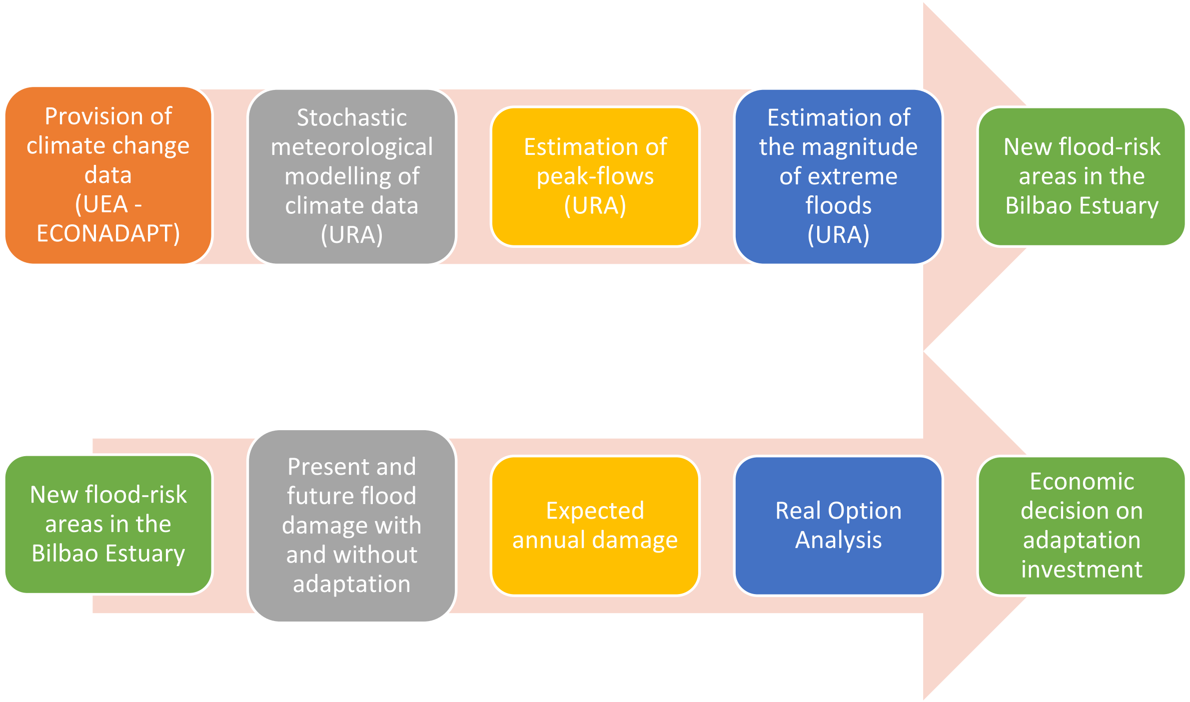

Figure 18. Conceptual framework of the methodology set up for the appraisal in the Bilbao case study.

3.1 Summary of the adaptation investment analysed and of its costs

The Bilbao case study handles the investment in adaptation to reduce the risk of flooding of a district of Bilbao, Zorrotzaurre, and its surroundings. The adaptation measure consists in the opening of a canal on the Deusto channel that will convert the Zorrotzaurre area from a peninsula into an island, which will alter the hydrodynamics of the river trait thus lowering the height of flooding (Fig. 19; see Deliverable 6.2 for details). The opening will be about 75 m wide, it should reduce the water depth in the event of extreme flooding (500-year) by on average 0.87 m. Works for the realization are planned to be completed in 2016.

In the remainder of this document, we will refer to the baseline case as to the “Peninsula”, and to the adaptation case as to the “Island”.

Figure 19. Computer graphics impression of the adaptation measure studied in the Bilbao case. The new development of the Zorrotzaurre district of Bilbao by its conversion from a peninsula into an island, by means of opening a 75 m wide channel. Source: Saitec (2007).

The cost of this measure is estimated at 12.1 M € and it will be financed entirely by the Bilbao City Council.

Further to this, plans for Zorrotzaurre include the implementation of an additional measure: the elevation of the urbanization level. This is not analysed in the present Deliverable, but will be considered descriptively in the guidelines in Deliverable 6.4.

3.2 Benefits of adaptation and associated uncertainties

3.2.1 Climate data

So far, in Basque hydrological assessments, the Basque Water Agency (URA) has been using data from climate models that adopt the SRES climate change scenarios of the IPCC (IPCC, 2000). In this case study the aim was to show the implementation of the more recent RCP scenarios.

Precipitation and temperature data

For this reason, we collaborated with the ECONADAPT project partners at the University of East Anglia (Clare Goodess), which provided to URA climate datasets for selected locations relevant to the case assessment.

Data were provided for the 1971-2000 and 2071-2100 period, representing the baseline and end-of-the-century climate change, respectively, and for RCP4.5 and RCP8.5 (Table 18). For this, 11 EURO-CORDEX RCMs (Jacob et al., 2013) were processed by the University of East Anglia (UEA). The full set of 11 runs sampled five Global Climate Models and four RCMs. The scatter plots in Figure 20 indicate that the results from the model HIRHAM forced by the ECEARTH Global Climate Model are fairly representative of the ensemble – and could be considered to provide some sort of central estimate in terms of changes in extremes of rainfall over southwestern Europe.

For the case study, UEA initially provided monthly mean data (mean rainfall and temperature, number of rain days) for the three requested locations (Bilbao, Donostia and Vitoria) extracted from the nearest ~12 km grid square from the HIRHAM-ECEARTH model. However, the RCMs driven by one particular GCM (HadGEM2) give larger temperature changes, and other models have larger decreases in summer rainfall, and a stronger tendency to increases in winter rainfall (Fig. 20). So it was recommended that URA should select two more runs – with the basis of selection depending on which variable/season they consider most important in terms of driving runoff extremes in the region.

In fact, URA took the approach of calculating mean percentage changes across the 11 RCMs (i.e., the multi-model ensemble mean change). These are shown in Table 19 for precipitation, number of dry days and temperature. An effect of using the inter-model average is that the inter-model variability of parameters is not retained. For example, the largest temperature changes simulated by some of the models (Figure 19) are not represented. Also, some models indicate wetter conditions in winter months, while others indicate dryer conditions, with these differences implying that the average multi-model change approaches zero. But for summer, particularly under the RCP8.5 scenario, most models indicate dryer conditions, so that the average change is larger than in winter, but also in this case the largest anomalies are not captured. A compromise of this method of processing projections is that inter-model uncertainties, and therefore the subsequent calculation of extremes in peak discharge, especially for the winter months, may be underestimated.

Table 18. Multi-model ensemble mean changes in the value of three climate parameters in the Bilbao case area as calculated by the Basque Water Agency using data for Bilbao provided by UEA. The data were used by the Basque Water Agency as main input for the hydrological modelling under 21st century climate change.

	Precipitation (mm)		**Number of dry days**		**Mean temperature (°C)**	
	RCP4.5	**RCP8.5**	**RCP4.5**	**RCP8.5**	**RCP4.5**	**RCP8.5**
January	-1.4%	-4.0%	2.6%	4.9%	22.3%	40.4%
February	5.9%	7.4%	-3.4%	-1.5%	18.5%	35.6%
March	-2.8%	1.0%	2.2%	2.9%	13.7%	28.0%
April	-7.8%	-14.1%	9.4%	16.5%	13.8%	26.4%
May	-6.6%	-23.6%	7.6%	18.9%	9.9%	20.7%
June	-11.6%	-32.2%	6.2%	18.3%	9.9%	20.7%
July	-6.9%	-36.3%	3.6%	9.1%	12.1%	22.9%
August	-20.2%	-34.8%	6.3%	10.0%	12.2%	23.6%
September	-18.7%	-29.3%	9.3%	14.3%	17.0%	28.8%
October	-14.0%	-18.0%	7.9%	14.0%	18.0%	30.7%
November	3.6%	8.0%	4.0%	5.3%	19.4%	35.8%
December	-3.9%	-6.1%	4.5%	8.1%	24.0%	45.1%
Annual change	**-5.9%**	**-12.4%**	**4.9%**	**10.3%**	**15.0%**	**28.1%**

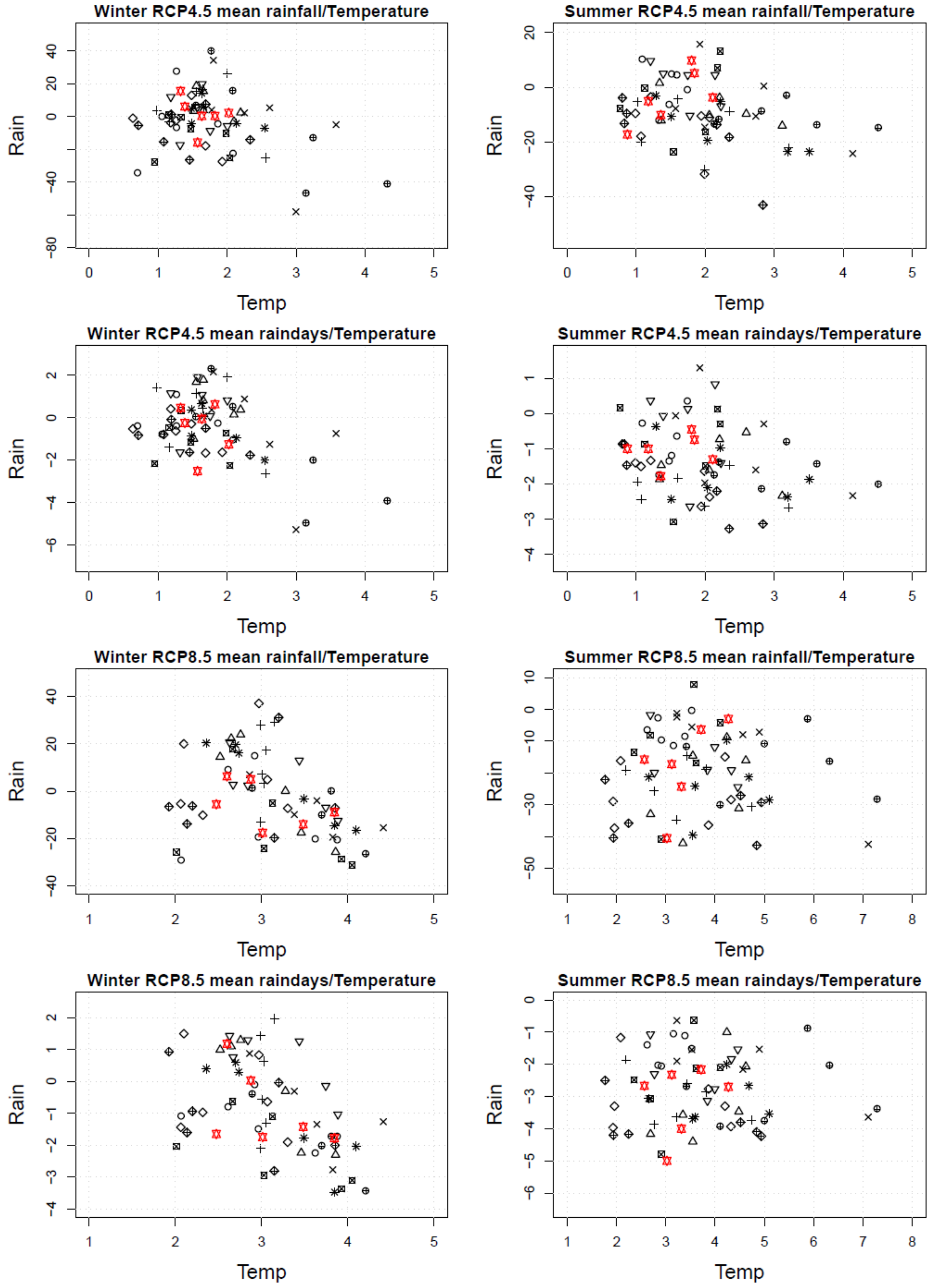

Figure 20: Scatter plot of projected changes (2071-2100 minus 1971-2000) in mean monthly temperature (horizonal axis, in °C), total monthly rainfall (vertical axis, in mm), and monthly rainy days (also vertical axis, in # of days) for Bilbao, for the six winter/coolest months (October to March; left) and six summer/warmest months (April to September; right), for RCP4.5 (top two rows) and RCP8.5

(bottom two rows). Plots show both total rainfall (mm) Data are from 11 EURO-CORDEX models – ECEARTH-HIRHAM is shown in red.

The climate projections are for mean monthly values so do not explicitly consider changes in day-to-day or year-to-year variability or in extreme events (such as heavy rainfall, drought or heatwaves). However, having information about both total precipitation and the number of dry/wet days does provide insights on changes in precipitation intensity (as discussed in Section 3.2.2).

Sea level rise data

Sea level rise projections data have been derived from Losada et al. (2014), who regionalised the latest IPCC RCP-specific data for the Spanish coast. For the coastal area close to Bilbao and the Nervión estuary the mean values for the end of the century are: 0.53 m under RCP4.5 and 0.74 m under RCP8.5.

Following the methodology defined by the Spanish Coastal Direction, four situations have been explored by URA: the overlaying of higher sea levels (as per the two RCP scenarios projections) to the 1-, 10-, 100- and 500-year river flood events (see table 20).

Table 19. Overview of the sea level anomalies (in m) obtained by overlaying the high sea levels with the hydraulic situation represented by river floods of four return periods.

River flood magnitude (return period)	Present	Year 2100 - RCP4.5	Year 2100 - RCP8.5
1-year	2.5	3.03	3.24
10-year	2.82	3.35	3.56
100-year	2.88	3.41	3.62
500-year	2.91	3.44	3.65

In the report, URA considered that due to the morphology of the Nervión river mouth, the effect of extreme waves could be considered negligible.

3.2.2 Stochastic meteorological modelling

Calibration of stochastic regional meteorological model for the Basque Country

Based on the climate data provided by the University of East Anglia, the stochastic regional meteorological model was adopted in order to reflect future conditions, by adjusting to main parameters: rain cell intensity (θ) and the frequency of storms (λ).

The procedure for the characterisation of meteorology in the two future scenarios is similar to that followed by URA for current climate in previous studies. Hourly precipitation and temperature series are obtained with a stochastic regional meteorological model for a period of 500 years for the entire considered grid. More than 3000 observations from 234 stations in the Basque Country were used to calibrate the model. These stations were clustered by means of a factorial analysis, and thus three climatic regions were defined in the area, with the Bilbao Estuary belonging to Region I.

The next step consisted in adjusting the above model to Region I, for every month of the year, based on existing climatic time series at high time resolution. In order to get a better representation of reality, it was decided to combine two spatial-temporal processes that correspond to the most common phenomena in the study area: Atlantic fronts with widespread, frequent and lasting rain; and convective rainstorms, with more localized and short-lived precipitation. The adjustment of the model parameters was achieved by minimizing the square error between simulations and observations for a combination of representative statistics. The model thus prepared satisfactorily captured three levels of aggregation considered (1, 6 and 24 hours), and other relevant variables as the percentage of dry days and autocorrelation.

Local meteorology by the end of the century

The results show a lower frequency of storms and a higher number of dry days proportional to the amount of climate change. The greater rainfall reduction is expected to occur from April to September (Figure 20). Rain intensity, on the contrary, increases slightly, potentially translating into a greater flash-flooding. Due to this effect, the reduction of total precipitation is not as strong.

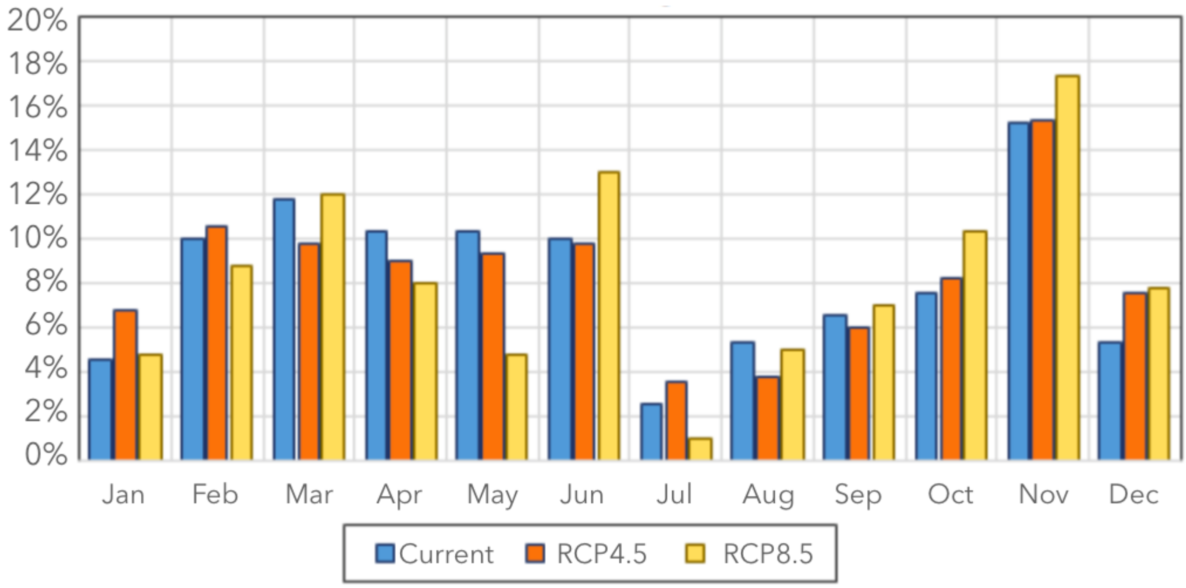

Figure 21. Temporal distribution of maximum precipitation in the study area, at present and at the end of the century under scenarios RCP4.5 and RCP8.5.

3.2.3 Hydrologic modeling of peak discharges under climate change

The simulated future climate regime under RCP4.5 and RCP8.5 was introduced into the TETIS v8.1 hydrologic model[3] (Francés et al., 2007; Bussi et al., 2013, 2014), in order to obtain potential peak-discharges for different return periods. TETIS uses three basic parameters: usable water height (Hu), surface permeability or saturated hydraulic soil conductivity (ks) and saturated hydraulic conductivity of the substrate (kp). The model was calibrated with data of historic events, with the aim of producing a single set of correction parameters and factors for the potential events in the Bilbao Estuary. Validation was

[3] Available at: http://lluvia.dihma.upv.es/ES/software/software.html

performed for the area to assess the capability of the model to reproduce extraordinary events. For this validation the 1983 floods were simulated, by compiling the daily isohyets registered on August 25th to 27th, 1983. The results of this simulation show orders of magnitude similar to the observations. Considering the typical complexity of this kind of modelling, the results are considered very satisfactory.

For future hydrologic projections, it has been assumed that the adjusted parameters of the TETIS model do not change. This means that the physical processes of the watershed (such as change in vegetation or soils) have been considered to remain constant.

The resulting design flows of the area's main rivers, as produced by TETIS, slightly decrease for the lowest return period events (Table 20). This can be explained by the increase in potential evapotranspiration, which is a result of temperature increase and of a higher number of dry days. Higher evapotranspiration reduces soil moisture in the hydrological models that could compensate a potential increase in future precipitation. On the other hand, there is an increase in the highest return-period events.

Table 20. Changes in design flows (in m^3/s) for RCP4.5 and RCP8.5 in different sections of the Bilbao Estuary. The Ibaizabal River, upstream of the Kadagua River (high estuary), is the most important station for the Zorrotzaurre area of the case study.

Scenario	1-year	10-year	100-year	500-year
Ibaizabal River, upstream of Kadagua River (high estuary)				
Current	273	832	1861	2510
RCP4.5	244	875	1996	2692
RCP8.5	232	849	1997	2754
Ibaizabal River, downstream of Kadagua River (lower estuary)				
Current	360	1120	2478	3216
RCP4.5	307	1162	2635	3444
RCP8.5	280	1079	2427	3152
Kadagua River (lower estuary, mouth)				
Current	91	438	806	1155
RCP4.5	75	434	892	1379
RCP8.5	58	361	776	1240

3.2.4 Delimitation of new flood-risk areas in the Bilbao Estuary

New flood-maps were developed by URA under RCP 4.5 and 8.5, considering changes in precipitation, temperature and sea level, as previously explained. The hydraulic modelling was carried out using the HEC-RAS v4.1 model (Pappenberger et al., 2005). The river course geometry and flood plains are defined using transverse profiles, perpendicular to flow lines, approximately every 50 m. Relevant infrastructural elements, such as bridges and dams, are included. The Manning friction coefficients for the riverbed were estimated based on its nature and morphological features, characterised through Cowan formulation. In the case of flood plains, the different kinds of land uses were considered. Contraction and expansion coefficients between sections, as well as the choice of the structure calculation method most appropriate for the flow in each section, follow the recommendations of the HEC-RAS model. The resulting flood maps provided by URA are included in the Appendix.

3.2.5 Avoided damages and risk

A previous study commissioned by the Bilbao City Council estimated the economic benefits of the opening of the Deusto channel in terms of avoided damages under present-day climate (Osés Eraso et al., 2012). The study assessed river floods with 10-, 100- and 500-year return periods, whose main features are known: flood-extension, depth and water speed. This information was combined with socio-economic data about those elements exposed to the risk of flooding. As in most cities, in Bilbao the main elements at risk are houses, shops, businesses, historic buildings and citizens.

Baseline damages, i.e., before the opening of the canal, were taken from a study by the Basque Government (2007), which used the same methodology as Osés Eraso et al. (2012). In order to define the new adaptation scenario several new variables were incorporated in the analysis:

- The opening of a 50 m-wide canal [4].
- According to a report commissioned by URA (SAITEC, 2007), the new water level varies from 1.07 m in the baseline to 0.70 m after the opening, so an average level of 0.885 m was considered. This new level was considered to be equal in every section.
- No new data on water speed was available, so it was assumed to be the same as in the baseline.

Five categories of damages were used to estimate the new costs of flooding after the opening of the Deusto channel. The first category accounts for damages to residential property, which can be classified into direct costs (to property, furniture or other appliances, including cleaning costs) and indirect damages (relocation). Direct costs estimates were transferred to Bilbao based on a study developed in the UK (Penning-Rowsell et al., 2006). These costs depend on water depth, the type of housing, the age of the affected buildings, the social class and the duration of flooding. Relocation costs were based on another study in the UK (DETR, 1999). The second category of costs includes damages to non-residential property, which accounts for damage to (non-residential) buildings, machinery or stored items and indirect damage due to a possible temporary cessation of activity. These estimates were also based on Penning-Rowsell et al. (2006).

The third type of damage is related to impacts on cultural heritage, which were based on a study from Taylor (2006) that used a contingent valuation method to obtain the willingness to pay to avoid the risk of flooding in two buildings of heritage interest in Lewes (UK). The results were transferred to Bilbao. The fourth type of damages refers to flood impacts on human health which may result from the even itself (risk to life, hypothermia and injuries during or immediately after) and from the subsequent activities related to the event (stress, post-traumatic anxiety…). Estimates for health damages were based on several studies from DEFRA (2003, 2004, 2006). This category includes foregone benefits related to the willingness to pay for increasing the level of protection, and is closely related to anxiety resulting from previously experienced events. The fifth category of damages includes temporary disruption of transportation, increasing the number of emergencies and so -called second -round effects following the approach by Penning-Rowsell et al. (2006).

The results obtained by Osés Eraso et al. (2012) show a significant reduction of damages in the adaptation scenario. Floods of 10-year return period would not cause any damage, while

---

[4] The final width of the canal is 70 m therefore the benefits of adaptation are expected to be higher than those estimated by Osés Eraso et al. (2012).

they decrease by 67.4% for 100-year floods. For 500-year floods, damages are reduced by 30.7%. The results are presented in Table 21.

Table 21. Benefits, in terms of avoided damages, resulting from turning Zorrotzaurre into an island by opening of the Deusto channel. Baseline flood damages, in the “peninsula” case, are taken from Basque Government (2007) and damages after building the canal were estimated by Osés Eraso et al. (2012). Data are shown in millions of Euros per event and include low and high cost estimates, based on the values transferred from Penning-Rowsell et al. (2006).

Category of damage	**10-year flood**						**100-year flood**						**500-year flood**					
	Peninsula		**Island**		**Benefits**		**Peninsula**		**Island**		**Benefits**		**Peninsula**		**Island**		**Benefits**	
	Low	High	Low	High	Low	High	Low	High	Low	High	Low	High	Low	High	Low	High	Low	High
Direct property damage																		
Residential property	4.67	5.72	0	0	**4.67**	**5.72**	164.83	197.59	61.36	73.49	**103.47**	**124.10**	235.15	276.45	192.05	228.34	**43.10**	**48.11**
Non-residential property	0	0	0	0	**0**	**0**	24.67	25.95	0	0	**24.67**	**25.95**	101.03	106.26	41.81	43.98	**59.22**	**62.28**
Cultural heritage	0	0	0	0	**0**	**0**	0.20	2.01	0.20	2.01	**0.00**	**0.00**	1.02	10.13	1.02	10.13	**0.00**	**0.00**
Other effects																		
Temporary accommodation	0.04	0.04	0	0	**0.04**	**0.04**	1.07	1.07	0.40	0.40	**0.67**	**0.67**	1.68	1.68	1.35	1.35	**0.33**	**0.33**
Additional power use	0.26	0.26	0	0	**0.26**	**0.26**	7.56	7.56	2.77	2.77	**4.79**	**4.79**	8.68	8.68	8.13	8.13	**0.55**	**0.55**
Health (anxiety)	0.02	0.02	0	0	**0.02**	**0.02**	0.61	0.61	0.22	0.22	**0.39**	**0.39**	0.67	0.67	0.65	0.65	**0.02**	**0.02**
Health (injuries and fatalities)	0.03	0.16	0	0	**0.03**	**0.16**	13.22	26.89	6.76	13.18	**6.46**	**13.71**	46.38	80.14	28.24	50.32	**18.14**	**29.82**
Emergency services	0.50	0.61	0	0	**0.50**	**0.61**	20.28	23.78	6.57	7.86	**13.71**	**15.92**	35.97	40.39	25.02	28.91	**10.95**	**11.48**
Forgone profit	0	0	0	0	**0**	**0**	8.30	8.30	0	0	**8.30**	**8.30**	12.19	12.19	8.30	8.30	**3.89**	**3.89**
Rail disruption	0	0	0	0	**0**	**0**	0.21	0.21	0.21	0.21	**0.00**	**0.00**	0.86	0.86	0.86	0.86	**0.00**	**0.00**
Secondary effects	0.01	0.01	0	0	**0.01**	**0.01**	0.38	0.45	0.12	0.15	**0.26**	**0.30**	0.67	0.79	0.47	0.56	**0.20**	**0.23**
TOTAL	5.53	6.82			**5.53**	**6.82**	241.33	294.42	78.61	100.29	**162.72**	**194.13**	444.30	538.24	307.90	381.53	**136.40**	**156.71**

Due to contingencies in the case study, it has not been possible to update the damage results of Osés Eraso et al. (2012) to incorporate the future effects of climate change for the selected RCPs. While on the one hand sea level rise will surely increase the damages of floods, it is not clear whether changes in precipitation and temperature will impact the damages in a positive or negative fashion (see Table 21 above). The following sections, nevertheless, explicitly include the effects of climate change in the economic risk modeling and in the resulting decision-making rules, at least in a conceptual manner.

3.2.6 Economic modeling

Using the damage data of Osés Eraso et al. (2012), we explain in this section a new methodology that enables the calculation of the expected accumulate damages at a given time, with and without adaptation, applying a new stochastic function.

We start with the assumption that the intensity of the extreme events does not change. The expected damage $E(D)$ in an interval dt can be expressed as:

$$E(D) = E(D_1) + E(D_2) + E(D_3) = E(d_1 \times d^1 q + d_2 \times d^2 q + d_3 \times d^3 q) = \quad (1)$$

$$d_1 \lambda_1 dt + d_2 \lambda_2 dt + d_3 \lambda_3 dt \quad (2)$$

Where D_1, D_2 and D_3 are the damages of events with return period λ_1, λ_2 and λ_3, and the independent Poisson process $d^i q$ has a value of 1 with probability $\lambda_i \times dt$ and 0 otherwise. The expected damage between the initial time $\tau_1 = 0$ and the final time τ_2 can be presented as:

$$E(D_i^{0,\tau_2}) = \int_0^{\tau_2} d_i \lambda_i e^{-\rho t} dt = \frac{d_i \lambda_i}{\rho} [1 - e^{-\rho \tau_2}] \quad (3)$$

where ρ is the discount rate with risk and d_i is the corresponding value from Table 21 that indicates the damage if there is a flood event of type i.

In the long run, we can consider that time tends to infinite ($\tau_2 \to \infty$), and thus Equation 3 can be simplified as follows:

$$E(D_i^{0,\infty}) = \int_0^{\infty} d_i \lambda_i e^{-\rho t} dt = \frac{d_i \lambda_i}{\rho} \quad (4)$$

As we are considering floods with return periods of 10, 100 and 500 years, there is an expected damage $E(D_i^{0,\tau_2})$ for each frequency λ_i. When there are three types of events the present value of the total expected damage for the interval $[0, \tau_2]$ is:

$$E(D^{0,\tau_2}) = E(D_1^{0,\tau_2}) + E(D_2^{0,\tau_2}) + E(D_3^{0,\tau_2}) \quad (5)$$

We acknowledge that to postulate that floods recur with three specific periodicities, such as the ones above, is a simplification, which nevertheless allows us to explore a novel methodology that handles floods as behave as in a Poisson process.

The effect of climate change and socio-economic development on the expected damage

Future damages could increase due to the effect of climate change, making flood events more frequent and/or more intense, and to socio-economic development, by which the value of the exposed assets increases. Also, the urban development of the Zorrotzaurre district implies a higher number of assets that could be potentially affected by flooding.

If climate and socio-economic effects are factored in, damage could increase at a rate of μ_C due to climate effects and μ_S due to socio-economic effects, so that a total Expected growth in damage μ can be defined as the sum of both effects: $\mu = \mu_C + \mu_S$. As the Expected growth in damage and the discount rates have opposite sign, the expected damage will depend on the difference between the two. In other words, assuming event i takes place at time t, the expected damage in the interval $[0, \tau_2]$ is as follows:

$$E(D_i^{0,\tau_2}) = \int_0^{\tau_2} d_i \lambda_i e^{(\mu-\rho)t} dt = \frac{d_i \lambda_i}{\rho - \mu}[1 - e^{-(\rho-\mu)\tau_2}] \tag{6}$$

As previously done, when $\tau_2 \to \infty$ then:

$$E(D_i^{0,\infty}) = \int_0^{\infty} d_i \lambda_i e^{(\mu-\rho)t} dt = \frac{d_i \lambda_i}{\rho - \mu} \tag{7}$$

Note that Equation (7) would only make sense if $\mu < \rho$. However there is nothing to prevent the sum of the climate and socio-economic effects from being greater than the discount rate, in which case we should consider Equation (6) for a finite time intervals.

In summary, the stochastic damage function defined by Equation (7) enables the calculation of flooding damages for any given time, depending on the difference between the increase of damages due to climate change and to economic growth and the discount rate. Using the data from Table 21 as input, we can measure stochastically the damages related to flood of different return periods, but we can also estimate the benefits of adaptation, in terms of avoided impacts. The latter is shown in Table 22.

Table 22. Total damages (in M €) for the baseline and adaptation cases, and damage reduction resulting from the adaptation investment, for different values of $\rho - \mu$ and different time periods (τ_2, in years).

$\rho - \mu$	1: Baseline (Peninsula)			2: Adaptation (Island)			Damage Reduction (1-2)		
	τ_2=50	τ_2=85	τ_2=100	τ_2=50	τ_2=85	τ_2=100	τ_2=50	τ_2=85	τ_2=100
-0.02	367.75	957.52	1,367.40	136.09	354.35	506.03	231.66	603.18	861.37
-0.01	277.68	573.43	735.50	102.76	212.21	272.18	174.92	361.22	463.32
0	214.02	363.84	428.04	79.20	134.64	158.40	134.82	229.19	269.64
0.01	168.42	245.09	270.58	62.33	90.70	100.13	106.10	154.39	170.44

0.02	135.29	174.92	185.06	50.07	64.73	68.48	85.22	110.19	116.57
0.03	110.84	131.54	135.58	41.02	48.68	50.17	69.83	82.86	85.41
0.04	92.53	103.44	105.05	34.24	38.28	38.88	58.29	65.16	66.18
0.045	85.10	93.05	94.06	31.49	34.43	34.81	53.60	58.61	59.25
0.05	78.58	84.39	85.03	29.08	31.23	31.47	49.50	53.16	53.56
0.06	67.79	70.91	71.16	25.09	26.24	26.34	42.70	44.67	44.83
0.065	63.30	65.59	65.75	23.42	24.27	24.33	39.87	41.32	41.42
0.07	59.30	60.99	61.09	21.95	22.57	22.61	37.36	38.42	38.48

The reduction of damages due to the adaptation measure can also be observed in Figure 21.

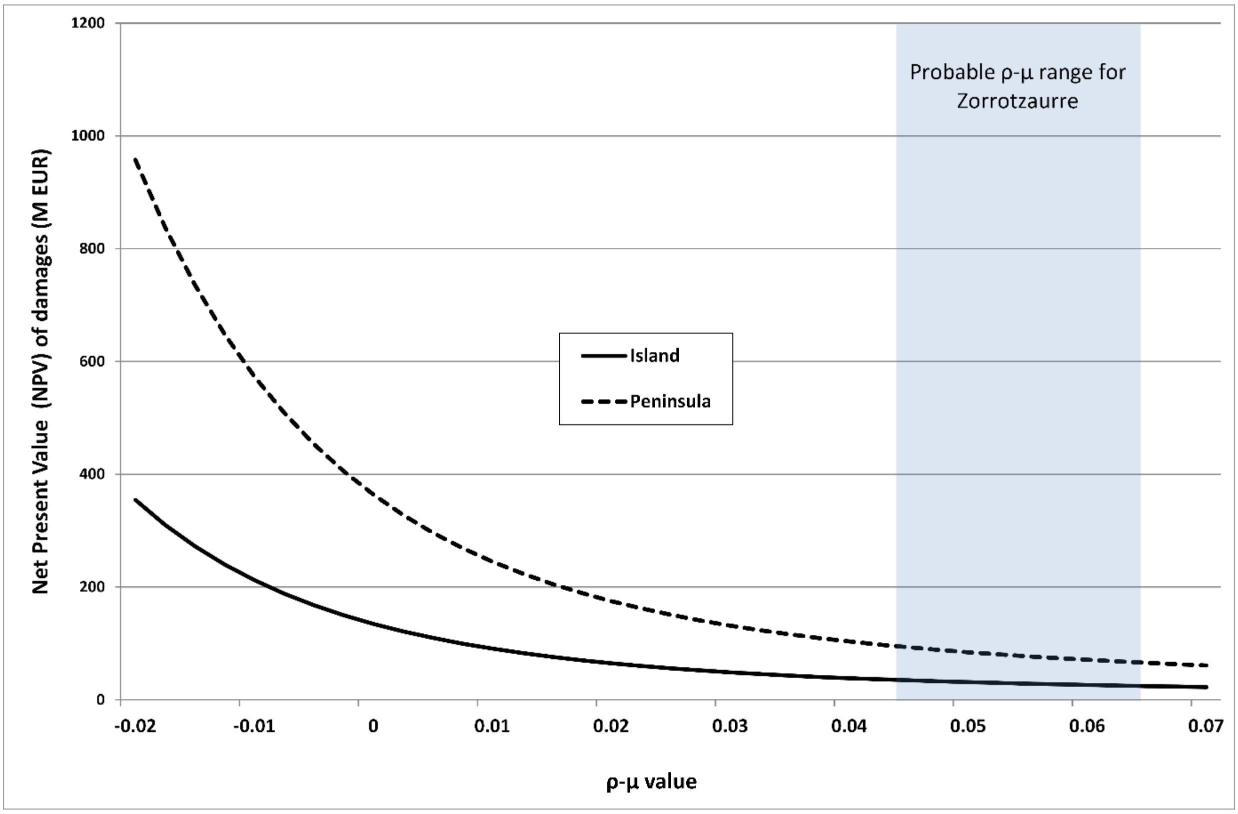

Figure 22. Net present value (in M €) of the cumulative damage with a time horizon of 85 years ($\tau_2 = 85$), for the baseline (Zorrotzaurre as a peninsula) and the adaptation scenario (Island), as a function of $\rho-\mu$.

An assessment of risk

In situations in which uncertainty needs to be accounted for, measures of risk have proven to be very useful tools. This is a quite novel approach in economics of adaptation, even though it has been frequently used, for example, to consider price uncertainties (Abadie and Chamorro, 2013).

There are two main risk measures that can be used for this purpose: Value-at-Risk (VaR) and Expected Shortfall (ES). The first is the most standard measurement and well recognised by international financial regulatory bodies. The VaR(α) at the confidence level α is the value at which the probability of obtaining higher values is 1-α. In our Bilbao case study, the VaR of damage resulting from river flooding in the case study area expresses the losses that could occur with a given confidence level α of 95%, for a time interval of 85 years.

The second risk measure is the ES, which in our case represents the expected damage when VaR is exceeded. ES is, therefore, a better measure of risk for low probability but high damage events. Both measures of risk will be estimated for the Bilbao case study.

The opening of the canal is expected to reduce not only the expected damage but also the level of risk, that is, the damages that would occur in the worst 5% of the cases. A risk assessment follows, with and without the opening up of the canal, considering time interval of 85 years $(\tau_2 = 85)$, and the rate is 6.5% ($\rho - \mu = 0.065$). One million MonteCarlo simulations were run, each with 50 steps per annum $\Delta t = 1/50$.

Figure 4 shows the probability distribution before and after opening the Deusto channel with $\rho - \mu = 0.01$. Results are presented in Figure 4, which shows that both the expected damage and the risks decrease significantly due to the opening of the canal. For example, in the adaptation case we found that in 360,926 of the million simulations performed damage is zero, which is equivalent to say that there is a 36.1% probability of there being no damage due to 100- and 500-year flood events.

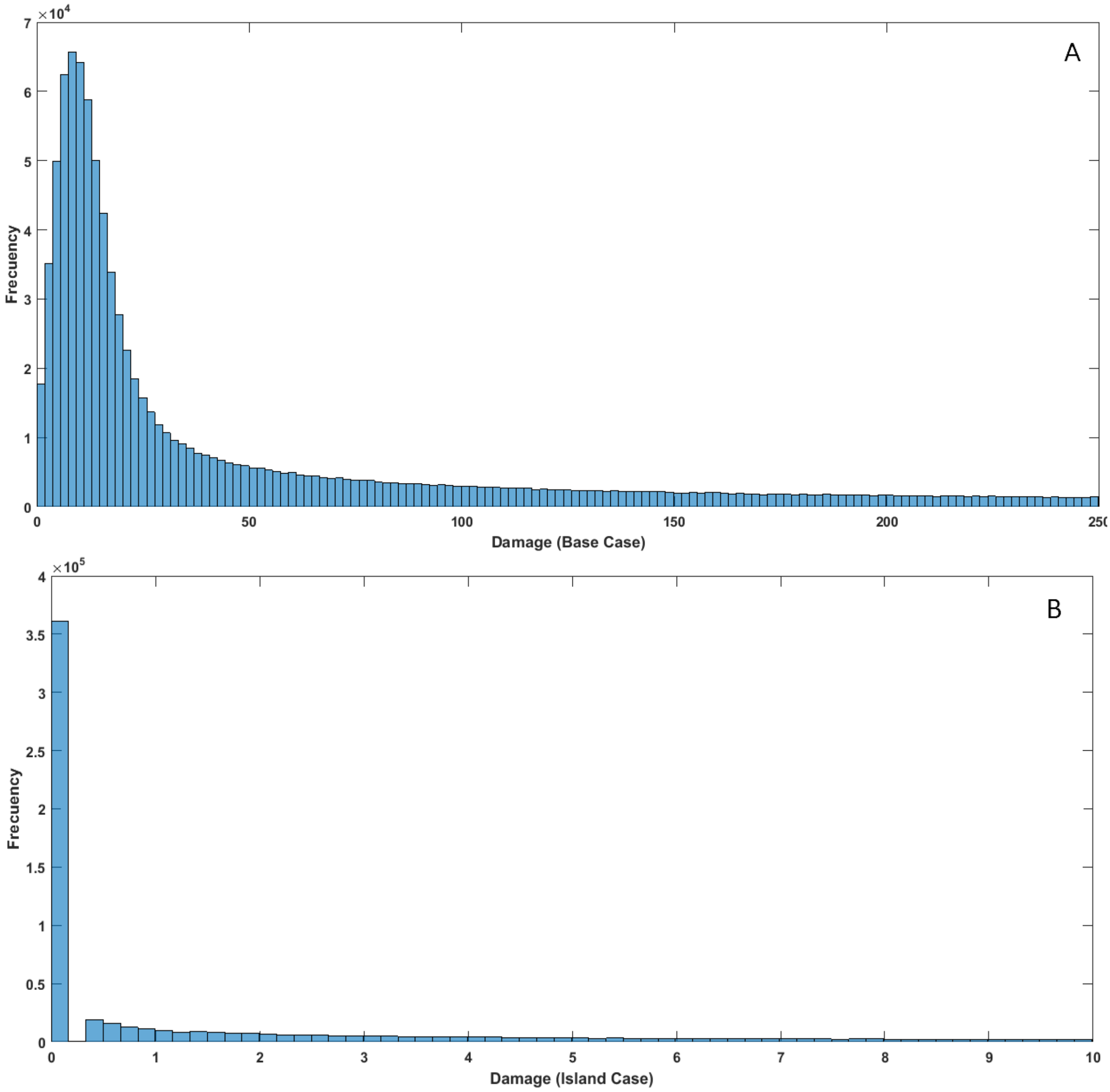

Figure 23. Frequency distribution of damages of extreme events (y axes indicates occurrences in the Monte Carlo simulation), for the case $\rho - \mu = 0.065$. The upper and lower figures represent the distribution in the baseline (peninsula) and in the adaptation (island) case, respectively. Note the different axes scales.

The Poisson distribution indicates the likelihood of a certain number of events happening within a given interval:

$$f(k, \Lambda_i) = \frac{e^{-\Lambda_i} \Lambda_i^k}{k!} \tag{8}$$

where k is the number of events and Λ_i is the average frequency of the i-event in the contemplated interval of 85 years ($T = \tau_2 - \tau_1$), corresponding to the time remaining until the end of the century, for which climate simulations are taken in the case study. Following this rule, we can estimate, for example, the possibility of not having any flood of 100- and 500-year magnitude in 85 years:

- For 100-year floods ($i=2$; $T=85$): $\Lambda_2 = T \times \lambda_2 = 0.85$
- For 500-year floods ($i=3$; $T=85$): $\Lambda_3 = T \times \lambda_3 = 0.17$

Once Λ_i is known, we can estimate the probability of zero events of both kinds of flood events:

- For 100-year floods ($i=2$; $T=85$): $f(0,\Lambda_2) = e^{-\Lambda_2} = e^{-0.85} = 0.4274$
- For 500-year floods ($i=3$; $T=85$): $f(0,\Lambda_3) = e^{-\Lambda_3} = e^{-0.17} = 0.8437$

The probability of there being no damage of type *i*=2 and $i=3$ by 2100, within 85 years after the opening up of the canal with the types of event being independent is:

$$f(0,\Lambda_2) \times f(0,\Lambda_3) = 0.3606$$

But in this case the present value of the damage may range from 89.46 if the type *i*=2 event takes place at the outset to 39.91 if it takes place at the end of the period. The distribution of probabilities in 85 years' time interval is presented in Table 23.

Table 23. Probabilities of 100- and 500-year flood events, event types $i=2$ and $i=3$, respectively, in the island (adaptation) case, with $\tau_2 = 85$.

No. 100-year floods (*i*=2)	**No. 500-year floods (*i*=3)**	**Probability**
0	0	0.3606
1	0	0.3065
2	0	0.1303
3	0	0.0369
4	0	0.0078
5	0	0.0013
0	1	0.0613
1	1	0.0521
2	1	0.0221
3	1	0.0063
4	1	0.0013
0	2	0.0052
1	2	0.0044
2	2	0.0019
3	2	0.0005
Other cases		0.0025
Total		**1.0000**

Based on Monte Carlo simulations, two measures of risk have been estimated, as a function of *ρ-μ*: the VaR(95%) and ES(95%). Table 24 shows the expected damage value and the risk measures in the island and peninsula cases as a function of *ρ-μ*:

Table 24. Measures of risk for the baseline and the adaptation scenario, in millions of €, showing mean damages, VaR(95%) and ES(95%). Risk reduction is also shown, as the difference between the previous two situations. The time horizon is 85 years ($\tau_2 = 85$).

	***ρ-μ* = 0.045**			***ρ-μ* = -0.065**		
	mean	**VaR(95%)**	**ES(95%)**	**mean**	**VaR(95%)**	**ES(95%)**

A. Baseline (peninsula)	92.81	330.49	444.65	65.41	266.80	370.73
B. Adaptation (island)	34.33	146.46	240.07	24.19	106.42	196.67
Damage reduction (A-B)	58.47	184.02	204.57	41.21	160.39	174.06

If we compare these results with the values presented in Table 22 for avoided damages, we observe that the averages obtained via the Monte Carlo simulation differ slightly from the theoretical values: for the case where $\rho - \mu = 0.045$, the mean avoided damage in Table 22 is 93.5 M € versus 92.81 M € presented above. Similarly small differences are observed with $\rho - \mu = 0.065$. This difference results from the use of two different methods, one numerical (Monte Carlo) and another one analytical (the Poisson distribution). Due to the number of simulations and the random numbers used with the Monte Carlo method, results slightly differ from those obtained through analytical methods. In turn, analytic methods such as the Poisson distribution are useful to estimate mean values, but not risk measures.

Figure 5 shows the reduction of risk, measured as ES(95%), for the baseline and adaptation cases. We observe that the reduction of risk due to the adaptation depends in a greater proportion on the sum of climate change and socio-economic development than on the discount rate used.

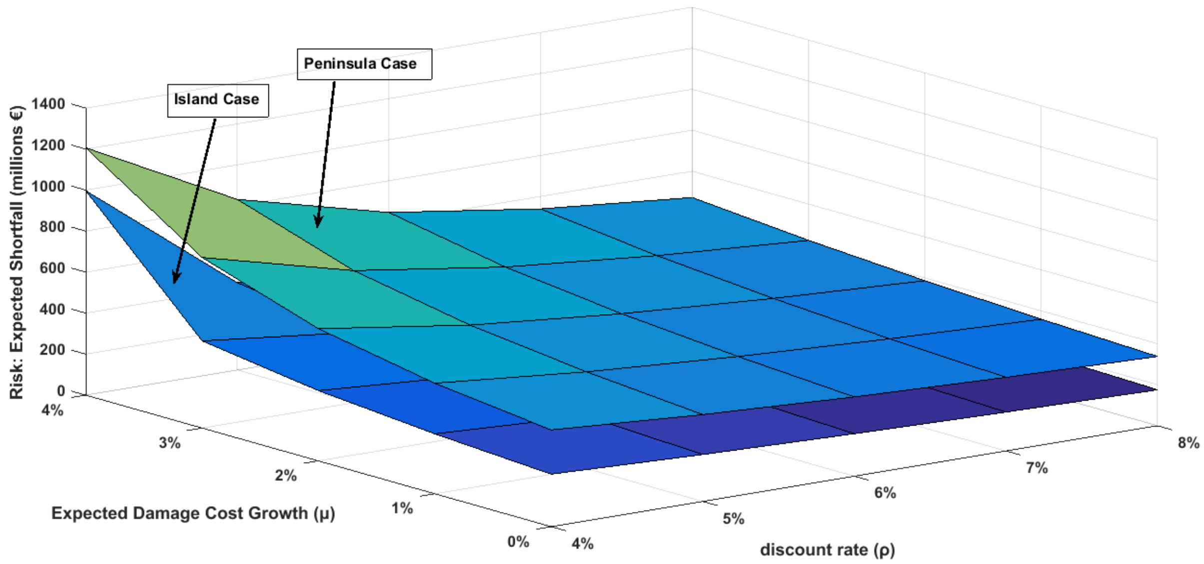

Figure 24. Representation of Expected Shortfall (ES) (95%) for the baseline (peninsula) and adaptation (island) cases, as a function of ρ (discount rate) and of μ (damage increase), respectively.

An assessment of risk with stochastic damage

We now consider the case in which damage does not increase deterministically but rather behaves stochastically, though with an expected value identical to the case of deterministic growth. This being so, if flood events in each class *i* take place, the damage is given by $d_i(t)=d_i(0)S_t$, where S_t is a variable that follows a stochastic process of the geometric Brownian motion type, as given by equation (9):

$$dS_t = \mu S_t dt + \sigma\ S_t dW_t \qquad (9)$$

where $S_0=1$, μ is the rate at which the present S_0 grows, σ is the instantaneous volatility, and dW_t stands for the increment to a standard Wiener (i.e., Brownian motion) process.

The significant characteristics of this model include the fact that it does not generate negative values, so $S_t > 0$ at all times. At a time t this distribution process generates a log-normal distribution, where the first moment is:

$$E_0(d_i(t)) = E_0(d_i(0)S_t) = S_0 d_i(0)e^{\mu t} = d_i(0)e^{\mu t} \qquad (10)$$

Table 25 shows the dependence of results on volatility. The expected values are the same as in the case of deterministic growth in damage. However, the risks now grow as volatility increases. In other words, risk *R* is a function of $\rho-\mu$ and σ, $R(\rho-\mu,\sigma)$.

Table 25. Risk reduction in the between the baseline (peninsula) and the adaptation (island) cases, for different values of volatility (σ).

Volatility	Case	ρ-μ=0.045			ρ-μ=-0.065		
		mean	VaR(95%)	ES(95%)	mean	VaR(95%)	ES(95%)
σ=0.00	Peninsula	92.81	330.49	444.65	65.41	266.80	370.73
	Island	34.33	146.46	240.07	24.19	106.42	196.67
	Change	58.47	184.02	204.57	41.21	160.39	174.06
σ=0.01	Peninsula	92.80	330.66	445.14	65.40	266.93	370.98
	Island	34.33	146.55	240.22	24.19	106.36	196.74
	Change	58.47	184.10	204.91	41.21	160.57	174.25
σ=0.02	Peninsula	92.80	331.24	446.45	65.40	267.38	371.69
	Island	34.33	146.66	240.72	24.19	106.33	196.97
	Change	58.47	184.58	205.74	41.21	161.04	174.72
σ=0.03	Peninsula	92.79	332.41	448.61	65.39	268.03	372.84
	Island	34.32	147.04	241.54	24.19	106.36	197.37
	Change	58.47	185.37	207.07	41.21	161.67	175.46
σ=0.04	Peninsula	92.79	333.83	451.64	65.39	268.93	374.43
	Island	34.32	147.39	242.72	24.18	106.56	197.95
	Change	58.47	186.44	208.92	41.20	162.37	176.48
σ=0.05	Peninsula	92.79	335.63	455.58	65.38	270.03	376.51
	Island	34.32	147.74	244.25	24.18	106.68	198.70
	Change	58.46	187.90	211.32	41.20	163.34	177.81

3.3 Economic decision: whether and when to invest in adaptation

In this subsection we develop a small example on real options analysis applied to the Bilbao case study adaptation project appraisal, about the opening the Deusto channel and turning the Zorrotzaurre peninsula into an island.

The time period is T, for which investment costs of I must be paid. If investment is made at time t, there is a current present value of damage avoided for a period of 85 years $[t, 85]$ given equation (11).

$$E_t(D_B^{t,85}) - E_t(D_A^{t,85}) = S_T \frac{(d_1^B - d_1^A)\lambda_1 + (d_2^B - d_2^A)\lambda_2 + (d_3^B - d_3^A)\lambda_3}{\rho - \mu}[1 - e^{-(85-t)(\rho-\mu)}] \quad (11)$$

where the scripts B and A refer to the cases of the baseline (*peninsula*) and of the adaptation (*island*), respectively, and where the remaining useful lifetime is $85 - t$.

At the final time T the decision made will be to invest if the expected present value of the avoided damage over the course of the 85 years is greater than the cost of investment, i.e., if equation (12) is met:

$$W_T = \max(S_T \frac{(d_1^B - d_1^A)\lambda_1 + (d_2^B - d_2^A)\lambda_2 + (d_3^B - d_3^A)\lambda_3)}{\rho - \mu}[1 - e^{-(85-T)(\rho-\mu)}] - I; 0) \quad (12)$$

If investment is postponed at an earlier time t for an interval Δt several things may happen:

a. During that period there may be damage with an expected present value as follows:

$$E_t(D^{t,t+\Delta t}) = S_t \frac{(d_1^B - d_1^A)\lambda_1 + (d_2^B - d_2^A)\lambda_2 + (d_3^B - d_3^A)\lambda_3}{\rho - \mu}[1 - e^{-(\rho-\mu)\Delta t}]$$
$$\approx S_t((d_1^B - d_1^A)\lambda_1 + (d_2^B - d_2^A)\lambda_2 + (d_3^B - d_3^A)\lambda_3)\Delta t \quad (13)$$

b. But the continuation value obtained will be the following:

$$W_t = (pW^+ + (1-p)W^-)e^{-\rho\Delta t}) \quad (14)$$

Where the values W^+ and W^- are the valuations of the nodes where S increases and decreases respectively. The valuation at an intermediate node is therefore:

$$W_t = \max(S_t \frac{(d_1^B - d_1^A)\lambda_1 + (d_2^B - d_2^A)\lambda_2 + (d_3^B - d_3^A)\lambda_3}{\rho - \mu}[1 - e^{-(100-t)(\rho-\mu)}] - I;$$
$$(pW^+ + (1-p)W^-)e^{-\rho\Delta t})) - S_t \frac{(d_1^B - d_1^A)\lambda_1 + (d_2^B - d_2^A)\lambda_2 + (d_3^B - d_3^A)\lambda_3}{\rho - \mu}[1 - e^{-(\rho-\mu)\Delta t}])$$

(15)

With this it is possible to build a binomial tree. The values of σ, μ and ρ are needed.

At the outset the value of immediate investment is given by (16):

$$NPV_0 = \frac{(d_1^B - d_1^A)\lambda_1 + (d_2^B - d_2^A)\lambda_2 + (d_3^B - d_3^A)\lambda_3}{\rho - \mu}[1 - e^{-100(\rho-\mu)}] - I \tag{16}$$

And the continuation value is given by equation (17):

$$C_0 = (pW^+ + (1-p)W^-)e^{-\rho\Delta t})) - S_t \frac{(d_1^B - d_1^A)\lambda_1 + (d_2^B - d_2^A)\lambda_2 + (d_3^B - d_3^A)\lambda_3}{\rho - \mu}[1 - e^{-(\rho-\mu)\Delta t}] \tag{17}$$

The values of I that give $NPV_0 = C_0$ define the optimal exercise boundary.

Initially we develop the calculations for a case in which $\sigma = 0.05$; $\rho = 0.08$; $\mu = 0.015$; $T = 1$; $\Delta t = 0.5,; I = 12.1$. This means building a tree with only two steps in which the investment option is only available for one year. Initially $S_0 = 1$. After one step $\Delta t = 0.5$ the value of S becomes uS if it increases with probability p_u or dS if it decreases with probability p_d, where

$$u = e^{\sigma\sqrt{\Delta t}} = 1.0360 \ ; \ d = e^{-\sigma\sqrt{\Delta t}} = 0.9653 \tag{18}$$

$$p_u = \frac{e^{\mu\Delta t} - d}{u - d} = 0.5976 \ ; p_d = (1 - p_u) = 0.4024 \tag{19}$$

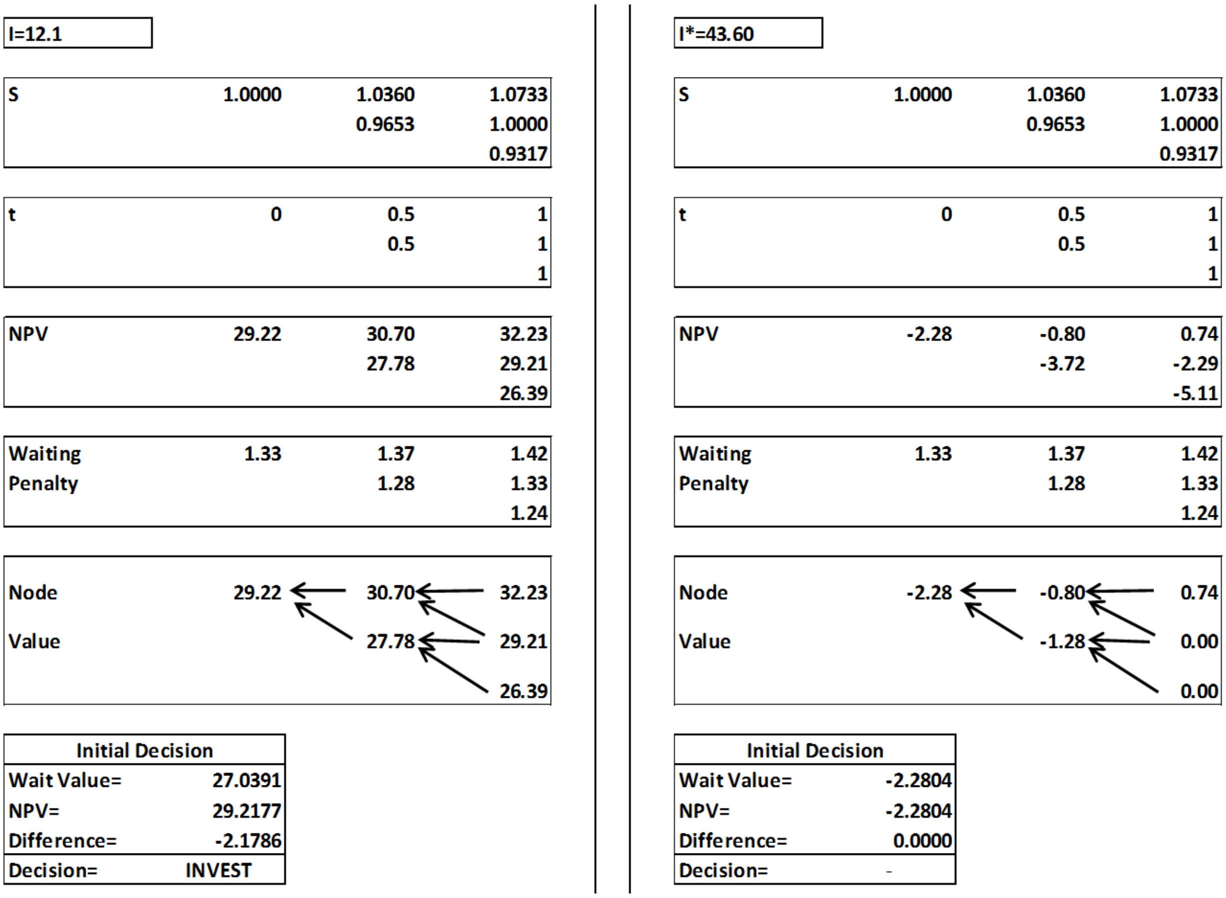

Figure 25. Summary of the essential parts of the decision making method, presenting the results for two investment options. The left chart uses an initial investment of 12.1 M €, the actual cost of the adaptation measure. The chart on the right shows the boundary value of the investment cost I between the "investment region" and the "wait region", this occurs for $I^* = 43.60$.

There are various parameters that influence the maximum cost that can be accepted for making investment immediately. For example, volatility can change the boundary of the wait-investment regions. As shown in Table 26, the greater the volatility, the lower the investment boundary. In other words, greater volatility makes potential investors more demanding and they invest only when the cost is lower.

Table 26. Changes in investment boundaries depending on volatility.

Volatility σ	Investment I^*
0.05	49.60
0.10	41.98
0.20	37.73
0.30	33.67

If the discount rate ρ increases, the future penalty increases. For the baseline scenario, with $\rho = 0.10$ the figure that results is $I^* = 34.28$, because the present value of the investment cost made in the future is lower. If damage grows as a result of climate change and/or socio-economic development, μ increases. For the baseline scenario, for $\mu = 0.035$ then the resulting figure is $I^* = 59.22$. The increase in μ results in higher investment costs being accepted.

Now consider a more elaborate case in which $T = 10$ years and $\Delta t = 1/50$. A binomial tree with 500 steps is built. In this case $I^* = 48.37$. The value is lower here because the period in which the option can be exercised is longer.

An optimal exercise boundary graph can be drawn up depending on volatility (Figure X). An increase in volatility, and therefore in uncertainty, results in investment being made immediately only if the cost is substantially lower. This example has been defined for a 20-year period in which the option can be exercised.

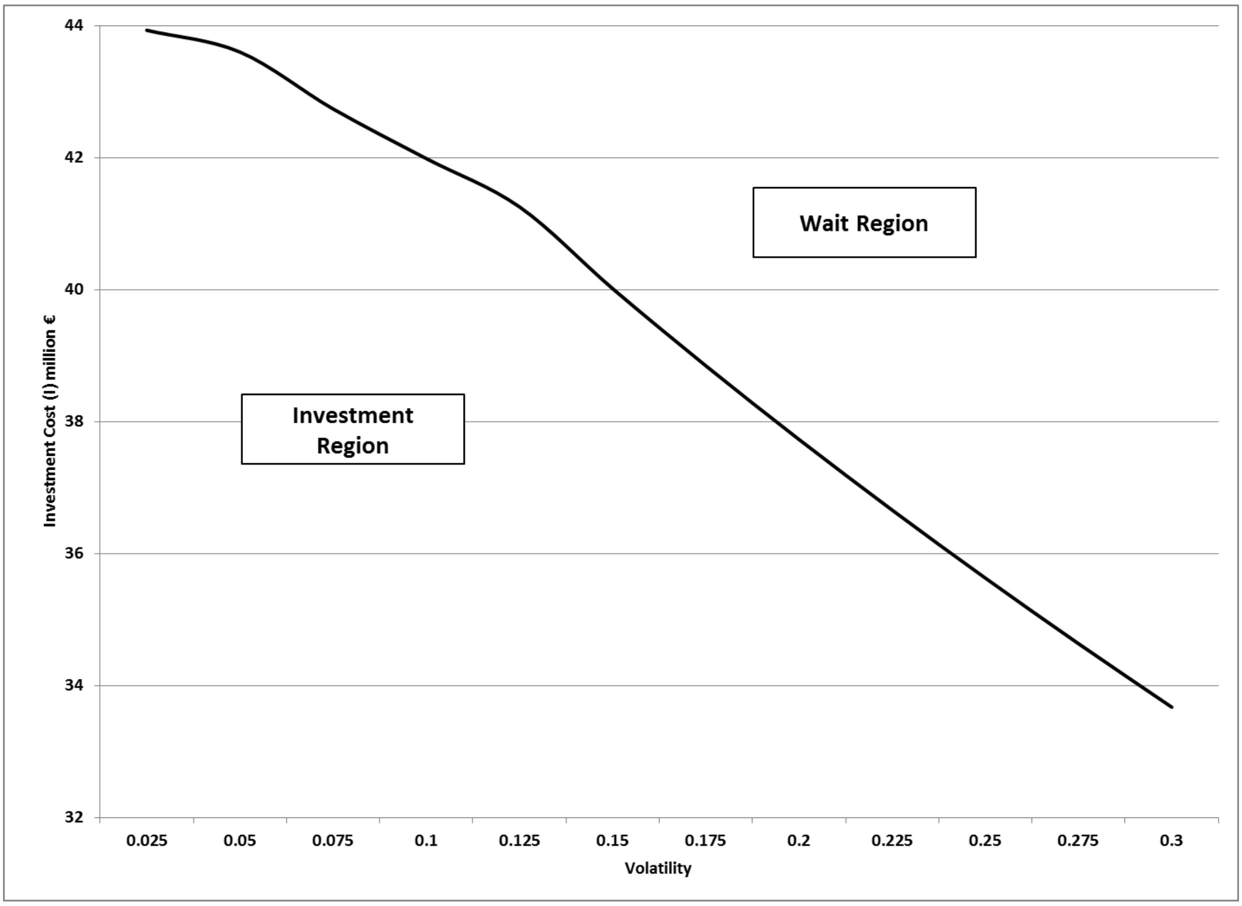

Figure 26. “Investment” and “Wait” regions depending on volatility and on the investment cost.

4 Treatment of uncertainty in the two appraisals

To provide an overview of the approaches taken in the Vltava and Bilbao case study to address the problem of uncertainties in investments in climate change adaptation, Table 27 tries to summarize them. For both cases, the uncertainties coming from the choice of the climate model simulation, from the scenarios of future socio-economic development, and from the rate of discounting applied appear to be the largest.

Table 27. Summary of the sources of uncertainty inherent with the appraisal in the Bilbao case study.

Source of uncertainty	**How is it addressed?**		**Degree of uncertainty**	
	Vltava case	**Bilbao case**	**Vltava case**	**Bilbao case**
Future emissions	Use of three RCPs: RCP 2.6; RCP 4.5; RCP 8.5	Use of two RCPs: RCP 4.5; RCP 8.5	Medium	Medium
Regional climate	Use of 14 climate simulations from several RCMs for precipitation and temperature	Use of 11 climate simulations from several RCMs for precipitation and temperature; for sea level rise a regionalization of IPCC mean global sea level change	**High**	**High**
Hydrological modeling	Cut-off of the events with the highest return periods, to reduce uncertainty from the extrapolation of extreme values from limited observation series	Not addressed	Low	
Socio-economic developments	Application of SSP- and RCP-dependent discount rates for future values. Also, two different sources of GDP projections are used (OECD, IIASA)	Results are provided for a range of values of increase in damage, also reflecting socioeconomic development	**High**	**High**
Damage calculation	Inclusion of uncertainties on exposure of assets and on the vulnerability curves for buildings: min, max and mean values are considered for these datasets	Inclusion of min and max values for the maximum possible damage to buildings	Medium/High	Medium/High
Costs of adaptation	Inclusion of a range of values for the cost of maintenance and for "one-off" costs for protection operations	Results of the decision-making process are provided for a range of values of investment costs	Low	Medium
Method of EAD calculation	Trapezoidal rule using 6 return periods vs. using full range of 141 return periods	Estimation of likelihood of occurrence of stochastic events of three return periods with Poisson process	Medium	Low
Discounting approach	Employing several approaches: constant rate; Ramsey formula with scenario-dependent discount rate; expanded Ramsey formula with uncertain growth; expanded Ramsey formula with RIRA. Also, two different sources of GDP projections are used (OECD, IIASA)	Results are shown for a vast range of discounting values	Medium	Medium
Discount rate	Two discount rates are used for the constant discounting approach	Results are shown for a vast range of discounting values	**High – This has the largest effect on the appraisal**	**High**

5 References

Abadie, L.M., Chamorro, J.M. (2013). Investment in energy assets under uncertainty: Numerical methods in theory and practice, 1st ed. Springer, London.

Arcadis (2004). Posílení rizikové analýzy a stanovení aktivních zón v českém vodním hospodářství. (Enhancement of risk analysis and determination of active zones in czech water management). Project report. Programme “Partners for Water” No. 110302/OF4/1O2/000852/LE, Ministry of Agriculture of the Czech Republic, Prague.

Arnell, N.W. (1989). Expected annual damages and uncertainties in flood frequency estimation. Journal of Water Resources Planning and Management 115 (1), p. 94–107.

Basque Government (2007). Metodología para valorar los costes de los impactos del cambio climático en el País Vasco. El caso de Bilbao - Methodology to value the costs of climate change impacts in the Basque Country. The case of Bilbao. Basque Government, Bilbao.

Brémond, P., (2011). Caractérisation et évaluation économique de la vulnérabilité des exploitations agricoles aux inondations. Thèse de doctorat, spécialité Sciences Économiques. Université de Montpellier 1, Montpellier, France (in French).

Brouwer, R., R. van Ek (2004). Integrated ecological, economic and social impactassessment of alternative flood control policies in the Netherlands. Ecological Economics 50, p. 1–21.

Bussi, G., Francés, F., Montoya, J.J., Julien, P.Y. (2014). Distributed sediment yield modelling: Importance of initial sediment conditions. Environ. Model. Softw. 58, 58–70. doi:10.1016/j.envsoft.2014.04.010

Bussi, G., Rodríguez-Lloveras, X., Francés, F., Benito, G., Sánchez-Moya, Y., Sopeña, A., (2013). Sediment yield model implementation based on check dam infill stratigraphy in a semiarid Mediterranean catchment. Hydrol. Earth Syst. Sci. 17, 3339–3354. doi:10.5194/hess-17-3339-2013

Chichilnisky (2011). Catastrophic risks with finite or infinite states. International Journal of Ecological Economics and Statistics 23(F11), p. 3-18.

City Hall of Prague (1997). Usnesení rady Zastupitelstva hlavního města Prahy č. 1094 ze dne 11. 11. 1997 k návrhu na realizaci protipovodňových opatření v hl.m. Praze. (Resolution of the Council of Prague no. 1094 of 11 November 1997 on the proposal of realisation of flood protection in the city of Prague.)

City Hall of Prague (2002). Usnesení rady Zastupitelstva hlavního města Prahy č. 2174 ze dne 17.12.2002 k postupu přípravy a realizace protipovodňových opatření v návaznosti na aktualizaci matematického modelu na úroveň hladiny srpen 2002. (Resolution of the Council of Prague no. 2174 of 17 December 2002 on the preparation and realisation of flood protection in connection to the update of mathematical model with the water level of July 2002.)

Czech construction standards (2015). Cenové ukazatele ve stavebnictví pro rok 2015 (Price indicators in construction industry for year 2015). (On-line.

URL:<http://www.stavebnistandardy.cz/doc/ceny/thu_2015.html>. Accessed on 12 July 2015.

Czech Hydrometeorological Institute (CHMI, 2013). Vyhodnocení povodní v červnu 2013. (Assessment of the flood in June 2013). 79 p. Ministry of Environment, Prague.

Czech Statistical Office (CZSO, 2014). Soupis ploch osevů – 2014 (Inventory of sowing areas – 2014). On-line. URL:< https://www.czso.cz/csu/czso/soupis-ploch-osevu-2014-aktclm38mi>. Accessed on 23 August 2015.

DEFRA, 2006. Flood Risks to People Phase 2 (No. R&D Technical Report FD2321). DEFRA & Environment Agency, Flood and Coastal Defence R&D Programme.

DEFRA, 2004. The appraisal of human related intangible impacts of flooding (No. R&D Technical Report FD 2005/TR). DEFRA & Environment Agency, Flood and Coastal Defence R&D Programme.

DEFRA, 2003. Flood Risks to People Phase 1 (No. R&D Technical Report FD2317). DEFRA & Environment Agency, Flood and Coastal Defence R&D Programme.

DETR, 1999. Flood and coastal defense project appraisal guidance FCD-PAG3 Economic appraisal. UK Department for Environmental, Transport and Regions, London.

Downtown, M.W., R. A. Pielke Jr. (2005). How accurate are disaster loss data? The case of U.S. flood damage. Natural Hazards 35, p. 211-228.

Dutta, D., S. Herath, K. Musiake (2003). A Mathematical model for flood loss estimation. Journal of Hydrology 277, p. 24-49.

Elleder, L. (2015), Historical changes in frequency of extreme floods in Prague, Hydrol. Earth Syst. Sci., 19(10), 4307-4315.

Ermoliev, Y., T. Ermolieva, G. Fischer, M. Makowski, S. Nilsson, M. Obersteiner (2008). Discounting, catastrophic risks management and vulnerability modeling. Mathematics and Computers in Simulation 79, p. 917-924.

Ermoliev, Y., T. Ermolieva, G. Fischer, M. Makowski (2010). Extreme events, discounting and stochastic optimization. Annals of Operations Research 177, p. 9-19.

Foudi, S., N. Osés-Eraso, I. Tamayo (2015). Integrated spatial flood risk assessment: The case of Zaragoza. Land Use Policy 42, p. 278-292.

Francés, F., Vélez, J.I., Vélez, J.J. (2007). Split-parameter structure for the automatic calibration of distributed hydrological models. J. Hydrol. 332, 226–240. doi:10.1016/j.jhydrol.2006.06.032

Fuguitt, D., Wilcox, S.J. (1999). Cost-Benefit Analysis for Public Sector Decision Makers. Westport, Conn: Quorum.

Groom, B. (2014). Discounting, in: Markandya, A., Galarraga, I., Sainz de Murieta, E. (Eds.), Routledge Handbook of the Economics of Climate Change Adaptation, Routledge International Handbooks. Routledge, Oxon (UK) and New York (USA), pp. 138–168.

Heal, G., A. Millner (2014). Reflections: Uncertainty and decision making in climate change economics. Review of Environmental Economics and Policy 8(1), p. 120-137.

Hanel, M., Vizina, A. (2015). Odvození změn extrémních průtoků a záplavových území v podmínkách klimatické změny. (Estimation of changes in extreme runoffs and floodplain areas under the climat change.) Internal report for Charles University Environment Center. Praha, srpen 2015.

Hanel, M., Buishand, T. A., Ferro, C. A. (2009). A nonstationary index flood model for precipitation extremes in transient regional climate model simulations. Journal of Geophysical Research: Atmospheres 114(D15), p. 1984–2012.

HM Treasury (2013). The Green Book: appraisal and evaluation in central government. On-line. URL:<https://www.gov.uk/government/publications/the-green-book-appraisal-and-evaluation-in-central-governent>. Accessed on 25. 11. 2015.

Horský, M. (2008). Metody hodnocení potenciálních povodňových škod a jejich aplikace pomocí prostředků GIS. (Methods of evaluation of potential flood damage and their application using GIS tools). Dissertation thesis, Czech Technical University in Prague, Faculty of Civil Ingeneering, Prague.

Institute of Agricultural Economics and Information (IAEI, 2014). Náklady avýnosy vybraných rostlinných a živočišných výrobků - předběžné výsledky (Cost and benefits of selected crops and animal products – preliminary results). 36 p. IAEI, Prague.

IPCC (2000), Nakićenović, N., and Swart, R., ed., Special Report on Emissions Scenarios: A special report of Working Group III of the Intergovernmental Panel on Climate Change (book), Cambridge University Press, ISBN 0-521-80081-1, 978-052180081-5 (pb: 0-521-80493-0, 978-052180493-6).

IPCC (2014). IPCC WGIII Fifth Assessment Report – Mitigation of Climate Change 2014. On-line. URL< http://mitigation2014.org/>. Accessed on 8. 12. 2015.

Janssen, R. (2001). On the Use of Multi-Criteria Analysis in Environmental Impact Assessment in The Netherlands. J. Multi-Crit. Decis. Anal. 10: 101– 109.

Koks, E.E., M. Bočkarjova, H. de Moel, J.C.J.H. Aerts (2015). Integrated direct and indirect flood risk modeling: Development and sensitivity analysis. Risk Analysis 35 (5), doi 10.1111/risa.12300.

Lasage, R., T. I. E. Veldkamp, H. de Moel, T. C. Van, H. L. Phi, P. Vellinga, J.C.H.C. Aerts (2014). Assessment of the effectiveness of flood adaptation strategies for HCMC. Natural Hazards and Earth System Sciences 14, p. 1441-1457.

Lebegue, D. (2005). Revision du taux d.actualisation des investissem-net publics. Rapport du groupe de experts, Commisariat Generale de Plan.

Li, W., Xu, B., Wen, J. (2016). Scenario-based community flood risk assessment: a case study of Taining county town, Fujian province, China. Nat Hazards, vol. 82, no. 1, pp. 193-208.

Losada, I., Izaguirre, C. & Diaz, P. (2014). Cambio climático en la costa española. Oficina Española de Cambio Climático, Ministerio de Agricultura, Alimentación y Medio Ambiente. Madrid, 133 pag.Walker, W. E. (2000), Policy analysis: a systematic approach to supporting policymaking in the public sector, *Journal of Multi-Criteria Decision Analysis*, *9*(1-3), 11-27.

de Moel, H., Van Vliet, M., Aerts, J.C.J.H (2014). Evaluating the effect of flood damage-reducing measures: a case study of the unembanked area of Rotterdam, the Netherlands. Reg Environ Change, vol. 14, pp. 895–908.

de Moel, H., J. Huizinga, and W. Szewczyk (2016), Flood damage curves for consistent global risk assessments, paper presented at EGU General Assembly, Vienna.

Mosegaard, K., Sambridge, M. (2002). Monte Carlo analysis of inverse problems. Inverse Probl. 18, R29.

Olsen, A.S, Zhou, Q., Linde, J.J., Arnbjerg-Nielsen, K. (2015). Comparing Methods of Calculating Expected Annual Damage in Urban Pluvial Flood Risk Assessments. Water, vol. 7, pp. 255-270.

Osés Eraso, N., Foudi, S., Galarraga, I., 2012. Análisis del impacto socio económico del daño por inundación en la Ría de Nervión: un cambio de escenario ante la apertura del Canal de Deusto. Informe de Avance del Proyecto. BC3 Basque Centre for Climate Change, Bilbao.

Pappenberger, F., Beven, K., Horritt, M., Blazkova, S., 2005. Uncertainty in the calibration of effective roughness parameters in HEC-RAS using inundation and downstream level observations. J. Hydrol. 302, 46–69. doi:10.1016/j.jhydrol.2004.06.036

Penning-Rowsell, E., Johnson, C., Tunstall, S., Tapsell, S., Morris, J., Chatterton, J., Green, C., 2006. The benefits of flood and coastal risk management. A manual of assessment techniques (Multi-coloured Manual). Flood Hazard Research Centre and Middlesex University.

Penning-Rowsell, E., C. Johnson, S. Tunstall, S. Tapsell, J. Morris, J. Chatterton, C. Green (2005). The benefits of flood and coastal risk management: A handbook of assessment techniques. Flood Hazard Research Centre, Middlesex University, Middlesex University Press.

Prague Institute of Planning and Development (2013): Technical use of the area. On-line. URL:< http://www.geoportalpraha.cz/cs/opendata/50C4A396-3C42-48EB-A6D9-42B59E588D6E#.VthaJRv2Z_s>. Accessed on 27. 06. 2014

Prague Institute of Planning and Development (PIPD, 2014). Územní analytické podklady 2014: 700 – Technická infrastruktura. (Planning analytical materials 2014: 700 – Technical Infrastructure.) On-line. URL:< www.iprpraha.cz/uploads/assets/soubory/data/uap2014/700_technicka_infrastruktura.pdf>. Accessed on 17-10-2015.

Ramsey, F. P. (1928). A Mathematical Theory of Saving. Economic Journal 38 (152), p. 543–559.

Rockafellar, R.T., Uryasev, S., 2002. Conditional value-at-risk for general loss distributions. J. Bank. Finance 26, 1443–1471. doi:10.1016/S0378-4266(02)00271-6

Saint-Geours, N., Bailly, J.S, Grelot, F., Lavergne, C. (2014). Multi-scale spatial sensitivity analysis of a model for economic appraisal of flood risk management policies. Environmental Modelling & Software, vol. 60, pp. 153-166.

SAITEC, 2007. Estudio hidráulico de la apertura del Canal de Deusto (No. P0744-NaN-NaN-NaN-V03). Bilbao City Council, Bilbao.

Sweco Hydroprojekt, a.s. and DHI a.s. (2014). Dokumentace oblastí s významným povodňovým rizikem - zpráva Dílčí povodí dolní Vltavy a Dílčí povodí Berounky (Documentation of the areas under significant flood risk – a report on Partial Lower Vltava River Basin and Partial Berounka River Basin). 51 p. Povodí Vltavy, s. e., Prague.

Taylor, T., 2006. Valuing cultural heritage and climate change risks, in: Quantifying the Cost of Impacts and Adaptation in the UK.

Thieken A.H., A. Olschewski, H. Kreibich, S. Kobsch, B. Merz (2008). Development and evaluation of flemops—a new flood loss estimation model for the private sector. In: Flood recovery, innovation and response I. WIT Press, Chichester, p. 315–324.

Traeger, C.P. (2014). Why uncertainty matters: discounting under intertemporal risk aversion and ambiguity. Econ. Theory, vol. 56, pp. 627–664.

T. G. Masaryk Water Research Institute (TGM WRI, 2009). Vyhodnocení povodní v červnu a červenci 2009 na území České republiky, ekonomické a sociální dopady povodní. Dílčí zpráva. (Evaluation of floods in June and July 2009 in the Czech Republic, economic and social impacts of floods. Partial report.) On-line. URL: < http://voda.chmi.cz/pov09/doc/11.pdf >. Accessed on 22-09-2014.

T. G. Masaryk Water Research Institute (TGM WRI, 2015). User manual model Bilan. On-line. URL:<http://bilan.vuv.cz/bilan/hydrologicky-model-bilan>. Accessed on 27. 2. 2015.

T. G. Masaryk Water Research Institute and Czech Hydrometeorological Institute (TGM WRI and CHMI, 2003). Hydrologické vyhodnocení katastrofální povodne v Srpnu 2002 (Hydrological assessment of the catastrophic flood of August 2002). Czech Hydrometeorological Institute, Praha.

T. G. Masaryk Water Research Institute (TGM WRI, 2009). Metodika tvorby map povodňového nebezpečí a povodňových rizik. (Methodology of creating maps of flood hazard and flood risks). 91 p. TGM WRI, December 2009.

T. G. Masaryk Water Research Institute and Czech Hydrometeorological Institute (TGM WRI, 2006). Vyhodnocení jarní povodně 2006 na území České republiky. Souhrnná zpráva. (Assessment of spring flood of 2006 in the Czech Republic. Summary report.). 164 p. Ministry of Environment, Prague.

T. G. Masaryk Water Research Institute (TGM WRI, 2002). Výsledná zpráva o projektu "Vyhodnocení katastrofální povodně v srpnu 2002 a návrhu úpravy systému prevence před povodněmi" (Final report on the project "Assessment of catastrophic flood in August 2002 and design of the adjustment of the system of the preventive flood protection). 174 p. Ministry of Environment, Prague.

de Vries, H., K. Katsman, and S. Drijfhout (2014), Constructing scenarios of regional sea level change using global temperature pathways, Environmental Research Letters, 9(11), 115007.

Ward, P.J., H. de Moel, J.C.J.H. Aerts (2011). How are flood risk estimates affected by the choice of return-periods? Natural Hazards and Earth System Sciences 11, p. 3181-3195.

Weitzman, M. L. (1998). Why the far-distant future should be discounted at its lowest possible rate. Journal of Environmental Economics and Management 36 (3), 201-208.

World Economic Forum (2016), The Global Risks Report 2016, 11th Edition. World Economic Forum®, Geneva, Switzerland.

6 Appendix

Fig. A1. Flood maps of the Bilbao estuary produced by URA for the Bilbao case study of ECONADAPT, covering the study area, the Zorrotzaurre peninsula (in the southern part), and the trait of the Nervión downstream (in the northern part). Red, yellow and blue areas represent the 10-, 100-, and 500-year return periods, respectively. Maps show the present ("actual") and the future simulations with RCP4.5 and RCP8.5 climate change scenarios, with ("Deusto") and without the adaptation measure.

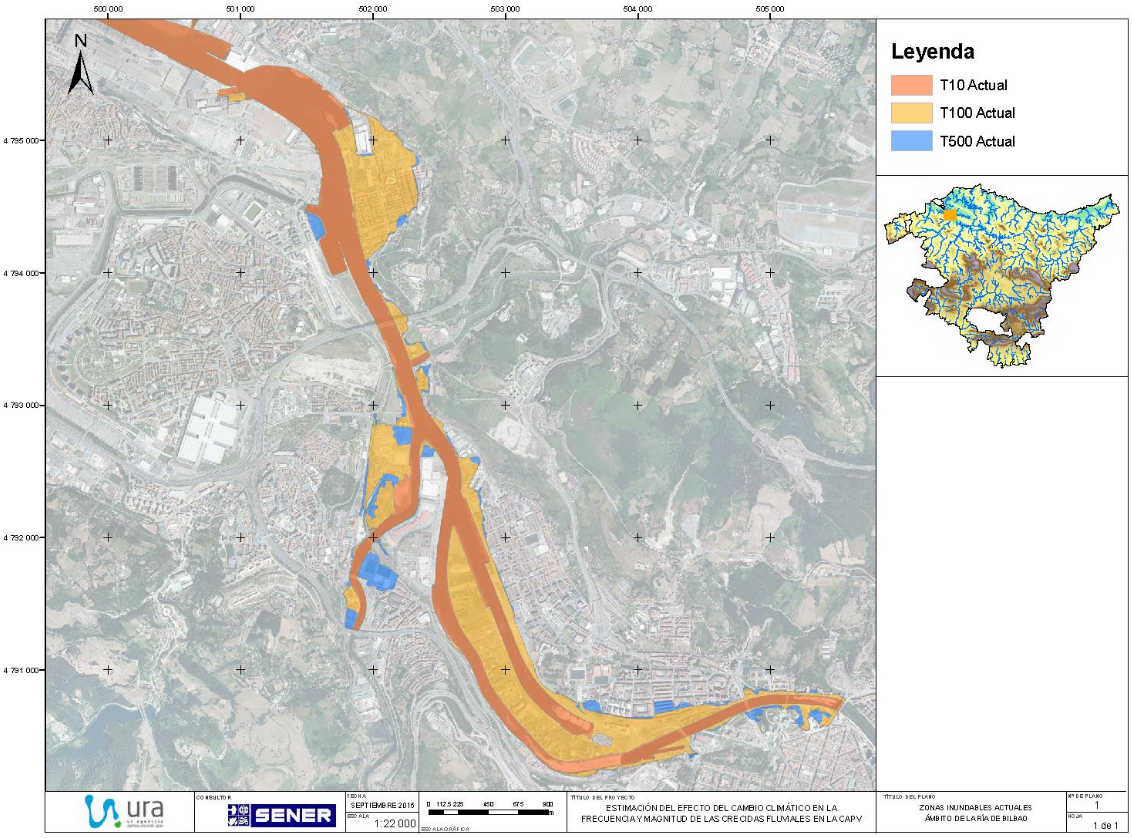

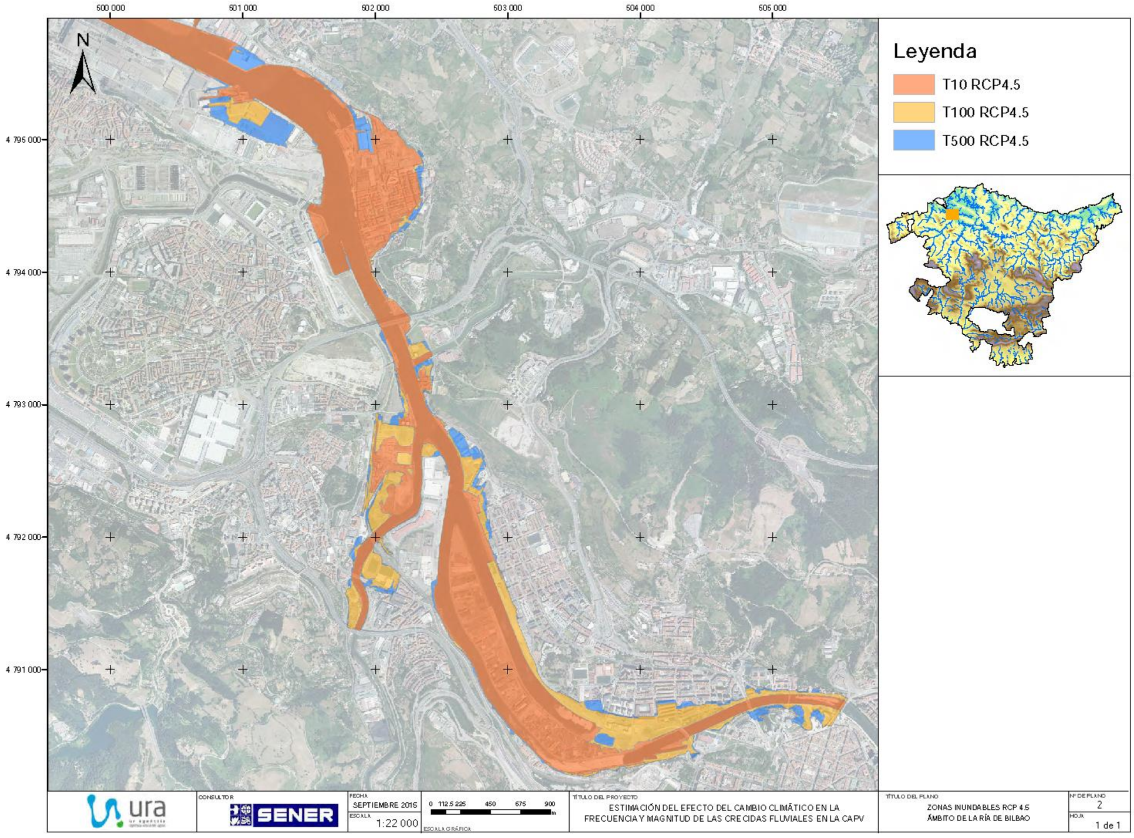
500 000
501 000
502 000
503 000
504 000
505 000
4 795 000
4 794 000
4 793 000
4 792 000
4 791 000
N
Leyenda
T10 RCP4.5
T100 RCP4.5
T500 RCP4.5
CONSULTOR
SENER
FECHA
SEPTIEMBRE 2015
ESCALA
1:22 000
0 112.5 225 450 675 900 m
ESCALA GRÁFICA
TÍTULO DEL PROYECTO
ESTIMACIÓN DEL EFECTO DEL CAMBIO CLIMÁTICO EN LA FRECUENCIA Y MAGNITUD DE LAS CRECIDAS FLUVIALES EN LA CAPV
TÍTULO DEL PLANO
ZONAS INUNDABLES RCP 4.5
ÁMBITO DE LA RÍA DE BILBAO
Nº DE PLANO
2
HOJA
1 de 1

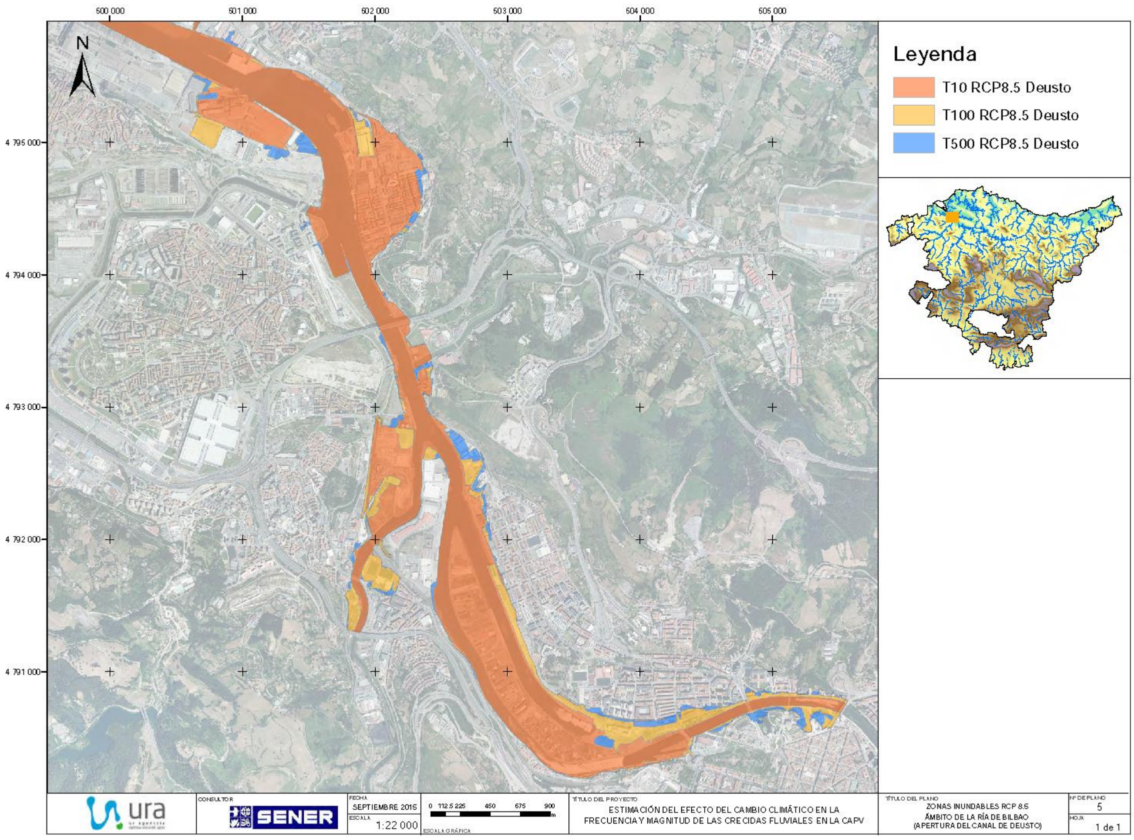
500 000
501 000
502 000
503 000
504 000
505 000
4 795 000
4 794 000
4 793 000
4 792 000
4 791 000
N
Leyenda
T10 RCP8.5 Deusto
T100 RCP8.5 Deusto
T500 RCP8.5 Deusto
CONSULTOR
SENER
FECHA
SEPTIEMBRE 2015
ESCALA
1:22 000
0 112.5 225 450 675 900 m
ESCALA GRÁFICA
TÍTULO DEL PROYECTO
ESTIMACIÓN DEL EFECTO DEL CAMBIO CLIMÁTICO EN LA FRECUENCIA Y MAGNITUD DE LAS CRECIDAS FLUVIALES EN LA CAPV
TÍTULO DEL PLANO
ZONAS INUNDABLES RCP 8.5
ÁMBITO DE LA RÍA DE BILBAO
(APERTURA DEL CANAL DE DEUSTO)
Nº DE PLANO
5
HOJA
1 de 1

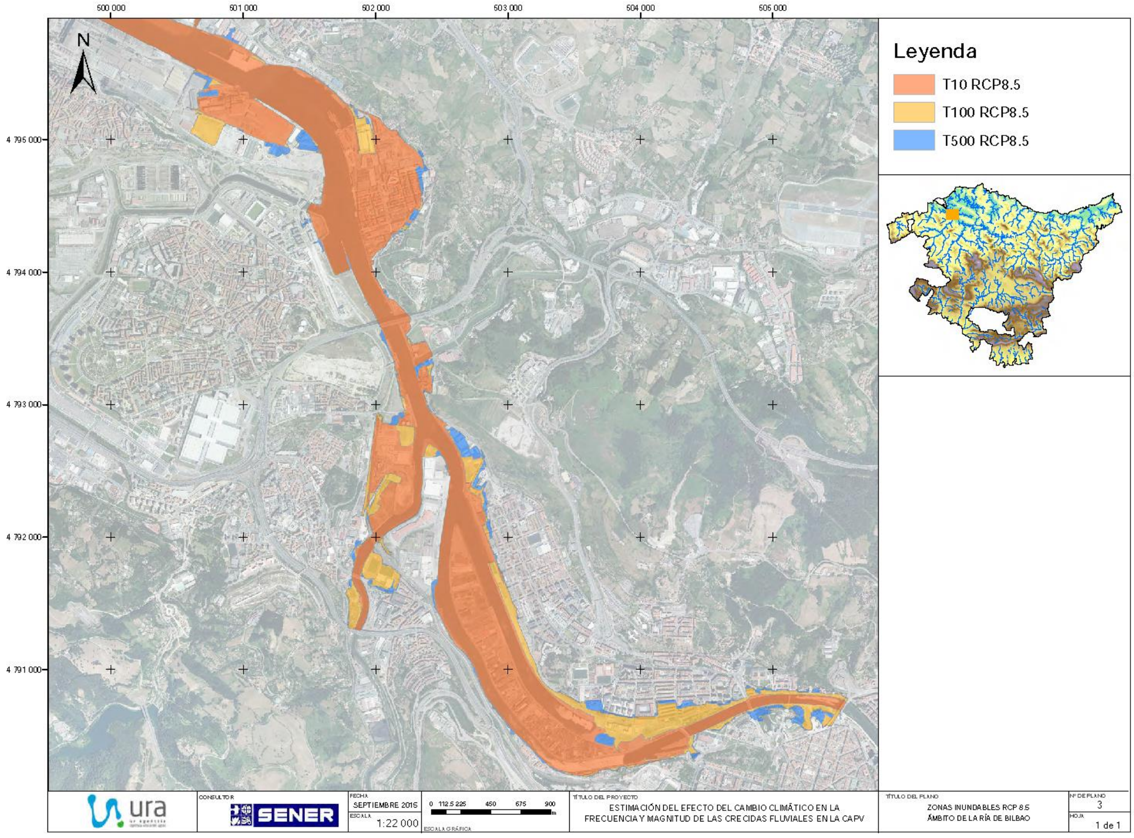

600 000
601 000
602 000
603 000
604 000
605 000
4 795 000
4 794 000
4 793 000
4 792 000
4 791 000
N
Leyenda
T10 RCP8.5
T100 RCP8.5
T500 RCP8.5
CONSULTOR
SENER
FECHA
SEPTIEMBRE 2015
ESCALA
1:22 000
0 112.5 225 450 675 900 m
ESCALA GRÁFICA
TÍTULO DEL PROYECTO
ESTIMACIÓN DEL EFECTO DEL CAMBIO CLIMÁTICO EN LA FRECUENCIA Y MAGNITUD DE LAS CRECIDAS FLUVIALES EN LA CAPV
TÍTULO DEL PLANO
ZONAS INUNDABLES RCP 8.5
ÁMBITO DE LA RÍA DE BILBAO
Nº DE PLANO
3
HOJA
1 de 1

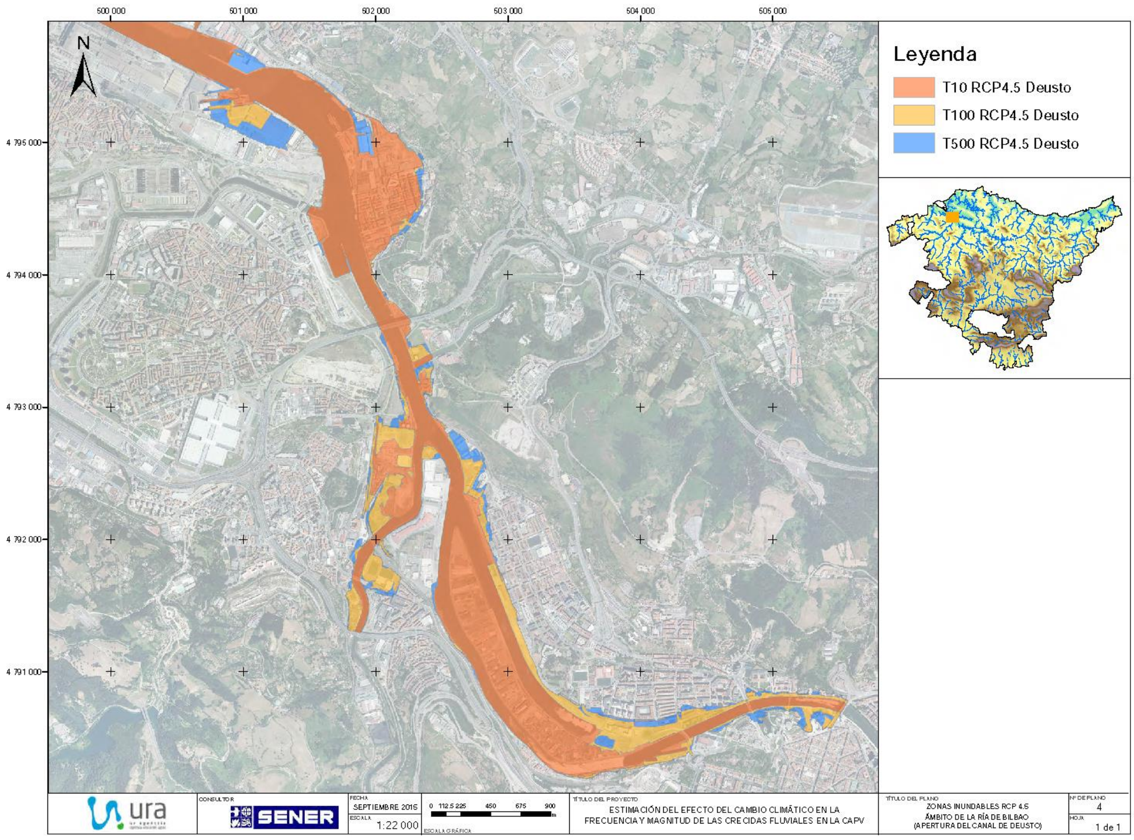

600 000
601 000
602 000
603 000
604 000
605 000
4 795 000
4 794 000
4 793 000
4 792 000
4 791 000
N
Leyenda
T10 RCP4.5 Deusto
T100 RCP4.5 Deusto
T500 RCP4.5 Deusto
CONSULTOR
SENER
FECHA
SEPTIEMBRE 2015
ESCALA
1:22 000
0 112.5 225 450 675 900 m
ESCALA GRÁFICA
TÍTULO DEL PROYECTO
ESTIMACIÓN DEL EFECTO DEL CAMBIO CLIMÁTICO EN LA FRECUENCIA Y MAGNITUD DE LAS CRECIDAS FLUVIALES EN LA CAPV
TÍTULO DEL PLANO
ZONAS INUNDABLES RCP 4.5
ÁMBITO DE LA RÍA DE BILBAO
(APERTURA DEL CANAL DE DEUSTO)
Nº DE PLANO
4
HOJA
1 de 1